Investigation of Plasma Processes in Surface Modification with Biodiagnostic Applications

A thesis for the degree of

PHILOSOPHIAE DOCTOR

Presented to:

DUBLIN CITY UNIVERSITY

By

Conor Coyle

B. Sc. (Hons)

Research Supervisor

Dr. Paul Swift

Co Supervisor

Dr. Stephen Daniels

Declaration

I hereby certify that this material, which I now submit for assessment on the programme of study leading to the award of Doctor of Philosophy, Ph.D. is entirely my own work, that I have exercised reasonable care to ensure that the work is original, and does not to the best of my knowledge breach any law of copyright, and has not been taken from the work of others save and to the extent that such work has been cited and acknowledged with the text of my work.

Signed: _____

ID No.: _____

Date: _____

Preface

The work contained in this thesis is entirely my own work, however I wish to acknowledge the contribution from a number of collaborators and groups.

- XPS data in *Chapter 4* was collected by technicians at the University of Auckland, New Zealand.
- The fibrinogen adsorption measurements using enzyme immunosorbent assay in *Chapter 5* were carried out by Dr. R.P. Gandhiraman of the BDI and NCPST, DCU.
- TIRF data was taken in collaboration with Dr. C. Charlton, BDI, DCU.
- TIRE data was taken in collaboration with Dr. N.C. Haoi Le, BDI, DCU.
- Samples were fluorescently spotted in collaboration with Dr. V. Gubala, BDI, DCU.

A number of research groups kindly allowed access to their equipment during this thesis work.

- National Centre for Plasma Science and Technology (NCPST) - PECVD chamber, Langmuir Probe, optical emission spectrometer, mass spectrometers, ellipsometer and consumables.
- Dr. P. McNally of Electronic Engineering DCU - Secondary ion mass spectrometer.
- Biomedical Diagnostics Institute (BDI) - TIRE, TIRF, consumables and materials.
- Dr. T. Cafolla of Surfaces and Interfaces Research Laboratory - AFM and consumables.
- National Centre for Sensor Research (NCSR) - UV/VIS spectrometer, FTIR, fluorescence spectrometer, contact angle goniometer and consumables.
- Impedans Ltd. - Retarding field energy analyser and Langmuir probe.
- DCU Physics School - Gold coater and consumables

Acknowledgments

I would like to thank first of all my supervisors Dr. Paul Swift and Dr. Stephen Daniels for their continuous support. I wish to particularly thank Dr. Ram Prasad Gandihraman for his kind help and guidance throughout this process, this work would not have been possible where it not for his dedication, expertise and encouragement.

I wish to thank the members of the physics department for making my time here enjoyable - Seamus, Eanna, Mossy, Jiang Xi, Colm, Nicky, Daragh, Ruth, Ciaran, Jack, Joe, Catherine, Hooi Ling, Tom, Conor, Ricky, Mairead, Paddy, Pauric and Vincent. I sincerely wish everyone all the best in the future.

I wish to thank the many people I had the pleasure of collaborating with over the past three and a half years. I am indebted to all those who have contributed to and guided the experiments contained in this work, in particular Christy Charlton, Vladimir Gubala, Nam C.H. Le, Ruairi Monaghan, David Williams, Chanel Hayden, Evgueni Gudimenko, Yang Zhang, Samir Ketchkar, Vladimir Milosavljevic and Conor Murphy. I am very grateful to have had the chance to work with many talented and enthusiastic scientists, all of whom were very willing to share with me their skills and knowledge and answer my questions. Thanks also to everyone who has helped me prepare manuscripts, posters and talks for trips and conferences.

Finally, I wish to thank my parents for their continuous support, both financial and emotional.

Abstract

Plasma enhanced chemical vapour deposition was investigated for the deposition of bioactive surfaces which can be categorised into two functions.

The first is in biosensor applications, immunoassay biodevices have been researched considerably but significant problems remain in particular non-specific adsorption. This work demonstrates a new method of reducing the non specific adsorption on the surface of cyclo olefin polymers for use as immunoassay biodevices. PECVD deposition of a silicon oxide bonding layer followed by an acrylic acid functional layer which contains carboxylic acid functional groups on cylic olefin polymers is achieved. The deposited film exhibits low non-specific adsorption of non target analytes and increased covalent attachment of target analytes. A comprehensive characterisation of the deposition is carried out and conclusions of the mechanisms involved in creating the surface are elucidated; surfaces are analysed using a combination of quantitative and qualitative approaches. The mechanisms behind the plasma deposition of acrylic acid are investigated and methods to increase carboxylic retention on the surface are considered, in particular the influence of background gas is investigated.

The function of the second surface is in anti-fouling devices. The production of anti-fouling films is a key element for the development of biomedical materials such as medical devices and implants. Anti-fouling coatings favour the biological integration by limiting the interactions between the implants and physiological fluids. Proteins present in the blood will be the first components to become adsorbed on the surface of the biomaterial. Fibrinogen present in the blood is the major initiator of inflammatory reactions and is involved in blood clotting. By minimising fibrinogen adsorption it is possible to reduce the contribution of the biomaterial surface characteristics to thrombosis and inflammatory reactions. Here in, a method to reduce fibrinogen adsorption is discussed and a characterisation of the plasma phase used to deposit the antifouling coating is investigated and a study on the properties of the surface for antifouling is examined. Using HMDSO and oxygen 'polymer-like' and 'silica-like' surfaces can be deposited, silica-like depositions when compared to the polymer-like depositions displayed lower fibrinogen adsorption, 42% compared to 23%.

Publications

- Christy Charlton, Vladimir Gubala, Ram P. Gandhiraman, Julie Wiechecki, Nam Cao Hoai Le, **Conor Coyle**, Stephen Daniels, Brian D. MacCraith, David E. Williams. 2011. TIRF Microscopy as a Screening Method for Non-Specific Binding on Surfaces. Journal Of Colloid And Interface Science, 1, 354, pp405-409.

- **Conor Coyle**, Ram P Gandiraman, Vladimir Gubala, Nam Cao Hoai Le, Christy Charlton, Paul Swift, Stephen Daniels, David E Williams. 2011. Tetraethyl orthosilicate and acrylic acid forming robus carboxylic functionalities on plastic surfaces for Biodiagnostics. Plasma Processes and Polymers. Volume 9, Issue 1, pages 2836, January 2012 DOI: 10.1002/ppap.201100070

- Nam Cao Hoai Le, Vladimir Gubala, Ram P. Gandhiraman, **Conor Coyle**, Stephen Daniels, David E. Williams. 2010. Total internal reflection ellipsometry (TIRE) as a label-free detection technique for the monitoring of bioassays on a functionalized cyclo olefin polymer surface. Analytical And Bioanalytical Chemistry, 398, pp 1927-1936.

- Ram P. Gandhiraman, Mohan Kumar Muniyappa, Magdalena Dudek, **Conor Coyle**, Cedric Volcke, Paul Burham, Stephen Daniels, Niall Barron, Martin Clynes, David C.Cameron. 2010. Interaction of plasma deposited HMDSO based coatings with fibrinogen and human blood plasma: the c orrelation between bulk plasma, surface characteristics and biomolecule interaction. Plasma Processes And Polymers (online), 7, , pp411-421.

- Vladimir Gubala, Nam Cao Hoai Le, Ram Prasad Gandhiraman, **Conor Coyle**, Stephen Daniels, David E. Williams. 2010. Functionalization of cyclo olefin polymer substrates by plasma oxidation: Stable film containing carboxylic acid groups for capturing biorecognition elements. Colloids And Surfaces B: Biointerfaces, 81, pp 544-548.

- V. Gubala, R. P. Gandhiraman, C. Volcke, **C. Coyle**, C. Doyle, B. James, S. Daniels and D. E. Williams. 2010. Silanation of Cyclo Olefin Polymer Surfaces. Comprehensive characterization of (3- Aminopropyl) tris-ethoxysilane coatings by PECVD, Insight from the top layer into the bulk. Analyst, 135, pp 1375-1381.

Contents

List of Figures

Chapter 1

Introduction

1.1 Background

Plasma polymerisation of films used in bioapplications has been a growing area of research over the last number of decades. A large number of books and review articles have been published in the research field which have highlighted the advantages of plasma polymerisation over other for example wet chemical means due to the variety and quality of surfaces that can be formed, cheaper production costs and lower environmental impact.

The 1960s saw the first studies of surface modification using plasma assisted processes [2] which focused on protective coatings and surface activation. In the 1970s, organic polymers were treated in plasma with non-polymerisable gases, Yasuda *et al.* used nitrogen and argon plasmas to modify the surfaces of organic polymers [3, 4]. With advances in the micro technology industry [5], plasma techniques progressed from the electronics industry to non-electronics in the late 1980s and early 1990s. Several reviews and journal articles related to polymer surface modification and polymerisation have been published [6–9]. Recent developments in the field explore plasma produced surfaces to control in-vivo biological interfacial interactions and the use of plasma deposited surfaces

to retain functional groups as interfacial bonding layers for the immobilisation of specific biological species for in-vitro devices [10, 11]. It is in this field of research which this thesis concerns itself.

The plasma polymerisation of acrylic acid to produce films containing carboxylic groups has become an active area of research due to its use in biodevices [12–16]. Acrylic acid is an important monomer as it contains carboxylic acid which can be used to immobilise biomolecules (proteins, DNA and RNA) covalently using the appropriate linker chemistries [11, 17, 18]. An aim of this area of research is to develop a surface that contains a high density of COOH functionality for the covalent immobilisation of biomolecules which display a high signal to noise ratio. Additionally, for biodevices there is a need to produce a stable plasma polymerised acrylic acid coating which is resistant to washing processes which occur in biodevices. A number of groups have researched the subject of acrylic acid coatings to produce carboxylic acid functional groups; Alexander and Duc [19] found stable cross-linked polymers obtained by copolymerising a mixture of acrylic acid and 1,7-octadiene under high plasma power. They obtained a percentage coverage of COOH of less than 6% after washing. Others using the co-polymerisation method have had similar success using acrylic acid with 1,7-octadiene [20, 21]. Beck *et al.* also incorportated hexane into the deposition process with the aim of controlling the concentrations of specific surface functionalities such as carboxylic acid and amines [22]. Detomaso *et al.* [23] investigated the increase in discharge power and influence of duty cycle in a pulsed plasma for the deposition of acrylic acid, they obtained a surface containing 4% of COOH groups after washing. Sciarratta *et al.* [24] studied the stability of acrylic acid in a continuous wave and pulsed discharge, they found a maximum COOH retention of 5% after washing. Jafari *et al.* [25] used a low frequency source of 70 kHz and were able to produce COOH groups with up to 15% retention after washing. Pistillo *et al.* [26] produced highly stable COOH surfaces using mixture of ethylene and acrylic acid in rf plasma with a retention of 11-12% of COOH after washing. This is not to say other methods to produce

COOH surfaces have not proved successful; plasma treatment employing CO_2 [27–29] and CO [30] have been used to produce carboxylated surfaces but such treatments have long term stability problems relating to the retention of functionality and lower COOH coverage.

Non-specific adsorption (NSA) is a common problem associated with biosensor devices. NSA interferes with the sensing species attached to the sensor, which increases the background signal and reduces a biosensors selectivity and sensitivity. Therefore it is desirable to develop a biosensor surface that is resistant to non-specific adsorption. Polyethylene glycol (PEG), has been widely shown to improve the biological compatibility of materials, the presence of a layer of PEG on a biomaterial surface is accompanied by reductions in protein adsorption and cell and bacterial adhesion [31–36]. It is difficult to compare the non specific adsorption properties of TEOS AA as it is a novel surface. However, PEG is the most employed protein-repellent polymer. It can act as a screen between the surfaces and the cells. PEG is highly soluble in water and as such exhibits a high chain mobility.

Surface morphology is one of a number of factors that can lead to non-specific binding of biomolecules, provided the surface roughness is comparable to or larger than the size of the biomolecule to be immobilised [37–39]. Poksinski and Advicula reported that films with roughness ranging from micrometer to nanoscale ($>$ 5 nm) enhance adsorption of proteins [40, 41]. For the immobilisation of DNA and also for the ultra sensitive detection of DNA, a surface with a roughness of 5 Å has been used [42, 43].

While film properties and potential applications receive much attention in the literature, this is not the case for the fundamental processes occurring in the plasma that lead to the formation and retention of desired film properties which consequently are not well understood. Studies of acrylic acid plasma deposition are sparse with most studies involving acrylic acid focusing on the surface properties of the deposited film. An ongoing debate exists in the literature as to the polymerisation mechanisms of acrylic acid.

Hegemann *et al.* [44] recently investigated the use of macroscopic kinetics to examine the plasma polymerisation of acrylic acid but the results have since been disputed by Short *et al.* [45]. The debate has resulted in a number of responses being published by Hegemann and Short [46, 47] but no consensus has been reached and further contributions to the debate are required which this thesis does.

For in-vivo devices it is widely accepted that in the interaction of an artificial bio-material surface with a biological system, the first observable event is the adsorption of proteins to the surfaces [48] and as such the success of in-vivo implantations is dependent on surface interaction between the bio-material and the biological system. The introduction of a foreign object into the body induces an inflammatory reaction caused by the accumulation of host proteins onto the surface of the implant [49, 50]. The adsorption of fibrinogen onto a bio-material surface has been linked to thrombogenic response to implanted materials for example on heart valves, vascular stents and artificial joints [51, 52]. Hence fibrinogen adsorption has to be controlled to prevent platelet adhesion and activation through adequate tailoring of surface properties.

The surface hydrophobicity strongly influences the adsorption properties of fibrinogen [53, 54]. Surfaces of different wettability result in different biological responses [55, 56]. A number of studies on fibrinogen adsorption onto biomaterial surfaces suggest that adsorption is higher on hydrophobic surfaces than hydrophilic surfaces [57–60]. Additionally, Ortega-Vinuesa *et al.* [53] showed that fibrinogen adsorption measurements carried out on hydrophobic methylated silica and hydrophilic silica showed that the hydrophobic methylated silica adsorbs more than the hydrophilic silica. Thus by tailoring the surface characteristics of the implant, through manipulation of the plasma deposition process, the adsorption of fibrinogen can be minimised.

A commonly used technique for surface modification is plasma enhanced chemical vapour deposition (PECVD). This is a one-step film-growth method which draws on

the chemistry of free-radical chain-growth polymerisation [1]. The use of PECVD is well established in the production of thin film polymeric materials [61–63] and allows the production of thin films with tailorable surface properties which importantly do not affect the bulk properties of the substrate [64, 65]. Plasma polymerisation is now employed in the production of biosensors and development of other biodevices, attracting considerable interest in medical diagnosis [66–68].

Rapid and sensitive detection of a specific biomolecule is critical to the success of any biosensor [69]. A biosensor consists of a biological recognition element, a transducer and a signal output system. Biological recognition elements are attached to the surface of the transducers and are used to preferentially select target analytes, resulting in a physical or chemical change, this change is then converted by the transducer into a quantifiable signal.

The signal can be in the form of a change in optical or electrochemical properties, piezoelectric, magnetic or other measurements. Other signal systems depend on labelling for the detection of the target species [68, 70, 71]. Many methods rely on the immobilisation of single-stranded oligonucleotides, i.e. DNA probes, onto sensor surfaces as the recognition elements, and the subsequent hybridisation of the surface attached probes with the complementary DNA target from a solution.

1.2 Radio Frequency Capacitively Coupled Plasma

Plasmas can be produced by a variety of methods [72–74], however for low-temperature plasma processing, capacitive and inductive radio-frequency (rf) power sources are predominantly used [61] as they can coat insulating materials, easy to replicate and can produce at an industrial scale. In both cases, a range of frequencies can be used but typically a frequency of 13.56 MHz is employed.

Radio frequency capacitively coupled plasmas (rf-CCP)[75, 76] consists of two electrodes within a vacuum chamber. An rf voltage is applied between the two electrodes

resulting in excitation and ionisation of the gas with electrons being accelerated by the rf field causing a current to flow through the plasma. An important characteristic of low temperature plasma is that the electrons are not in thermodynamic equilibrium with neutrals and ions [61]. The electron temperature ($\approx$ 1 - 4 eV), is much greater than the ion and neutral gas temperatures ($\approx$ 0.05 eV) which arises from the transfer of energy from the energised electrons to the heavy particles. This key property of plasmas has the facility to produce a chemical environment, characterised by a high temperature chemistry without inducing the associated physical damage to an object immersed in the plasma. This is critical to the retention of bio-functional groups in plasma depositions.

1.3 Plasma Enhanced Chemical Vapour Deposition

Plasma deposition and treatment processes have been used for the improvement of the adhesion, spreading and proliferation of cells on the surface of materials of biomedical interest, as well as for the improvements in membrane properties such as hydrophobic and hydrophilic character, non fouling properties, transport and capability of immobilising molecules [11, 77, 78]. The production of a thin film from a gas, through a set of gas and surface chemical reactions is called chemical vapour deposition (CVD). If a plasma is used to stimulate and dissociate the feed gas, through a set of gas and surface chemical reactions, the CVD process is called plasma enhanced chemical vapour deposition (PECVD) [61, 79–83]. The gas pressure in the PECVD discharges is low with operational pressures of 0.1 to 10 Torr ($\approx$ 10 to 1300 Pa) employed. Typical plasma densities in PECVD discharges are in the range of 10^9 - 10^{11} cm^{-3} and degrees of ionisation of 10^{-7} - 10^{-4}.

PECVD can be contrasted to plasma etching with the main difference being in the etching processes, the reaction results in the formation of volatile species that leave the surface. In the case of PECVD, this reaction bonds the chemically activated species to the surface.

The PECVD technique has a number of advantages over the multi step, wet chemical methods or chemical vapour deposition (CVD); it can be used to coat a large number of substrates at the one time, it avoids direct contact with a solvent thus reducing chemical waste and it operates at essentially room temperature maintaining required functionality. Significant fragmentation of monomers (precursors) occurs in glow discharges and as a result a wide range of functional groups appear in the deposited film.

1.4 Plasma Chemistry

The application of a sufficiently high voltage causes 'breakdown' of a gas in which a self-sustaining glow discharge plasma results which consists of electrons, ions and electrically excited species. The visible glow observed when this breakdown occurs is caused by electron-ion recombination and by relaxation processes of collisionally excited gas species. The electrical power is coupled into the gas via the plasma electrons, the high-energy tail of which ionises the background gas, the degree of which can be calculated using the Saha equation [84]. The chemical activity of the gas results primarily from dissociation of the molecules into smaller species called radicals. Radicals are chemically unsaturated and therefore capable of chemical reactions at high rates; they are the species that, upon contact with a surface react to form a thin film.

The surface processes in plasmas are influenced by a number of factors; reactive particles approaching the surface, the ion flux onto the substrate and the ion energy distribution function (IEDF). Reactive particles approaching the surface are mainly determined by plasma chemistry. The electron energy distribution function (EEDF) controls the plasma chemistry and an approach to control the EEDF is via the rf power. The ion flux onto the substrate is mainly governed by the ion density. The power coupled into the plasma controls the ion density and thus the flux onto the surface. The IEDF and kinetic energy of ions striking the substrate is a crucial parameter that is key for understanding and further developing the techniques used in surface processes. The type of ions and

their kinetic energy onto the electrode surface is dependent on properties of the boundary sheath The ability to manipulate ion transport in the sheath and thus tailor the IEDF at the substrate is highly desirable and is addressed in this thesis.

1.5 Plasma Polymerisation

Plasma polymerisation has been defined as 'the formation of polymeric materials under the influence of plasma' [85]. The term plasma polymerisation is often used to indicate a PECVD process when organic precursors are used to deposit the film [1]. Until the early 1990s plasma polymerisation methods were considered processes by which organic molecules could be polymerised in a physical process to produce films with an uncontrolled chemical structure. Depending on the chemical nature of the monomer the deposited films could contain a number of groups, for example fluorine, oxygen or nitrogen, however more specific molecular structures could not be identified. The last twenty years have demonstrated that this is no longer the case and careful tuning of the plasma power, electron temperature and density can lead to tailored film deposition with specific molecular structures. Employing analytical equipment permits detailed characterisation of both the deposited surface and the plasma phase, permitting insights into the entire deposition process.

The ionisation of a molecule by collision with an energetic electron is the essential process for creating and sustaining a plasma of a monomer and is the first step of plasma polymerisation. Non-plasma polymerisation is highly dependent on the structure of the monomer. However, in plasma polymerisation, monomers and any organic compound without a polymerisable structure such as a double bond can polymerise. Plasma polymerisation takes place through several reaction steps. In the initiation stage, free radicals and atoms are produced by collisions of electrons (and to a lesser extent ions) with monomer molecules, or by dissociation of monomers adsorbed on the surface of the sample. Secondly, propagation of the reaction is the actual formation of the polymeric chain.

This can take place both in the gas phase and on the substrate film. Finally, termination can also take place in the gas phase or at the polymer surface, by similar processes as in the propagation step, but ending either with the final product or with a closed polymer chain.

Plasma polymerisation allows films to be deposited on most substrates using a relatively simple one-step coating procedure. Films can be made as thin as desired, are mechanically and chemically stable because of their highly branched and cross linked structure and they can be tailored to accept a large number of biological components such as proteins, antibodies, viruses, cells, and enzymes, all of which contain amine, carboxylate, and/or thiol groups. [86]. Additionally, plasma polymerised surfaces have favourable environmental and economical advantages as compared to other processing methods [87]. These advantages have resulted in the rapid development of plasma technology during the past decades, for applications ranging from adhesion to composite materials and protective coatings [88–90].

1.5.1 Mechanisms of Plasma Polymerisation

The mechanisms that lead to the formation of the plasma polymerised films still remain poorly understood. Yasuda [1] described plasma polymerisation as a rapid step-growth polymerisation mechanism. The scheme put forward by Yasuda and shown in Fig. 1.1 is a general one, and is not intended to cover the entire range of conditions under which plasma polymerised deposits form. However, in the absence of other schemes, it is widely quoted [91–93]. There are two parallel cycles in the scheme, the reactive species are denoted here as monofunctional ($M_i^\bullet$), or difunctional ($^\bullet M_k^\bullet$) free radicals, but other activated species should also be considered in the reaction mechanism [85]. This radical can combine with a neutral species, to produce a further larger radical ($M_i^\bullet + M \rightarrow M_i\text{-}M^\bullet$), which reacts with another radical to produce a neutral species ($M_i^\bullet + M_j^\bullet \rightarrow M_{i+j}$). The neutral species can be reactivated in the plasma. The second difunctional

radical can react with a neutral species to yield a larger difunctional species ($^{\bullet}M_k^{\bullet}$ + M $\rightarrow$ $^{\bullet}M_k$-M$^{\bullet}$) or with another difunctional species ($^{\bullet}M_k^{\bullet}$ + $^{\bullet}M_j^{\bullet}$ $\rightarrow$ $^{\bullet}M_{k+j}^{\bullet}$). The cycles cross-over where a difunctional species reacts with a monofunctional species ($^{\bullet}M_k^{\bullet}$ + $M_i^{\bullet}$ $\rightarrow$ $M_{i+k}^{\bullet}$). This scheme implies that plasma-phase reactions are non-specific and that a wide range of new compounds may form in the plasma.

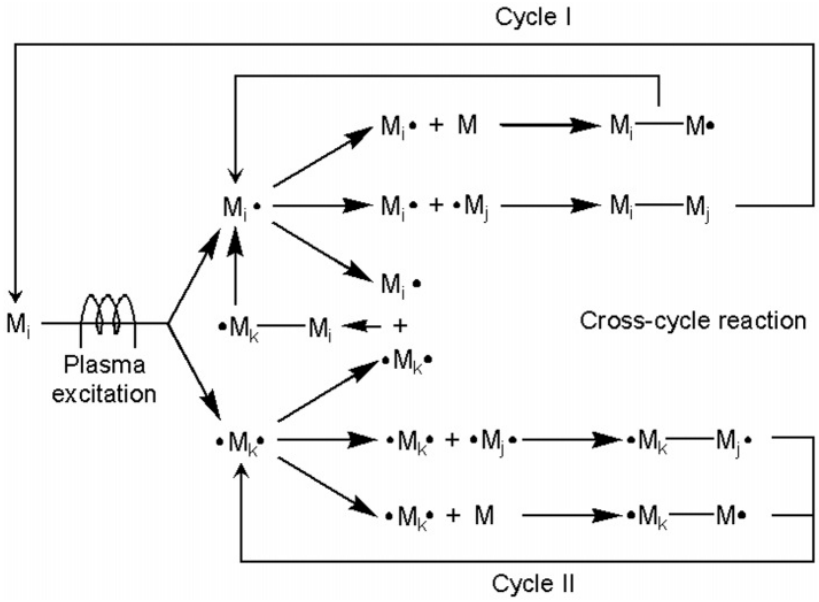

Figure 1.1: Schematic diagram of the rapid step-growth mechanism of plasma polymerisation [1].

1.6 Biosensors

An ideal immunoassay biosensor surface has a high specific binding and adhesion of target material, stability and resistance against washing steps and regeneration conditions such as hydrophobic recovery. Such a surface would possess, with respect to sensitivity in fluorescence based detection devices, the ability to tune the non-specific binding of the non-analyte components of the sample, resulting in a decrease in the background (non-specific) response and an increase of the signal to noise ratio [94, 95]. A better signal to

noise ratio offers better sensitivity in such devices and permits detection of diseases at lower concentrations and earlier stages in its growth.

Creating a biosensor surface that has long-term stability, high reactivity towards a particular molecule without binding non-specific constituents and which is inexpensive and easy to manufacture in a high-throughput industrial process are some of the challenges that need to be addressed.

The substrate used in biosensors is important and considerable effort has been invested in the production of new class of thermoplastic polymer, cyclo olefin polymer (COP) for point-of-care diagnostic applications [96, 97]. Such polymers are of great interest because of their favourable properties, such as low autofluorescence, optical clarity, resistance to organic solvents, low water uptake and easy machinability [98, 99]. Zeonor 1060R is a type of COP that includes these desirable properties while providing a cost effective platform for carrying out bioassays (or biosensors) in disposable biodiagnostic chips. The bioassays depend on surface-bound specific receptors, which must be efficiently immobilised in their active form. COPs consist of unreactive hydrocarbons and thus possess no native groups amenable for specific reactions with the capture elements. Therefore, in order to enable covalent attachment of biomolecules, such as antibodies and oligonucleotides, the COP surface needs to be functionalised. A number of methods have been described for this [1, 100].

COP shows light transparency in near-UV and visible light regions of the electromagnetic spectrum, it is for this reason that COP is used in fluorescent based bioimmunosassays. To investigate whether the film deposition process altered the optical transmission properties of the polymer, a COP sample was measured before and after film depositions using a UV-Vis spectrophotometer.

1.7 In-vivo Implantations

The success of in-vivo implantations is dependent on surface interaction between an implant and the biological system. The introduction of a foreign object into the body induces an inflammatory reaction caused by the accumulation of host proteins onto the surface of the implant [49, 50]. The modification of implants surface has been researched extensively in the literature [101, 102]. Studies have shown that fibrinogen is the major initiator of inflammatory response and is involved in blood clotting through the activation of platelets resulting in thrombosis [51]. Hence fibrinogen adsorption has to be controlled to prevent platelet adhesion and activation through adequate tailoring of surface properties. Studies have shown that fibrinogen adsorption is higher on hydrophobic surfaces than hydrophilic surfaces [58, 60]. Thus, by tailoring the surface characteristics of the implant the adsorption of fibrinogen can be minimised. This thesis addresses this subject by controlling the plasma environment to illicit specific properties on the substrate surface.

Fibrinogen is a globular protein with a molecular weight of 340 kDa and dimensions of 450 $\times$ 90 $\times$ 90 Å [103]. It is present in blood plasma at a concentration of about 3 mg/mL. As the precursor of fibrin it plays a major role in coagulation. Thrombin cleaves fibrinogen to allow fibrin formation, fibrin forms a network in which blood cells are trapped to form a clot [104].

1.8 Thesis Structure

The research described in this thesis deals with the surface modification of substrates by plasma polymerisation. A characterisation of the plasma is performed, which leads to better understanding of the deposited film surface behaviour and offers a method of controlling surface properties. One part of this work is directed towards the functionalisation of materials with carboxylic acid groups through the plasma polymerisation of acrylic acid. Thin films bearing carboxylic acid groups are of great interest for many ap-

plications because they are known to influence protein adsorption and cell adhesion and provide sites for the covalent immobilisation of biomolecules in immunoassay biodevices. Non specific adsorption is a problem associated with immunoassay biodevices and a novel method to reduce this effect is demonstrated through the incorporation of TEOS as a bonding layer to the acrylic acid deposition. For in-vivo devices fibrinogen is recognised as an initiator of inflammatory responses in a biological system and an investigation using HMDSO is carried out to mimimise it's adsorption and understand the plasma phase that leads to the plasma deposited anti-fouling coating.

In *Chapter 2* a description of the experimental arrangements are given. An introduction to the characterisation tools and materials used for the analysis of the plasma deposited films and plasma phase discussed in this thesis is provided. Surface sensitive techniques such as total internal reflection fluorescence microscopy and total internal reflection ellipsometry are introduced. The principles of a retarding field energy analyser for plasma phase investigations of ion energy distributions are presented.

The synthesis and characterisation of carboxylic acid functionalised on substrates of COP are discussed in *Chapter 3*. A plasma deposited surface that exhibits high signal to noise ratio made using the sequential deposition of tetraethyloxysilane and acrylic acid is described.

In *Chapter 4* the plasma characterisation and investigation of acrylic acid plasma under various plasma conditions that leads to carboxy retention in depositions is discussed, growth mechanisms are elucidated and influence of background gas is investigated. A major part of this section focuses on the functional group tuning of surfaces by variation of plasma parameters such as the input power and background gas

Chapter 5 describes the development of an anti-fouling surface for in-vivo implantations using hexamethyldisiloxane. The surface is characterised using a number of techniques such as contact angle goinometry, FT-IR spectroscopy, SIMS and an enzyme immunosorbent assay.

Chapter 6 is the thesis conclusion, ideas of future work and areas of research are presented.

Chapter 2

Experimental

2.1 Introduction

No one diagnostic tool can fulfill all of the needs to completey characterise the various deposited films and process plasma behaviour. Consequently, the work in this thesis relies on a combination of techniques which offers a broader characterisation of plasma processes and surface interaction. There are a number of well established plasma and surface analytical techniques that are widely used for the study of plasma-deposited films; contact angle goiniometry (CA), X-ray photoelectron spectroscopy (XPS or ESCA), attenuated total reflection Fourier transform-infra red spectroscopy (ATR-FTIR), UV/Vis spectrophotometry, secondary ion mass spectrometry (SIMS), atomic force microscopy (AFM) [105–109]. Langmuir probe (LP), mass spectrometry (MS) and optical emission spectroscopy (OES) are used to study the plasma phase [110–112]. These analytical techniques have been employed and reported widely and will not be discussed at length in this work. Details of specific equipment and experimental parameters are given in each result chapter where appropriate. Some equipment employed in this work will be briefly discussed here.

2.1.1 The Deposition Plasma Chamber

The thin films presented in this thesis were deposited using an industrial PECVD system (Europlasma CD300, Belgium). The deposition system is shown in Fig. 2.1. The power source is a 13.56 MHz radio frequency source with automatic power matching. The power source is capacitively coupled to the upper electrode and the lower electrode is grounded. A floating substrate holder is midway between the upper and lower electrodes, the film depositions were performed on the floating substrate holder. The vacuum chamber is made of aluminium and has dimensions 30 cm $\times$ 30 cm $\times$ 30 cm. An Edwards EH mechanical booster pump backed by an Edwards E1M40 rotary pump is used to pump down the chamber. The chamber has a base pressure of approximately 15 mTorr (2.0 Pa). The chamber pressure is measured using a MKS baratron pirani gauge. The flow of monomer vapour into the chamber is regulated through a manually operated needle valve. The monomer flow rate is monitored before and after the deposition to ensure the flow is constant. Oxygen and argon flow rates were regulated by mass flow controllers connected to a shower head at the top of the chamber. Side ports on the chamber permit probe access to the plasma.

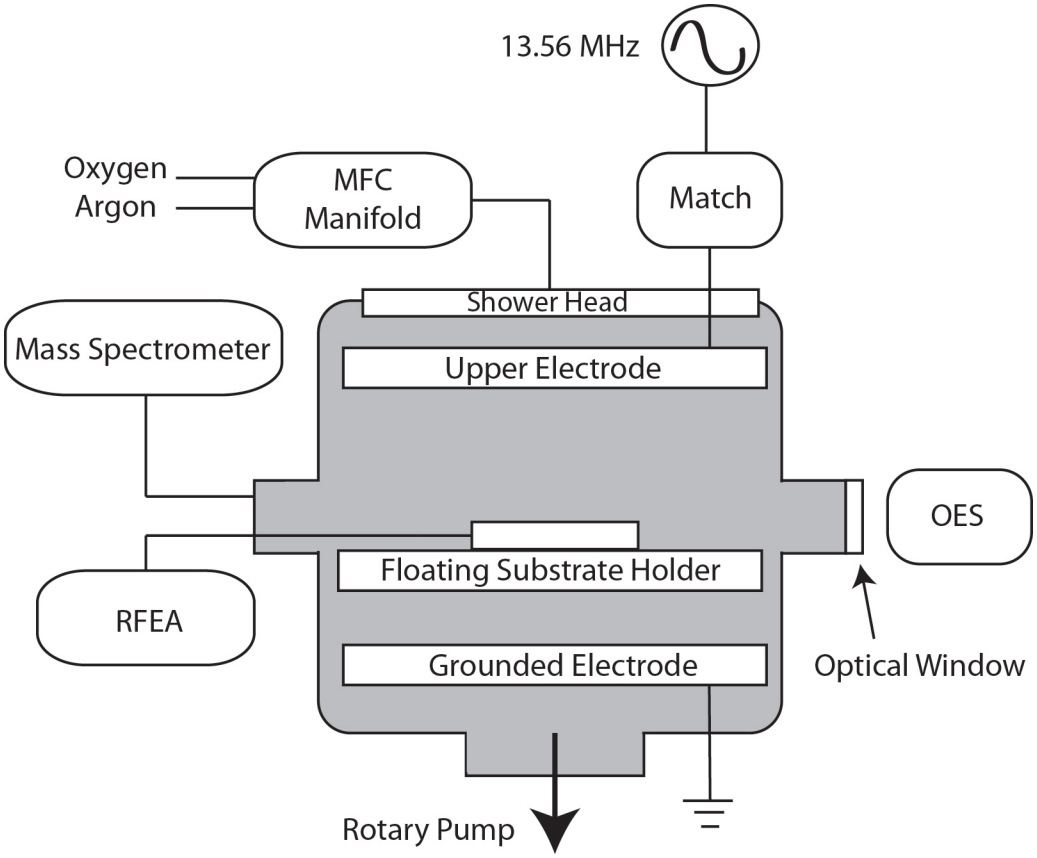

Figure 2.1: Schematic of PECVD chamber. Probe and momomer gas access via side ports.

2.1.2 Total Internal Reflection Ellipsometry

TIRE is very convenient for different sensing applications in both gaseous and liquid media, as well as for thin film characterisation. This work employs the TIRE method for the study of DNA hybridisation. Total internal reflection ellipsometry (TIRE) is a combination of the spectroscopic ellipsometry with surface plasmon resonance (SPR) [40]. TIRE is a useful and fast method to test the attachement of particles to a surface. A sharp minimum in the reflected light intensity occurs when the light is resonantly coupled to the surface plasmon modes. At this point, the energy and the momentum between the incoming photons and the surface plasmon waves are matched and the reflectivity goes to a minimum. TIRE is also used to test the stability of the the attached particles in long exposure time in a buffer envioronemt. TIRE shows much higher sensitivity to small changes in optical parameters, thickness and refractive index of thin films, as compared to both traditional external reflection ellipsometry and SPR. TIRE is convenient for different sensing applications in both gases and liquids, as well as for thin film characterisation. A schematic of a TIRE system is shown in Fig. 2.2.

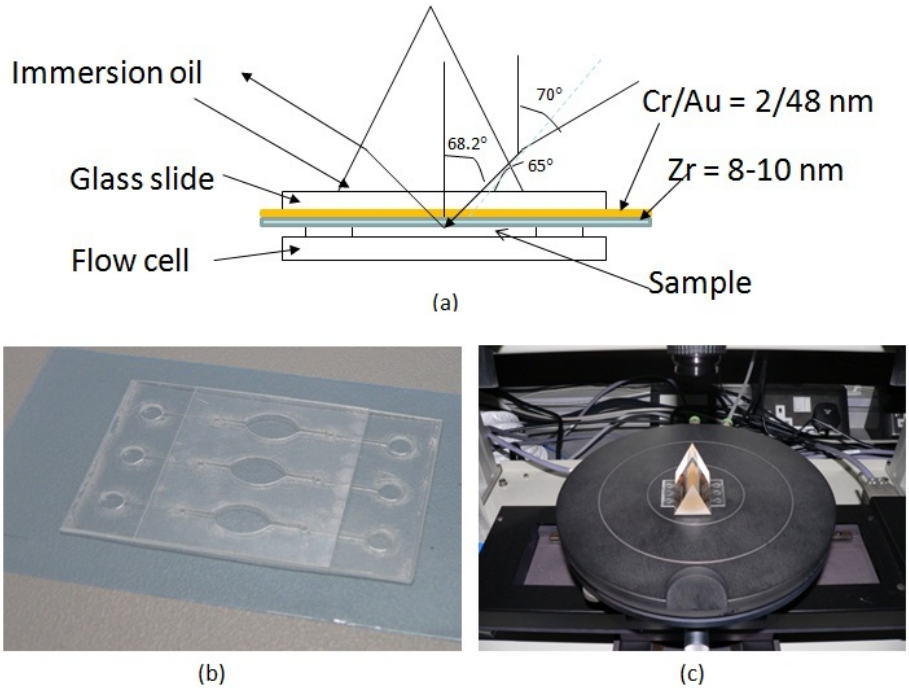

Figure 2.2: (a) Schematic view of the TIRE system. It shows the index-matching liquid inserted between the prism and substrate and the metal layer deposited on the other side of the substrate. (b) Flow cell with three wells. (c) Image of TIRE setup.

2.1.3 Total Internal Reflection Flourescence Microscopy

Total internal reflection flourescence microscopy (TIRF or TIRFM) [113] uses light that propagates through a medium which meets an interface with a second medium of lower refractive index. Total internal relfection occurs at all angles of incidence that are greater than a critical angle. The incident beam creates an evanescent electromagnetic field that penetrates into the second medium and decays exponentially with the distance from the interface.

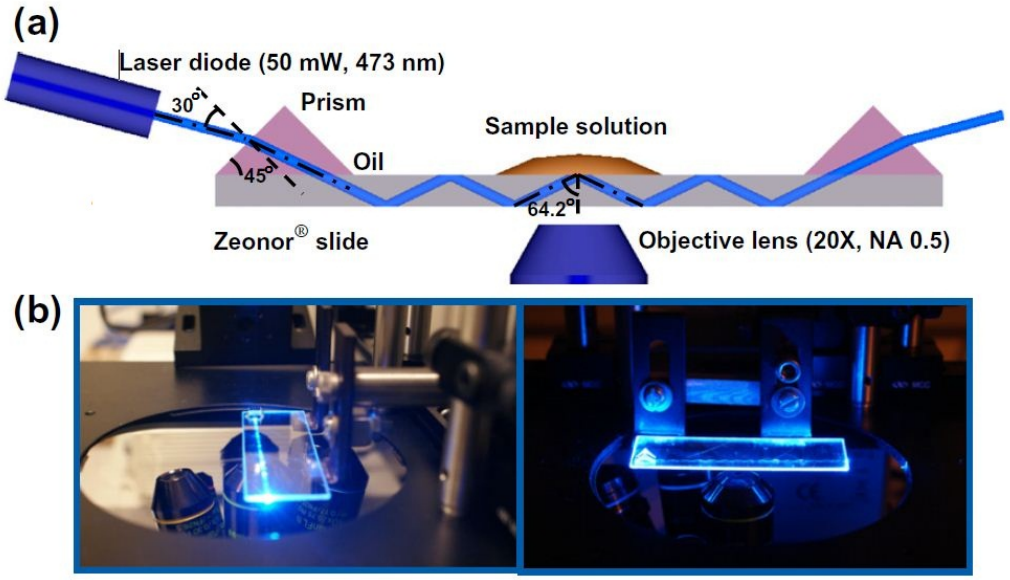

Figure 2.3: (a) Schematic of TIRF setup (b) Images of TIRF setup

TIRF is a useful and fast method to compare non-specific adsorption of detection molecules on different surfaces. This method allows rapid screening of surfaces to determine their ability to prevent non-specific binding. Figure 2.3 illustrates how light is coupled to the substrate to allow for characterisation of surface coatings by counting the adsorbed particles on the substrate. TIRF allows surface-molecule interactions to be investigated, as it excites only particles within the evanescent field of the excitation light, providing surface specificity and improving signal to noise compared with conventional

microscopy.

2.1.4 Retarding Field Energy Analyser (RFEA)

Of particular importance to plasma deposition of functional films is the rate at which ions bombard the substrate surface and the energy they have at impact. Specifically, the ion current flux and ion energy often determine the characterisitics of the plasma process. The ion energy analyser used in this study is a planar gridded energy analyser (Semion, Impedans, Dublin, Ireland) [114], which is mounted on the floating electrode in the chamber as shown in Fig. 2.4. The RFEA probe is designed to sit on the floating substrate holder in place of the substrate with the signal cables fed through the reactor side port. The analyser is 60.0 mm in diameter and 3.0 mm thick, it consists of an array of 800 μm holes over an area of 1.0 cm^2. A series of three grids are used; the first grid is maintained at the electrode floating potential, the second grid is swept to provide the ion retarding potential, only ions with energies greater than the voltage on the second grid will be detected. The third grid is biased negative with respect to the first grid so as to repel electrons that may enter the analyser and to inhibit secondary electron emission from the collector. A collector plate is used to attract any ions passing through the second grid. The ion energy distribution is obtained by taking the derivative of the collector current versus retarding potential. Gahan *et al.* have published a full description of the RFEA [115].

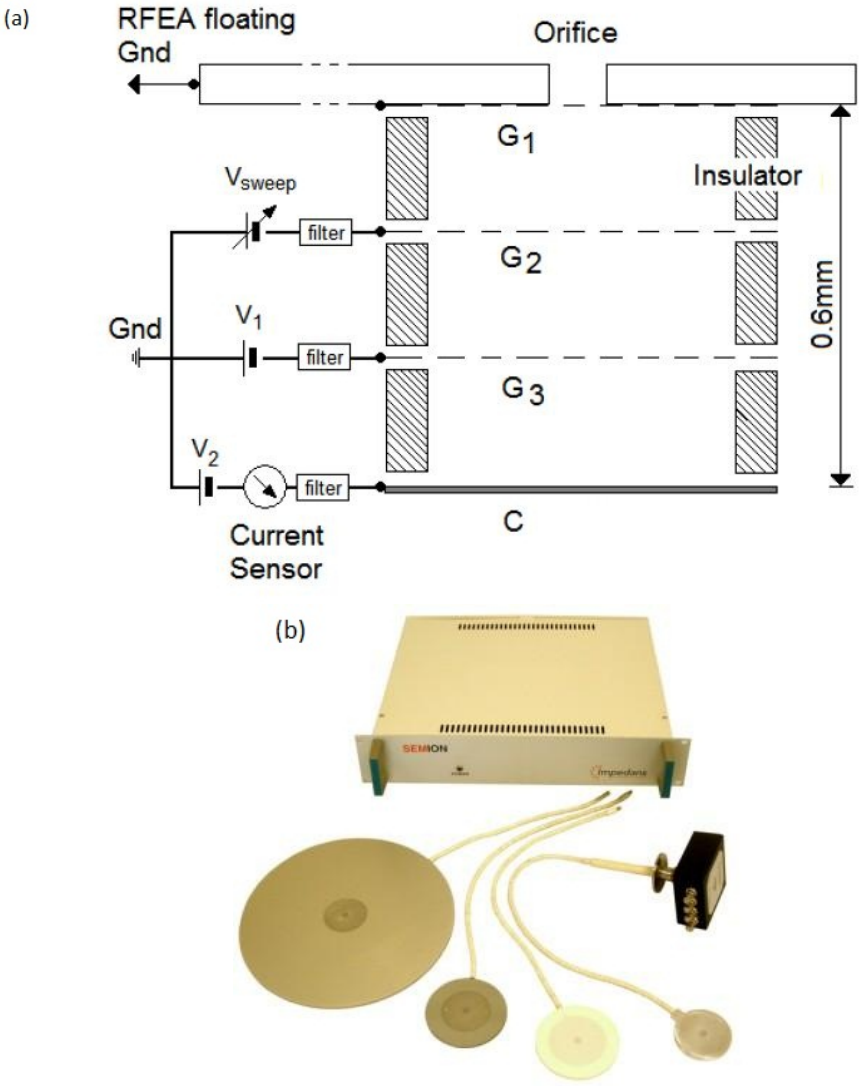

Figure 2.4: (a)Cross section of retarding field analyser. (b) Image of RFEA probe. Images taken with approval from Imdeans Ltd.

2.2 Materials and Substrates

Specific details of materials and substrates are described in the experimental section of each relevant chapter. The monomers used in this work are acrylic acid (AA), tetraethyl orthosilicate (TEOS), hexamethyldisiloxane (HMDSO), which were purchased from Sigma-Aldrich, Germany. Their chemical structures are shown in Fig. 2.5.

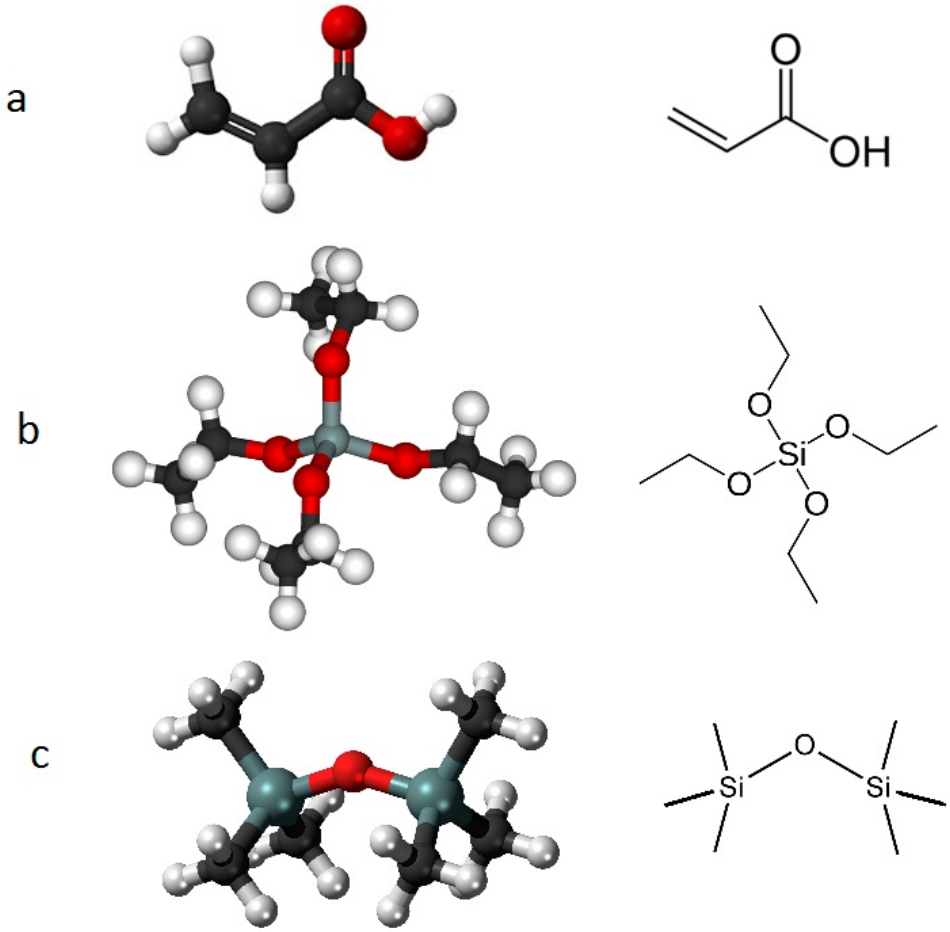

Figure 2.5: Three major monomers used in this work and their chemical structure; (a) acrylic acid (b) TEOS (c) HMDSO

2.2.1 EDC and NHS

1-Ethyl-3-[3-dimethylaminopropyl]carbodiimide hydrochloride (EDC) and sulfo-NHS were purchased from Sigma-Aldrich, Germany. EDC is a crosslinking agent used to couple carboxyl groups to amines. The activation and cross linking with EDC and NHS is shown in Fig. 2.6. EDC reacts with a carboxyl to form an amine-reactive O-acylisourea intermediate. If this intermediate does not encounter an amine, it will result in hydrolysis and return to the carboxyl state. But with the addition of N-hydroxysuccinimide (NHS), EDC can be used to convert carboxyl groups to amine-reactive NHS esters thus stabilising the process.

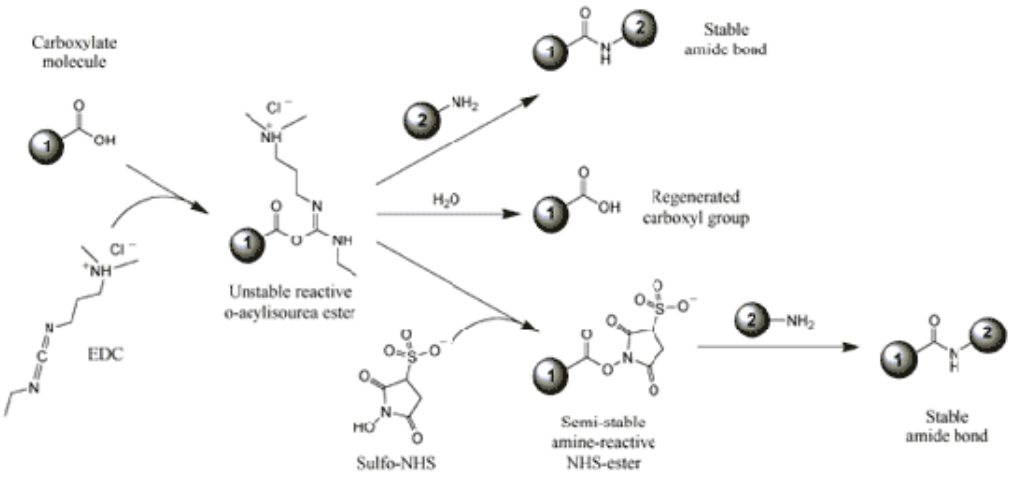

Figure 2.6: Carboxylic attachment with amine group using EDC and NHS

2.2.2 Substrates

Considerable effort has been invested in a production of a new class of thermoplastic polymer, cyclo olefin polymer (COP), for point-of-care diagnostic applications [96, 97]. Such polymers are of great interest because of their favourable properties for biodevices, such as low autofluoescence, optical clarity, resistance to organic solvents, low water up-

take and easy machinability [98, 99]. Zeonor 1060R is a type of COP that includes these desirable properties while providing a cost effective platform for carrying out bioassays (or biosensors) in disposable biodiagnostic chips and is the COP substrate used in this thesis. The bioassays depend on surface-bound specific receptors, which must be efficiently immobilised in their active form. COPs consist almost exclusively of unreactive hydrocarbons and thus possess no native groups amenable for specific reaction with the capture elements. Therefore, in order to enable covalent attachment of biomolecules, such as antibodies and oligonucleotides, the COP surface needs to be functionalised.

QMT epoxy substrates are widely used for covalent immobilisation of oligonucleotides and DNA. Additionally amino-modifications of the nucleic acids are not required. The hydrophobic surface allows small spot diameters (100 to 130 μm) to create high density arrays. The surface chemistry is very stable and remains active even during long spotting runs.

For in-vivo applications 316L medical grade stainless steel is used as it is recognised as a safe substrate within the human body. For this thesis 316L steel substrates were used for fibrinogen adsorption measurements. The steel is widely used for medical applications including; implants, in-vivo pins and screws and orthopaedic implants like total hip and knee replacements [116].

Chapter 3

Carboxylic Acid Functionalised Surface Demonstrating a High Signal to Noise Ratio in Bioassays

3.1 Introduction

In the work presented in this chapter surfaces of cyclo olefin polymer (COP) substrates were modified using PECVD to produce carboxylic groups for applications in biosensors. A technique for the modification of substrates using tetraethyl orthosilicate (TEOS) and acrylic acid (AA) as monomer sources to produce a polymer-like coating is presented. A comparison of the TEOS and AA film with an AA deposition is given. Polymerisation of AA to form carboxylic films on various substrates has been studied extensively [14, 117, 118] and while this is of interest in itself and the research area remains active, the novel

aspect of the work presented in this chapter is the introduction of a silicon oxide bonding layer onto the COP substrate followed by an AA functional layer deposition. Although the adhesion of the AA polymer by itself to a COP substrate is sufficient for most biosensor applications the plasma polymerised AA with TEOS exhibits high non-specific binding as well as other desirable characteristics sought for immunoassay biosensors.

Other groups have demonstrated that the combination of precursors with two distinct functions is an effective approach to increase the film stability and reactivity and consequently to gain better control over non-specific binding [119, 120]. Hence the use of TEOS as an adhesion and network building layer was attempted with the sequential deposition of AA. Upon activation with 1-Ethyl-3-[3-dimethylaminopropyl] carbodiimide hydrochloride (EDC) and N-hydroxysuccinimide (NHS), the -COOH group can be used to perform an aminolysis reaction with free amines. Such groups are abundant in proteins and can be easily incorporated into the $5'$ or $3'$ end of oligonucleotides. The low acid dissociation constant (pK_a) values of carboxylic acid (pK_a = 4.0 - 4.2) means that under standard physiological conditions, the equilibrium is shifted towards its deprotonated species, hence providing significant negative charge on the surface. Charged films with low zeta potential can take advantage of electrostatic repulsions between the surface groups and other negatively charged molecules, such as DNA thus effectively reducing the non-specific binding.

The surface modification procedure was characterised by contact angle measurement to monitor changes in wettability and ageing effects, fluorescence microscopy to study the nonspecific binding, X-ray photoelectron spectroscopy (XPS) and Fourier transform-infrared spectroscopy (FT-IR) to determine the chemical composition and the nature of chemical bonding present in the film, atomic force microscopy (AFM) for surface morphology and total internal reflection ellipsometry (TIRE) to investigate the stability of the coatings upon contact with aqueous buffer and for studying biomolecule immobilisation and total internal reflection fluorometry (TIRF) to demonstrate low non-specific binding

of sample target. SIMS was employed to investigate the interfacial characteristics of the TEOS & AA film. Measurements were taken using a UV/Vis spectrometer to characterise optical transmission of depositions on COP substrates to confirm the suitability of the deposited film substrate for labelled biosensor devices.

3.2 Experimental

COP slides (Zeonor © 1060R) 75 × 25 mm^2 were supplied by Åmic AB (Uppsala, Sweden). Acrylic Acid ($C_3H_4O_2$) of 99% purity and tetraethyl orthosilicate ($C_8H_{20}O_4Si$) of 99.999% purity, N-(3-dimethylaminopropyl)-N' -ethylcarbondiimide hydrochloride (EDC) sulfo, N-hydroxysuccinimide (NHS) and xylene were purchased from Sigma-Aldrich. All chemicals were used as received without further purification. Amino modified single stranded DNA (19 bp), one base pair corresponds to around 3.4 Å of length along the strand, with and without Cy5 label was purchased from Eurofins MWG Operon (Ebersberg, Germany).

Depositions were carried out in a plasma chamber described in section 2.1.1. Particular to this operation, oxygen and argon pretreatment both had flow rates of 100 sccm. During deposition the oxygen flow was stopped and the argon flow rate was reduced to 50 sccm. The flow of TEOS & AA into the chamber were regulated through a manually operated needle valve. The operating pressure during deposition was 80 mTorr (13.3 Pa), TEOS was flowed in until pressure reached 100 mTorr, after TEOS deposition stopped, AA was flowed in until pressure reached 100 mTorr, thus partial pressures of TEOS and AA were 20 mTorr. The monomer flow rate through the needle valve was carefully controlled to maintain the operating pressure at 100 mTorr. The rf power into the system was 250 W during the pretreatment for 150 s and then reduced to 10 W during the 30 s deposition time.

Contact angles were measured with a contact angle goniometer (First Ten Angstroms FTA200) using a high purity HPLC grade water (Sigma Aldrich) as the probe liquid.

Surface morphology and roughness on plain COP, TEOS-coated COP, AA-coated COP and TEOS & AA-coated COP surfaces were measured with a Digital Instruments BioScopeTM II (Veeco Instruments Inc., Plainview, NY, USA) in tapping mode in ambient conditions. Silicon cantilevers with integrated tips (TESP, Veeco Probes, Camarillo, CA, USA) and with resonant frequencies between 327 and 349 kHz, and with $\approx$ 30 N/m spring constant were used. For each surface, three locations with surface area of 2.0 $\times$ 2.0 μm^2 each were imaged at a rate of 0.5 Hz. Research NanoScope 7.30 software (Veeco Instruments Inc., Plainview, NY, USA) was used to analyse the measured data and estimate the RMS roughness.

The XPS data[1] was collected on a Kratos Axis UltraDLD equipped with a hemispherical electron energy analyser. Spectra were excited using monochromatic Al Kα X-rays (1486.69 eV) with the X-ray source operating at 100 W. This instrument illuminates a large area on the surface and a hybrid magnetic and electrostatic lenses collects photoelectrons from a desired location on the surface. In this case, the analysis area was a 220 $\times$ 220 μm^2 spot. The measurements were carried out in normal emission geometry. A charge neutralisation system was used to alleviate sample charge build up, resulting in a shift of approximately 3 eV to lower binding energy. Survey scans were collected with 160 eV pass energy, while core level scans were collected with a pass energy of 20 eV. The analysis chamber was at pressures 10^{-9} Torr throughout the data collection. Data analysis was performed using CasaXPS. Shirley backgrounds were used in the peak fitting. Quantification of survey scans utilised relative sensitivity factors supplied with the instrument. Core level data were fitted using Gaussian-Lorentzian peaks. The binding energy scale was corrected for the neutraliser shift by using the C1s signal from saturated hydrocarbon at 285.0 eV as an internal standard.

Fourier transform infrared spectroscopy spectra were recorded on a Perkin Elmer - Spectrum GX FTIR used in the attenuated total reflection mode (ATR-FTIR). The

[1]XPS data was collected by technicians in New Zealand, as access to XPS system that could operate with charge build up on samples was not available locally.

system uses a ZnSe crystal which is used in contact with the sample. The detector and sample chamber were purged with nitrogen gas during measurements. For all data presented, unmodified COP slides were used as background. Scans were collected between 4000 and 400 cm^{-1} wavenumber range, with a 32 scan average per image. number range, with a 32 scan average per image.

Fluorescence spectroscopy was carried out using a Perkin Elmer LS 45 fluorescence spectrometer. Fluorescence images were analysed using the ScanArray Gx software (Perkin Elmer). Carboxylic acid coated COP slides were scanned at 635 nm, the absorbance wavelength of Cy5, using a laser activated confocal scanner (ScanArray Gx; Perkin Elmer) at a 20 μm resolution.

For TIRE measurements a COP slide was cut into small pieces and dissolved in xylene at 0.25 wt% w/v to make the COP solution. The COP solution was then spin coated onto a gold coated glass slide at 1300 rpm for 30.0 s with spin up time in 2.0 s and then at 2000 rpm for 5.0 s with spin down in 2.0 s. The xylene solvent was evaporated at ambient conditions, leaving a COP layer of approximately 23 nm in thickness, as measured by a spectroscopic ellipsometer (UVISEL, JobinYvon Horiba, France). The substrate was subsequently introduced to an oxygen and argon plasma treatment for 60.0 s, during which its thickness was reduced to approximately 10 nm which was measured using the same ellipsometer. TEOS and AA were then deposited onto the substrate in the same PECVD chamber with the same conditions as the other COP substrates.

The substrate was then assembled into a specialised flow-cell with a BK7 prism for TIRE measurements with the UVISEL spectroscopic ellipsometer. The flowcell contains three wells, labelled '1', '2', '3', on the same TEOS and acrylic acid functionalised COP surface for three TIRE measurements at angle of incidence of 70° with wavelengths ranging from 500 to 900 nm. A stability test was performed of the TEOS and AA surface under continuous immersion in PBS buffer (pH 7.0) in well 1. Ψ and Δ spectra were measured after PBS buffer was pumped in and replaced in well 1 after 1.0 hr and 2.0 hr. The

baseline Ψ and Δ spectra were also measured for the TEOS and AA surface in well 2 and 3 filled with PBS buffer before DNA attachment. 30 µls of aminated 19 bp single strand DNA (ssDNA) 10×10^{-6}M in MES buffer (pH 8.0) without EDC NHS and with 50 mM EDC NHS were then pumped in well 2 and 3, respectively, and allowed to react with the TEOS and AA surface for 1.0 hr. Ψ and Δ spectra were recorded for well 2 and 3 after 1.0 hr of reaction. Ψ and Δ spectra were recorded for well 2 and 3 before they were rinsed thoroughly with PBS. PsiDelta 2 software (Jobin Yvon Horiba, France) was used for fitting the data from the measured Ψ and Δ spectra from TIRE to obtain the thickness of the ssDNA layers.

Gold-coated standard glass slides (Ti/Au 2 nm/48 nm, 26 mm×76 mm, 1 mm thick) were purchased from Phasis Sarl (Geneva, Switzerland). N-(3-Dimethylaminopropyl)-N'-ethylcarbondiimide hydrochloride (EDC), N-hydroxysuccinimide (NHS) and xylene were purchased from Sigma-Aldrich (Dublin, Ireland). All chemicals were used as received without further purification. Amino-modified single-stranded DNAs (ssDNAs) (5'-ACG-GCA-GTG-TTT-AGC-3') (Sa19 ssDNA, 15-mer), complementary ssDNAs (5'-GCT-AAA-CAC-TGC-CGT-3') (Sa19 rev comp ssDNA, 15-mer) and non-complementary ssDNAs (5'-AAG-TTTCTT-CTA-AAC-AGA CT-3') (Sa20 non-comp ssDNA, 20-mer) were purchased from Eurofins MWG Operon (Ebersberg, Germany).

The DNA hybridisation assay was conducted in a fresh microwell after the baseline Ψ and Δ spectra of the COOH surface in PBS had been recorded. Thirty microlitres of 10^{-5} M aminated Sa19 ssDNA in 100 mM EDC in 2-(N-morpholino)ethanesulfonic acid (MES; pH 8.0) buffer was then pumped into the microwell and allowed to react for 60 min. A second set of Ψ and Δ spectra, which correspond to the registration of the binding of the capture Sa19 ssDNA, were measured after the microwell had been rinsed with 50 µl PBS. Next, 30 µl of 10^{-5} M complementary Sa19 rev comp ssDNA in hybridisation buffer (150 mM NaCl, 150 mM saline/sodium citrate buffer, pH 7.0) was pumped into the microwell and also allowed to react for 60 min before rinsing the microwell with 50 µl PBS. A

third set of Ψ and Δ spectra were then recorded, corresponding to the registration of the complementary Sa19 rev comp ssDNA to the capture Sa19 ssDNA. Also conducted were two negative control experiments in two different microwells. The first negative control experiment was conducted with mismatched Sa20 non-comp ssDNA at concentration of 10^{-5} M in the same hybridisation buffer to confirm the specificity of the captured ssDNA probes. The second negative control experiment was performed to assess the COOH surface capture efficiency of the aminated Sa19 ssDNA without EDC in the MES buffer.

TIRF analysis used a 473 nm laser with a maximum output of 50 mW (Photop Technologies Inc, Fujian, China) which was coupled to the COP slide through a BK7 prism (BRP-5, Newport, Oxfordshire, UK) which was index matched to the slide using immersion oil. Light entered the slide at an angle of 15° from horizontal giving an angle of reflection at the slide/water interface of approximately 65° from the vertical. This angle is below the critical angle of 61° causing the light to undergo total internal reflection. This setup was placed above the objective on an Olympus IX81 (Olympus, Essex, UK) inverted fluorescence microscope. A drop of fluorescent dye-doped latex particle (Kisker Biotech, Steinfurt, Germany) solution was placed on top of the slide at a location where the laser beam was being reflected from the top surface giving an evanescent field at that point. As particles interact with the surface, they enter the evanescent field and are excited, emitting fluorescence which is collected through the slide from below. The objective used was a 20×0.50 NA (UPlanFLN, Olympus, Essex, UK) giving a viewing area of 0.144 mm^2. An Olympus U-MWIBA filter blocked the laser excitation light and allowed collection of fluorescence emitted by the particles. Images were recorded every 10.0 s for 2000.0 s with a 5.0 s exposure time on an Olympus DP71 camera. Image colour was adjusted using ImageJ software to remove background noise before particles were counted using Matlab image processing software.

Secondary ion mass spectroscopic studies were carried out using a quadrupole apparatus MiniSIMS developed by Millbrook Instruments Ltd. It incorporates a gallium ion gun

for the primary beam. Ga^+ ions (6.0 keV) were focused perpendicularly to the substrate. To mitigate charging of the electrically insulating COP substrate an electron gun charge neutralisation was used for all the measurements. The operating pressure was 3.1×10^{-7} mbar.

Optical transmission measurements were carried out using a Perkin Elmer LAMBDA 850 UV/Vis spectrophotometer. Scans were collected between 1000 and 220 nm range, with a step rate of 1 nm. Unmodified COP substrates were used as background.

3.3 Results and Discussion

3.3.1 Attenuated Total Reflection Fourier Transform Infrared Spectroscopy

Two different coatings have been deposited in the FTIR study; (a) an AA coating using acrylic acid precursor in an argon plasma for 30.0 s at 14 W RF power and (b) a sequential deposition of TEOS & AA coating for 30.0 s each in argon plasma at 14 W RF power. A plasma pre-treatment of 180.0 s using argon and oxygen plasma at 250 W was used for both cases. The nature of chemical bonding present in the film was determined by Fourier-transform infrared spectroscopy used in the attenuated total reflection mode (ATR-FTIR), the spectra of which are shown in Fig. 3.1. This figure shows the absorbance spectra of four substrates; (a) a plasma treated COP substrate, (b) AA deposited on COP, (c) TEOS deposited on COP, (d) TEOS & AA deposited on COP. In all spectra, the absorption at 2850 - 2950 cm^{-1} region is the C-H stretching vibration modes of CH_2 and CH_3 from the polymer substrate. Additionally, the peak at 1453 cm^{-1} represents the wagging mode of CH_3 in the polymer backbone.

The TEOS (Fig. 3.1 c) and the TEOS & AA deposition (Fig. 3.1 d) may show two absorption peaks at 1196 cm^{-1} and 1075 cm^{-1} were both assigned to the asymmetric SiOSi vibration mode, where oxygen atoms move back and forth along the axis line of

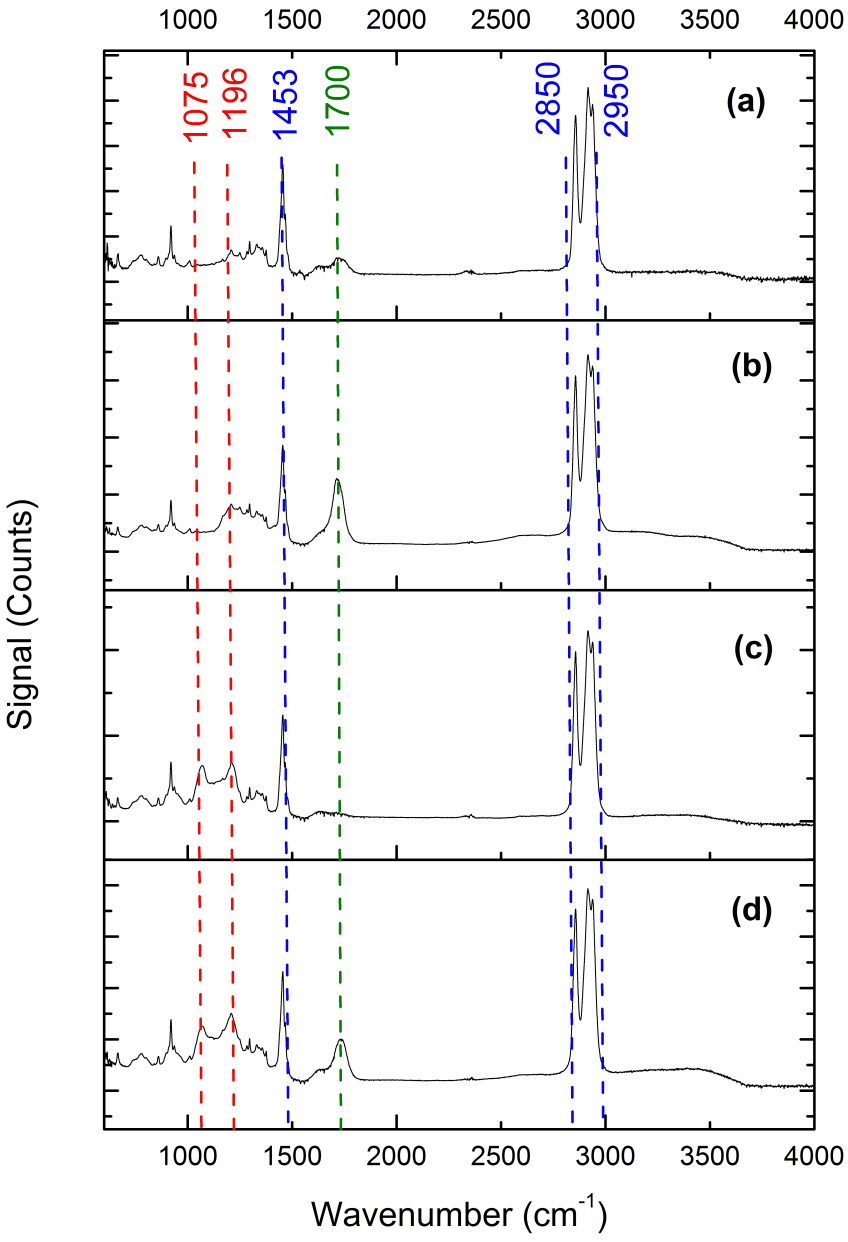

Figure 3.1: (a) Plasma treated COP with no depositions (b) AA deposition (c) TEOS deposition (d) TEOS & AA deposition. The red lines are contributions from TEOS, the green line are contribution from AA and the blue lines are contributions from the COP substrate.

the silicon atoms which have been reported in the literature [121, 122]. By comparison, these bands do not appear in the spectrum of the plasma treated COP sample or AA deposition, which suggests a successful deposition of Si-O layer.

At 1700 cm^{-1} the carbonyl (stretch) mode is visible in the AA (Fig. 3.1 b) and TEOS & AA depositions (Fig. 3.1 d), by comparison, this band did not appear in the spectrum of the TEOS deposition. A small peak is present on the plasma treated COP substrate this can be explained by the formation of the reactive species on the surface by a plasma treatment. It is possible that this could be used for the attachment of biorecognition elements. Nonetheless, films with carboxyl groups prepared by PECVD deposition have significantly higher binding capacity when compared to the plasma treated surface. It should also be noted that the reactive species on plasma treated COP surfaces are prone to degradation in air and do not show long term storage properties [123].

3.3.2 XPS

XPS survey scans are shown in Fig. 3.2 showing contributions from C1s, O1s, Si2s and Si2p. A detailed study of the C1s region revealed differences in the chemical composition of the different layers. Qualitatively, the C1s spectra for the films, shown in Fig. 3.3, are similar with one saturated hydrocarbon peak of 285.0 eV and additional peaks at higher binding energies of 286.2 eV and 289.3 eV. The 286.2 eV peak is assigned to C-O-C as well as C-OH, while the higher binding energy peak at 289.3 eV is characteristic of O-C=O [124]. It is observed that the proportion of the total C1s signal due to carboxyl peaks is higher for the TEOS & AA coating (16.4%) than for the AA coating (6.5%) for the same acrylic acid exposure time in the plasma (Table 3.1). This demonstrates that the plasma polymerisation of acrylic acid depends strongly on the nature of the interfacial layer and the presence of a siloxane intermediate layer enhances the carboxylic functionality in the coating.

Comparing the work, Mourtas et al. [125] attempted to increase the C1s peak C1s

signal of a plasma deposited AA coating deposited using a 27.12MHz RF power supply. Mourtas et al. achieved a carboxy signal of 5.3% of the C1s peak through plasma tuning they could at reach <8% which can be compared to 16.4% in this work. Furthermore Mourtas et al. attempted to reduce non specific binding of liposomes and at best were able to achieve a S/N ration in a bioassay of 4.07 compared to 12 using a TEOS underlayer in this work which is improved further with tuning of the plasma.

XPS survey spectra shown in Fig. 3.2 confirm the introduction of Si onto the surface layer by TEOS deposition by the appearance of Si2s and Si2p. The Si2p peak at 103.8 eV is attributed to SiO_2 [126, 127]. This supports the result obtained by FTIR analysis that the chemical bonding states in the film prepared using TEOS are close to those in silicon dioxide. In Fig. 3.4 black lines represent the raw data and the coloured lines were obtained by the curve-fitting calculation.

A lower intensity reading of the Si2p (and Si2s) spectra from Fig. 3.4(b) to (c) suggests that a deposited layer from AA is formed on the silicon oxide surface and thus a reduced contribution from the bonding layer is recorded.

The Si2s peak can be assigned to SiO_2, at 155.3 eV with a small contribution from elemental Si at 150.5 eV [128, 129]. The XPS analysis of the TEOS & AA sample shows that the outer layer of the deposition contains small amounts of silicon, mainly as SiO_2 but mostly acrylic acid deposition appears on the surface.

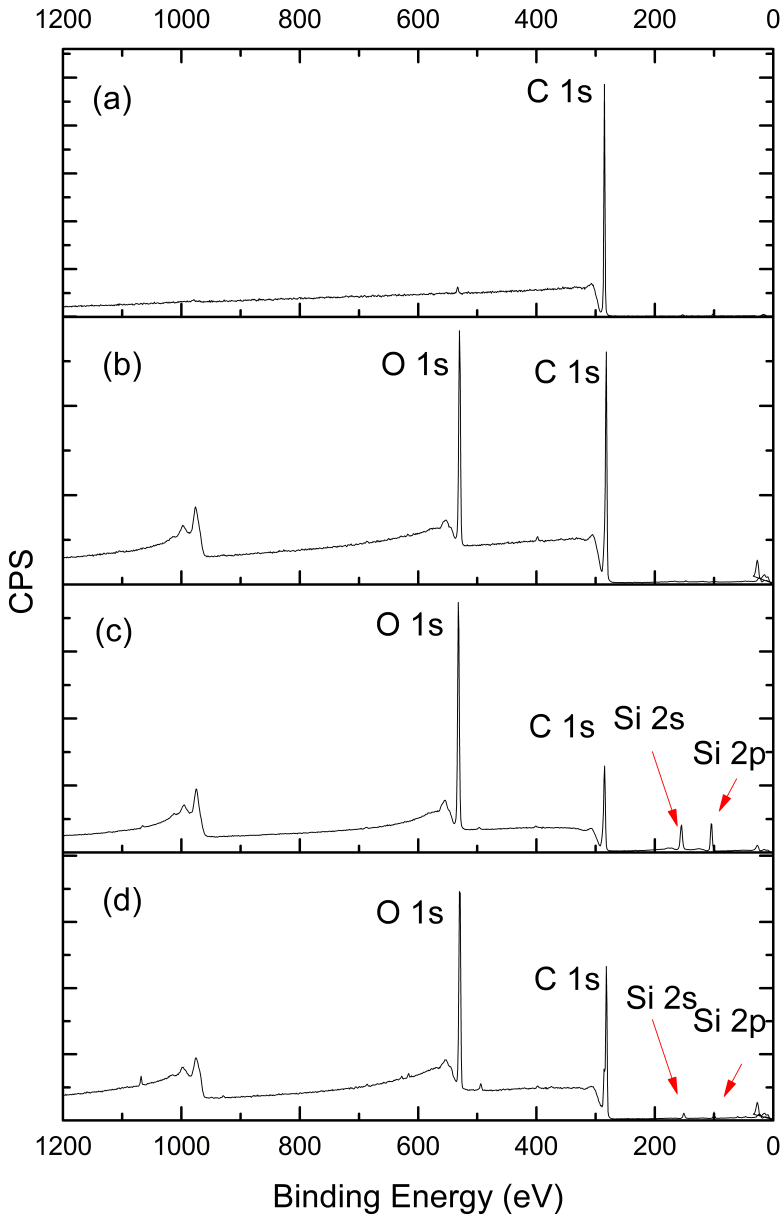

Figure 3.2: XPS survey scans collected with 160 eV pass energy using monochromatic Al Kα monochromatic X-rays (a) Untreated Zeonor (b) Acrylic acid (c) TEOS (d) TEOS & AA

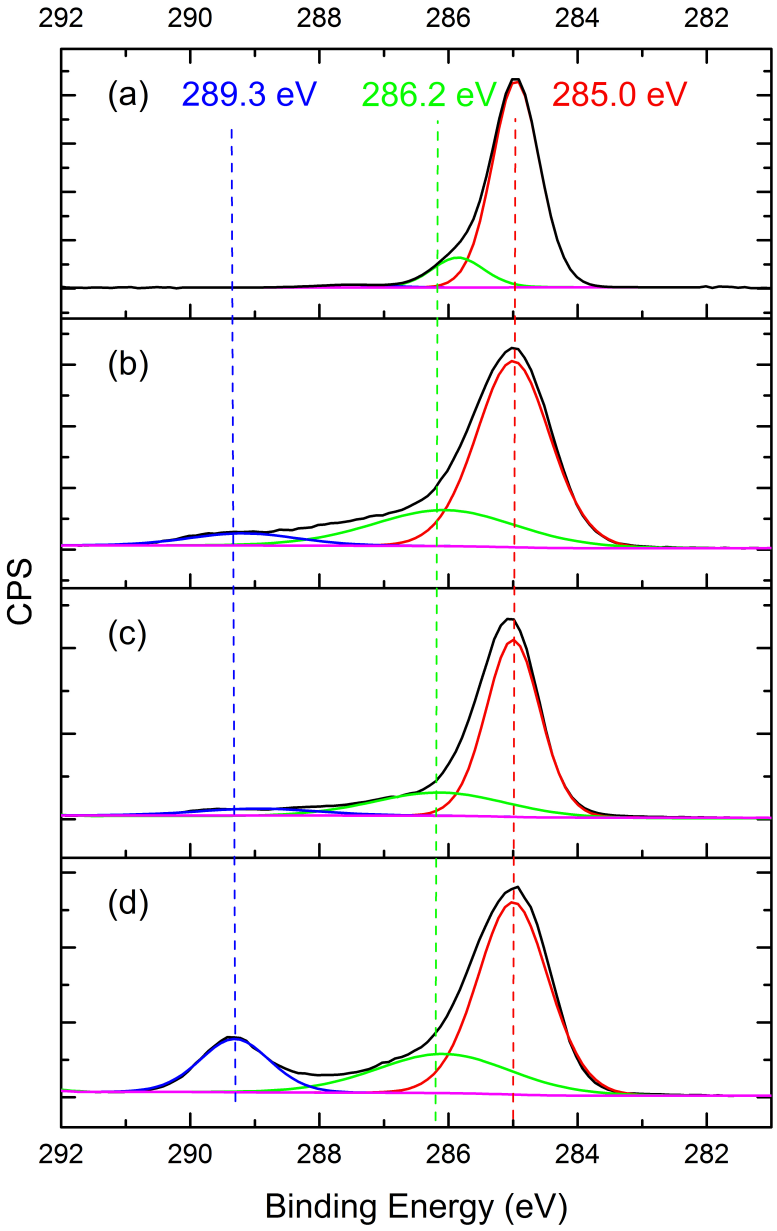

Figure 3.3: High resolution C1s core level photoemission spectra of (a) Untreated COP substrate (b) Acrylic acid coated COP substrate and (c) TEOS (d) TEOS & AA coated COP substrate, taken with a pass energy of 20 eV using monochromatic Al Kα monochromatic X-rays. The C1s peak is deconvoluted to show the various bonding environments in carbon. This demonstrates that the plasma polymerisation of AA depends strongly on the nature of the interfacial layer and the presence of a plasma polymerised siloxane intermediate layer enhances the carboxylic functionality in the coating.

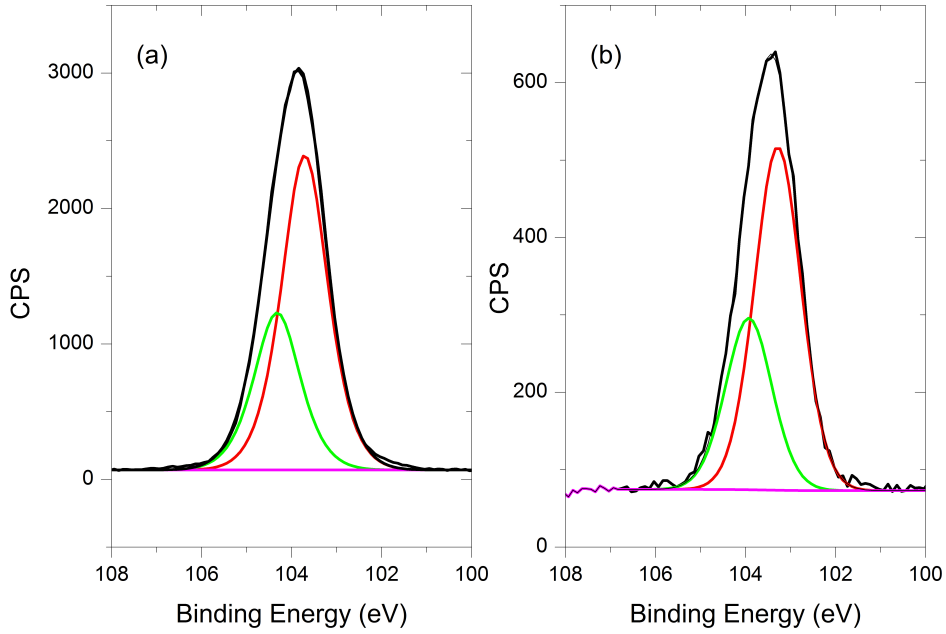

Figure 3.4: High resolution Si2p xps spectra of (a) TEOS (b) TEOS & AA. The Si2p peak is deconvoluted to show the various bonding environment in silicon.

Table 3.1: Analysis of the C1s region of the XPS spectra

Sample	C-C	C-C	Surface Oxide	C-OH	O-C=O
	Binding energy (eV) (% of total C1s peak area)				
Untreated COP	285.0 (84%)	285.9 (13.9%)	287.5 (2.1%)	-	-
Acrylic Acid	285.0 (68.1%)	-	-	286.5 (25.3%)	289.2 (6.5%)
TEOS & AA	285.0 (60.5%)	-	-	286.3 (23.1%)	289.3 (16.4%)

3.3.3 Surface Morphology and Thickness

AFM investigations on the effect of surface modification have been shown capable of providing information on surface morphology at the nanometre level. AFM studies were carried out on the modified surfaces to establish the roughness of the coatings compared to the plain COP surface. Using AFM, it is possible to determine the mean roughness of the morphological features within a given area. The value of rms roughness of the pristine COP surface containing pinholes and scratches was 1.73 ± 0.09 nm. This roughness has been smoothed significantly by the coatings of TEOS which displayed an RMS roughness of 0.71 ± 0.02 nm. AA deposition exhibited an RMS roughness value 0.49 ± 0.20 nm. Upon sequential coatings of TEOS and AA, the roughness of resulting TEOS & AA film was 1.10 ± 0.21 nm which exhibits a slight increase compared to the coatings of the individually deposited TEOS and AA, but is still within acceptable levels of roughness for biosensor applications. The observed post deposition surface roughness for TEOS & AA film is comparable with that found for films formed from liquid phase silanisation using organosilanes on silica, mica and glass surfaces [130, 131]. AFM measurement images are shown in Fig. 3.5. The surface roughness increased with the addition of a SiO layer. Increased surface roughness thus depends on the presence of both the TEOS and AA precursors.

Thickness measurements using optical ellipsometry techniques showed that the thickness of TEOS is 4.8 ± 0.2 nm, the thickness of acrylic acid coating is 12.6 ± 0.7 nm and thickness of TEOS & AA coating is 16.5 ± 0.7 nm.

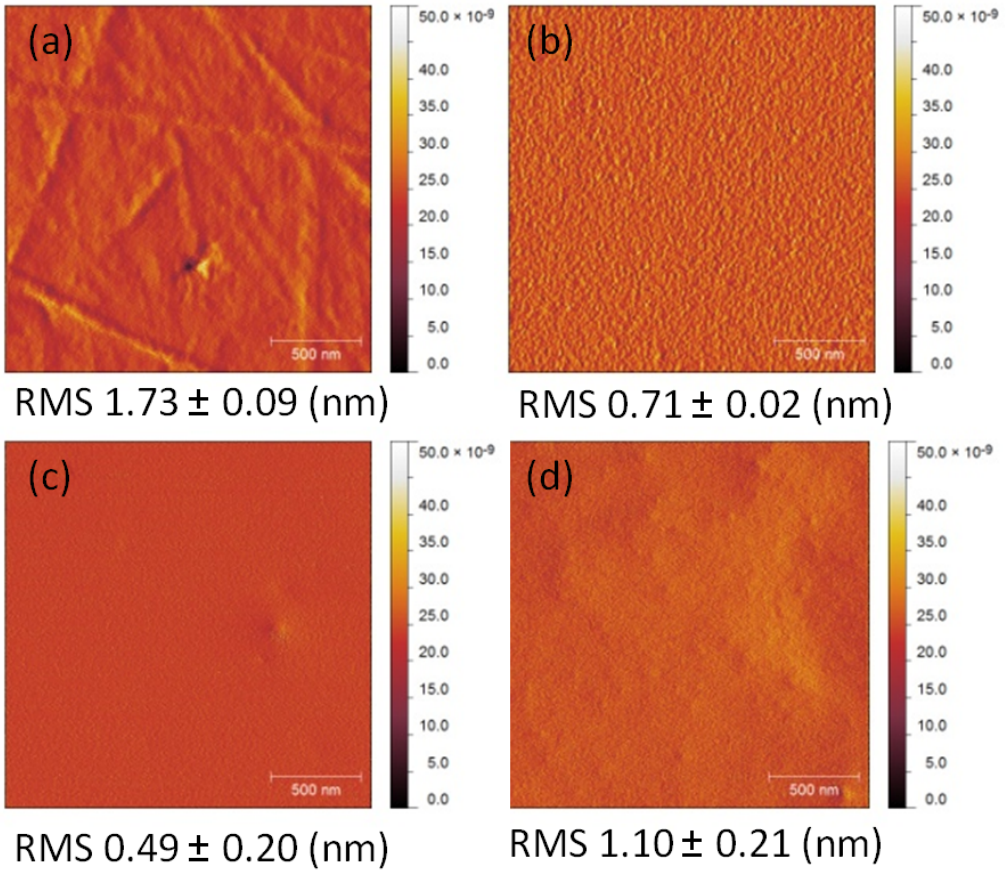

Figure 3.5: Atomic force microscopy images of (a) plain untreated COP (b) TEOS coating (c) Acrylic acid coating and (d) TEOS and acrylic acid coating. AFM measurements show that the prisitne COP surface contains scratches with RMS roughness of 1.73 nm, this can be smoothed to 0.71 nm with a layer of TEOS, AA on COP with RMS value of 0.49 nm and TEOS & AA with RMS value 1.10 nm.

3.3.4 Ageing

It is known that exposing COP to a plasma treatment changes it from its native hydrophobic state (water contact angle (WCA) $> 85°$) to a hydrophilic state (WCA $< 10°$). These contact angle changes are unstable over short time intervals and return to their original state with a time scale that depends on the discharge power exposed to substrates [132, 133]. Under the pretreatment settings used in this work, COP substrates went from their native hydrophobic state of WCA 86° to a WCA of 5°. After 48 hours the contact angle had returned to near original hydrophobic state (80°). Hydrophobic recovery is a well-known phenomenon of plasma exposed polymers, which can be attributed to the rearrangement of polymer chains at the surface along with migration of low molecular weight residues [134]. Figure 3.6 shows that coatings of AA and TEOS & AA retain their hydrophilic nature for longer periods of time compared to a plasma treated COP substrate. The AA coating had a lower water contact angle than the AA & TEOS coating.

3.3.5 Bioattachment

The ability of the coating to covalently bind biomolecules was assessed by attaching a fluorescently labelled (Cy5) single strand DNA (ssDNA). Specific surface binding and capture efficiency was assessed through immobilisation of DNA with NH_2- group via aminolysis. Non-specific binding was determined via physical adsorption of dye labelled DNA without the NH_2 group. A routine manipulation with substrates in immunoassays involves extensive washing with aqueous solutions, often containing detergents. Good adhesion and stability of coatings against washing and hydrolysis are necessary to ensure reproducibility and precision of a biodevice. The coated substrates were subjected to washing with PBS Tween and deionised water, dried with nitrogen and the fluorescence intensity was measured. This process was repeated five times. Both AA and TEOS & AA films showed comparable adhesion strength and resistance against washing with water and PBS Tween. The signal to noise ratio, measured as fluorescence signal of specifically

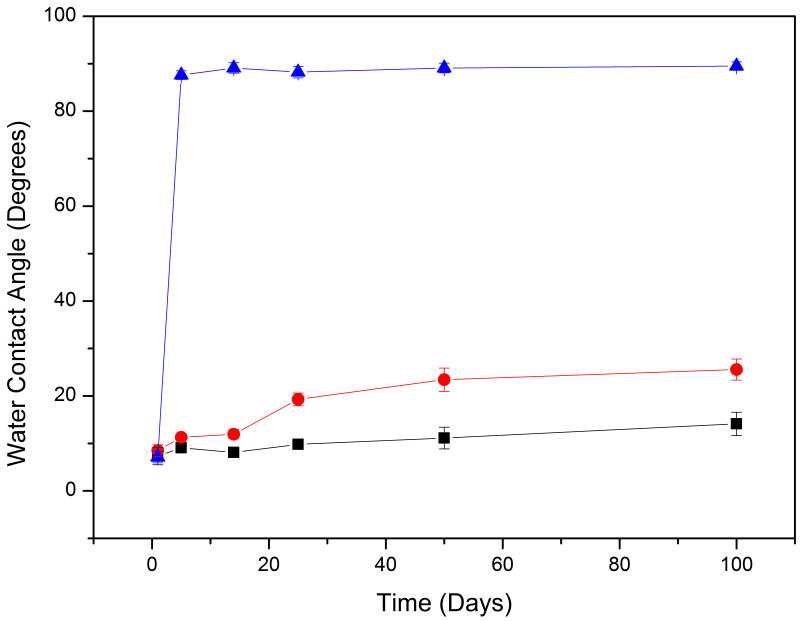

Figure 3.6: Variation of water contact angle with time (ageing effect) of deposited coatings on COP substrate. Red circle: TEOS & AA, Black square: AA Blue Triangle: Plasma treated COP. This image demonstrates that coatings of AA & TEOS and AA retain their hydrophilic nature over long periods of time compared to plasma treated COP.

bound DNA to unspecifically adsorbed DNA, was higher for TEOS & AA than that of AA (Fig. 3.4).

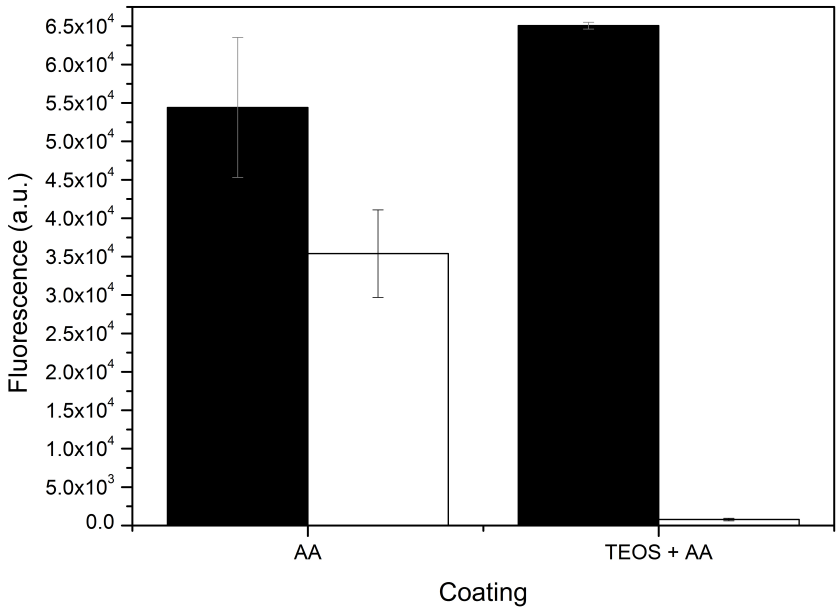

Figure 3.7: The ability of the coating to covalently bind biomelecules was assessed by attaching a fluorescently labelled ssDNA. Specific surface binding capture efficeincey was assessed through immbnolisation of DNA with NH2 group. Non specific binding was determined via adsorption of dye labelled DNA without the NH2 modification. Cy5 labelled IgG was attached to acrylic acid coated COP using EDC NHS. Black: Specific Binding, White: Non-specific Binding

Figure 3.8 shows the signal to noise ratio of AA and TEOS & AA coatings against washing steps. The increase in S/N ratio in bioassays can be explained by the washing off of physisorbed particles with each wash. The conditions the coatings were exposed to in washing are more extreme than the surface a biodevice would endure in regular operation. Figure **??** displays the role EDC NHS activation has in promoting attachment of the ssDNA to the surface; EDC NHS activation doubles the captured species.

Also, considering the fluorescence intensities as shown by Fig. 3.4, a higher density of

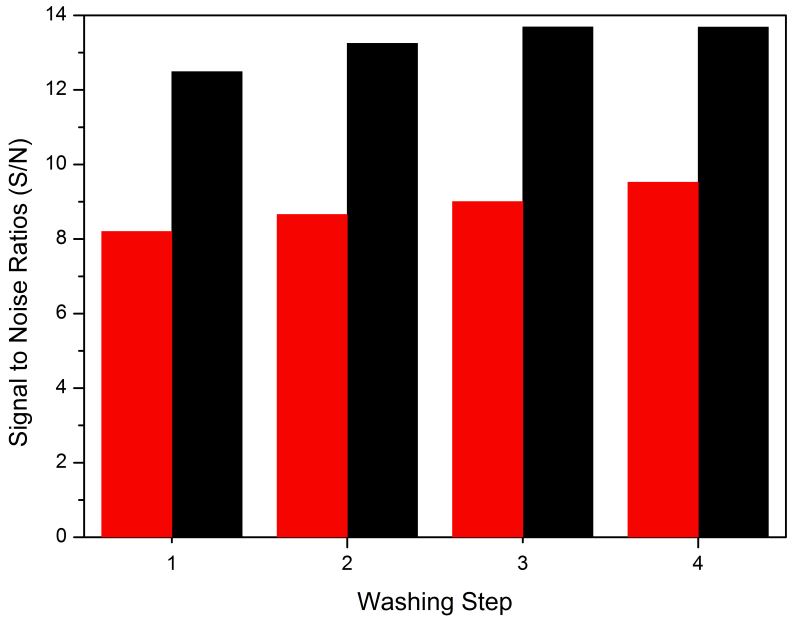

Figure 3.8: Signal to noise ratios of Black: TEOS & AA, Red: AA

captured DNA molecules was observed on AA & TEOS coatings. This polymer consisting of COOH-siloxane network also showed very good adhesion to the COP surface even after the washing steps.

3.3.6 Total Internal Reflection Ellipsometry

Total internal reflection ellipsometry (TIRE), was used to corroborate the fluorescence results on the TEOS & AA surface [135]. TIRE was also used to test the stability of TEOS & AA surface under long exposure to PBS buffer to simulate operating conditions.

As shown in Fig. 3.9 a, the Δ spectra remained the same over a period of 2.0 hr suggesting that the TEOS & AA is indeed stable against hydrolysis in aqueous environment. Replacing the PBS buffer with solution of ssDNA resulted in a large shift in Δ spectra. (Fig. 3.9 b). However, extensive rinsing with PBS revealed that the DNA is effectively immobilised only when the activating agent, EDC NHS, was present in the reaction mixture. In the absence of EDC NHS, the shift in Δ spectrum has been reduced to be close to the original Δ spectrum of TEOS & AA surface. It is possible that some small amount ssDNA have been non-specifically adsorbed to the TEOS & AA surface even without EDC NHS activation. Fitting of Ψ and Δ spectra gave corresponding thickness of ssDNA bound to the surface. It was found that with the EDC NHS activation, the thickness of ssDNA bound to surface was 17.8 $\pm$ 2.2 Å, while that without EDC NHS activation was as small as 2.6 $\pm$ 1.4 Å.

Ψ and Δ spectra of the complete DNA hybridisation assay are plotted in Fig.3.10 a and b, respectively. The introduction of the capture aminated Sa19 ssDNA (15-mer) solution and then the complementary Sa19 rev comp ssDNA (15-mer) solution resulted in large shifts in both Ψ and Δ spectra from the initial Ψ and Δ spectra of the COOH surface when the microwell was filled with PBS. In the first negative control experiment, a mismatched Sa20 non- comp ssDNA solution (20-mer) was incubated for 60 min after the capture Sa19 ssDNA had been immobilized to assess the non-specific hybridisation and non-specific binding effect. As seen in Fig. 3.10 c and d, the introduction of the non-complementary ssDNA solution did not result in any shifts in the Ψ and Δ spectra. Therefore, the effects of non-specific binding and non-specific hybridisation were minimal. The second negative control experiment, conducted by incubating the aminated Sa19

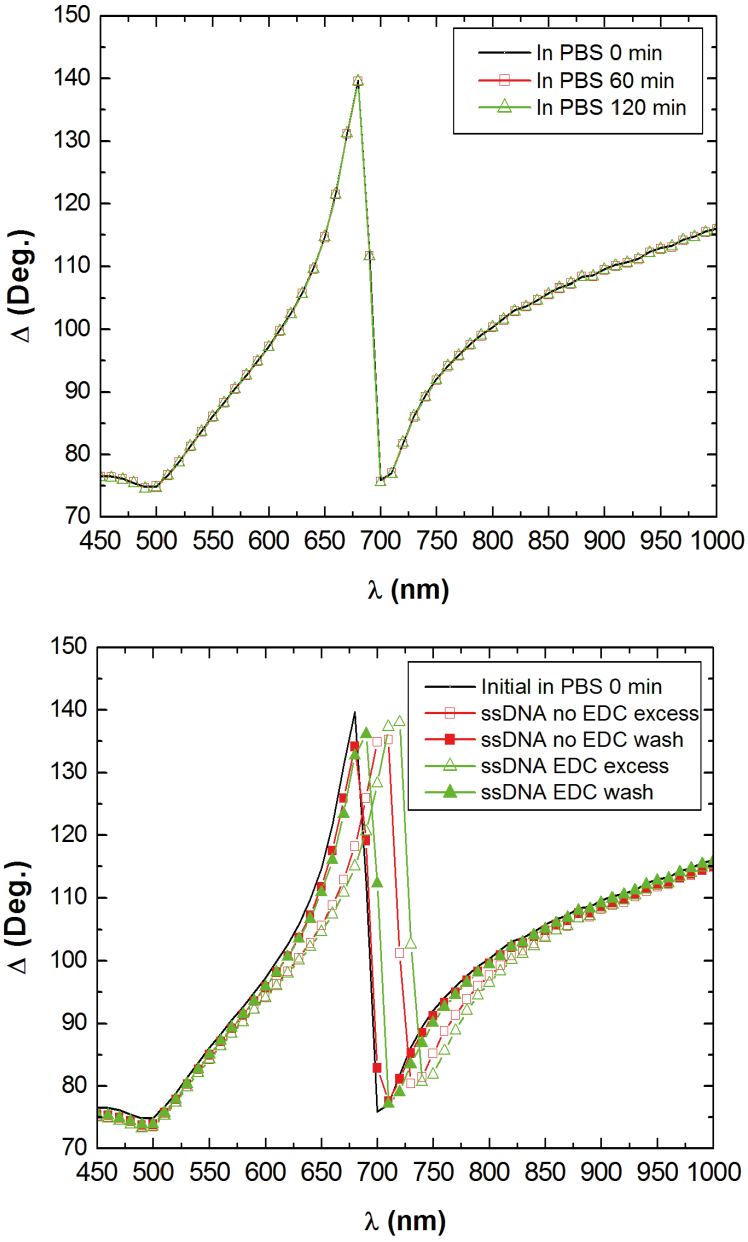

Figure 3.9: TIRE was used to test the stability of TEOS and AA surface under long exposure to PBS buffer and used to check the fluorescence results on the TEOS and AA surface (a) Δ spectra measured on TEOS & AA functionalised COP surface, with the cell first filled with PBS and then replaced with new PBS after 1hr and 2hrs. (b) Δ spectra measured on original TEOS & AA functionalised COP surface first filled with PBS buffer (representative from well 2), then reacted with excess ssDNA 10×10^{-6} M without EDC NHS (well 2) and with EDC NHS (well 3), and after rinsing with PBS buffer.

ssDNA solution without the activating agent EDC, showed that only a very small shift in Ψ and Δ spectra was observed after 60 min, Fig. 3.10 e, f).

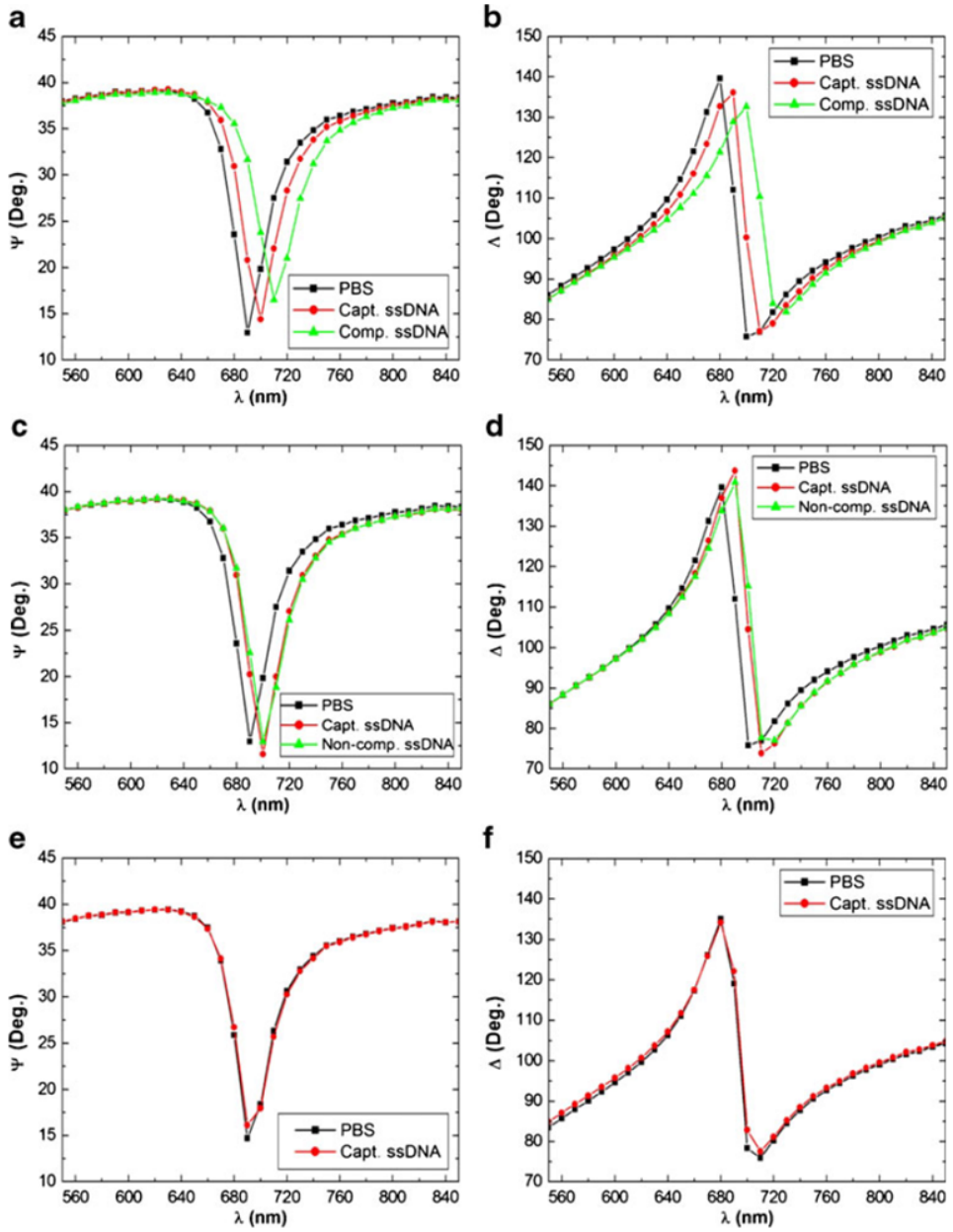

Figure 3.10: (a) (b) Ψ and Δ spectral shifts after binding of the capture of aminated Sa19 ssDNA (15-mer) at 10^{-5} M and hybridized with complementary Sa19 rev comp ssDNA (15-mer) at 10^{-5} M. (c)(d) Ψ and Δ spectral shifts were only observed for binding of the capture Sa19 ssDNA (15-mer) at 10^{-5} M but not for the mismatched Sa20 non-comp ssDNA (20-mer) at 10^{-5} M. (e)(f) Capture of aminated Sa19 ssDNA (15-mer) at 10^{-5} M without EDC activation; Ψ and Δ spectral shifts were minimal

3.3.7 Total Internal Reflection Fluorescence

Dye-doped nanoparticles (NP) are often used as labels in bioassays to increase signals and improve sensitivity. The benefits of sensitised NPs as bright detection molecules can only be realised if the particles have good colloidal stability and the non-specific interactions between the particles and the substrate surface is kept at minimum. The latter was of great interest in the context of the presented work. Although the commercial NPs are typically negatively charged to avoid aggregation, they often show high levels of particle-surface binding even in absence of biomolecules [136]. This subsection investigates the non-specific adsorption of dye-doped NPs on the TEOS & AA surface and compared it with a standard, commercially available, epoxy-coated glass slide, commonly used in bioassays, by use of total internal reflection fluorescence (TIRF) microscopy [113]. As expected, the electrostatic forces between the negatively charged NP surface and the negatively charged carboxy groups on the substrate dominate in this binding event. Fig. 3.3.7 illustrates low particle count on the TEOS & AA surface compared with that of the epoxy slide indicating the suitability of this surface for bioassays based on fluorescent particles.

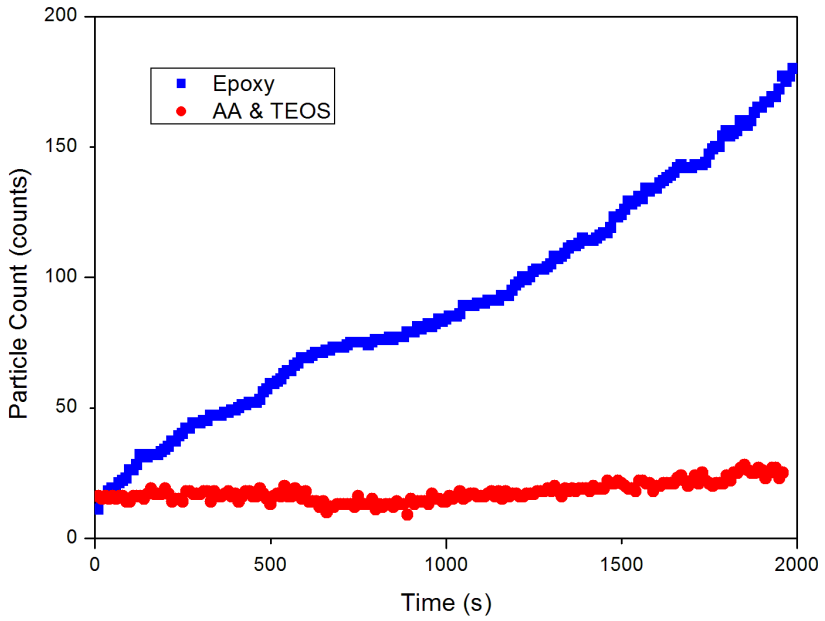

Figure 3.11: Particle count versus time for nanoparticles accumulating on TEOS & AA surface and epoxy surface. Scheme Caption: Carboxylic functionalised surface displaying low non-specific binding of ssDNA

3.3.8 Secondary Ion Mass Spectroscopy

In order to study the interfacial characteristics of the TEOS & AA film, the TEOS coating on its own (without acrylic acid) was deposited on a gold substrate and a surface secondary ion mass spectroscopy SIMS studies was carried out. The quadrupole apparatus miniSIMS was used for the chemical identification of the samples. The analysis of the surface fragments, produced by Ga+ ion bombardment, based on its mass by charge ratio (m/z) corresponds to the chemical structure of the coating. The miniSIMS measurement carried out on the top surface of TEOS coating and scanned through the film into the interface showed the presence of SiOH (m/z= 45 amu), hydrocarbon containing $SiOCH_x$ (m/z=58 amu) and SiO_2 species (m/z =60 amu). It is also observed that the carbon content decreased and the silicon related compounds dominated at the interface, see Fig. 3.12.

During the subsequent AA deposition, the plasma would not only activate both the reagent and the surface, but also promote mixing and reorganisation within the layer as it grows, resulting in a graded composition.

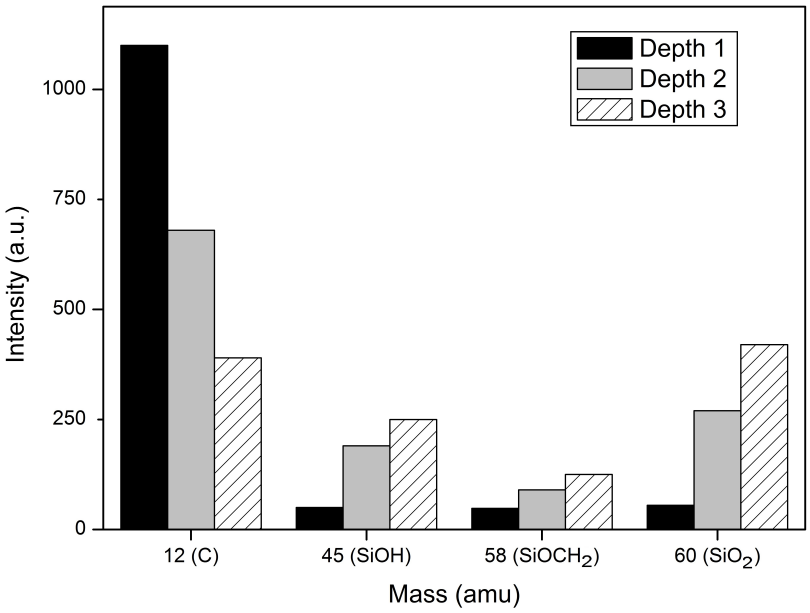

Figure 3.12: SIMS measurements taken of TEOS deposition on gold substrate. The SIMS measurement carried out on the TEOS coating showed the presence of SiOH (m/z 45 amu), hydrocarbon containing SiOCHx (m/z 58 amu) and SiO2 species (m/z 60 amu).

3.3.9 Optical Transmission

The optical transmission spectra of COP substrates were taken at normal light incident under the ambient conditions. As shown in Fig. 3.13, the transmittance of the hybrid sample was close to 100% from 1000 nm to 400 nm; it gradually decreased to around 80% at 360 nm and quickly fell when the wavelength approached 200 nm. The UV-Vis spectrum of the AA and TEOS & AA was almost identical to that of the untreated COP substrate in the full measured range, which indicated that the plasma deposition did not cause polymer surface damage or material deformation by either ionic bombardment or surface functionalisation. Furthermore, the high transmission characteristic of the hybrid material in the near UV range (>350 nm) implied that this coating technique can be applied to the optical COP devices in different applications, which require surface coating with hybrid materials for light irradiation without sacrificing the high transmission characteristics. The experiment was repeated again after a hundred days, no deterioration was observed in the optical properties of the deposited substrates, this data was not included in Fig. 3.13.

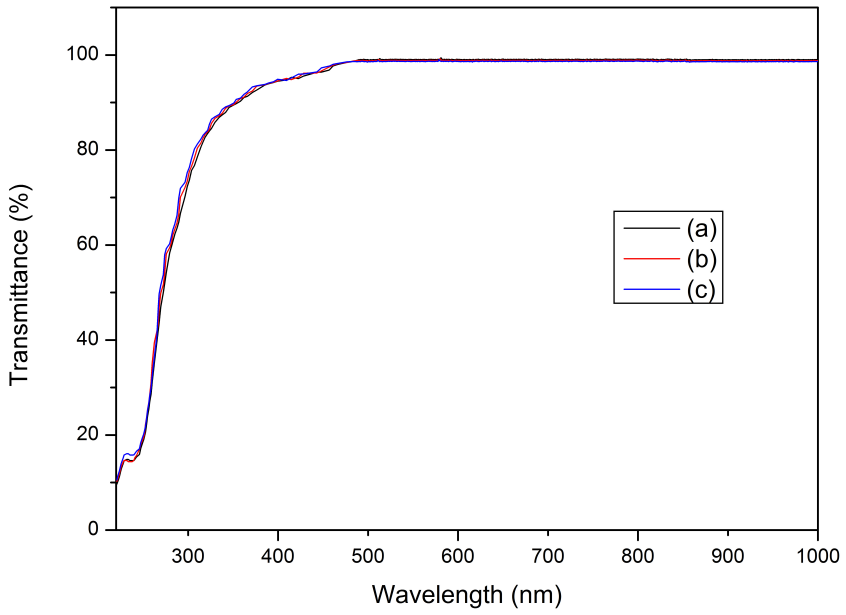

Figure 3.13: UV/Visible transmission of (a) Untreated COP (b) AA deposition on COP (c) TEOS & AA depsotion on COP. The UV-Vis spectrum of the AA and TEOS AA was almost identical to that of the untreated COP substrate in the full measured range, which indicated that the plasma deposition did not cause polymer surface damage or material deformation by either ionic bombardment or surface functionalisation. The experiment was repeated again after a hundred days, no deterioration was observed in the optical properties of the deposited substrates, this data was not included in the figure above for clarity.

3.4 Discussion

From the results a schematic can be deduced that represents the different stages of deposition on the COP substrate. Figure 3.14 shows the binding scenario and illustrates the process of deposition; a pretreatment of an argon oxygen plasma creates sites amenable to covalent attachment of the TEOS monomer, followed by the introduction of acrylic acid to illicit carboxy functionality for the immobilisation of biospecific markers. Using EDC NHS, amino terminated species were attached to the carboxy functionality, flourescently labelled DNA with and without NH_2 terminations were used as a means of testing specific and non-specific adsorption on the surface. The surface exhibited an improved signal to noise ratio from 9 to 12 by the introduction of the TEOS layer.

Eun-Sik Kima [137] demonstrated the effect of plasma treatment on Aldrich humic acid fouling. Results of bovine serum albumin (BSA) adsorption demonstrated that the protein adsorption decreased with increasing plasma treatment time. The plasma treatment resulted in a more hydrophilic and negatively charged surface which could better prevent Aldrich humic acidattachment on the substrate surface. A similar effect is observed in this work where non specific adsorption of ssDNA is reduced due to the increased number of negatively charged carboxy groups on the surface. Bioattachment measurements confirmed the immobilisation of amino-terminated species (ssDNA). High signal to noise ratio is critical to the success of biosensor devices. The non-specific binding can be explained by the low pK_a values of carboxylic acid (pK_a = 4.0 - 4.2) means that under standard physiological conditions, the equilibrium is shifted towards its deprotonated species, hence providing significant total negative charge on the surface. Charged films with low zeta potential can take advantage of electrostatic repulsions between the surface groups and other intrinsically negatively charged molecules, such as DNA and low isoelectric point proteins, thus effectively reducing the non-specific binding.

The picture that emerges from the different characterisations is that the role of the siloxane network, formed by fragmentation and activation of TEOS in the plasma, fol-

lowed by condensation and polymerisation on the COP surface is three-fold. Firstly, the TEOS deposition serves as a bonding layer to the COP substrate for enhanced adhesion. Secondly, it provides a reactive ground for cross-linking with acrylic acid, thus increasing the content of -COOH functionality. And thirdly, the presence of silanols (Si-OH) can facilitate large uptake of water molecules and cause significant hydration of the layer which in combination with high total negative charge crucial parameters for low non-specific adsorption of molecules.

Different powers, monomer pressures, polymerisation times and reactors location were also studied and optimal conditions were established for acrylic acid plasma polymerisation onto COP substrates i.e. Power 15 W, time 30 sec, monomer pressure 100 mTorr. This yields uniform layers of approximately 16 nm thickness with good adhesion to the substrate. The more the RF power was increased the more the polymerisation occurred and layers obtained were not uniform. Layers deposited using a lower RF source power and a same polymerisation time, were uniform and had a high degree of acidic functional groups in its surface. The ssDNA was spotted in multiple locations across the substrate, each spot gave similar fluorescence intensities. This is demonstrated in figure . TEOS & AA showed smaller error bars compared to AA confirming good surface coverage of carboxy groups and uniform deposition.

The investigation of the surface characteristics shows: ATR-FTIR confirmed the deposition of a Si-O coating using the TEOS monomer and the successful deposition of COOH using acrylic acid. These results were supported by XPS data confirming the presence of both COOH and Si-O. Other functional groups were identified including contributions from CH. XPS data demonstrated that on analysis of C1s peak, 6.5% was attributed to COOH from an acrylic acid deposition, 16.4% was attributed to COOH from a TEOS and acrylic acid deposition. Thus the inclusion of TEOS has beneficial effects in the retention of COOH with quantitative analysis by XPS revealing that the amount of carboxylic acids available on the surface was 2.5 times higher in films containing TEOS as an intermedi-

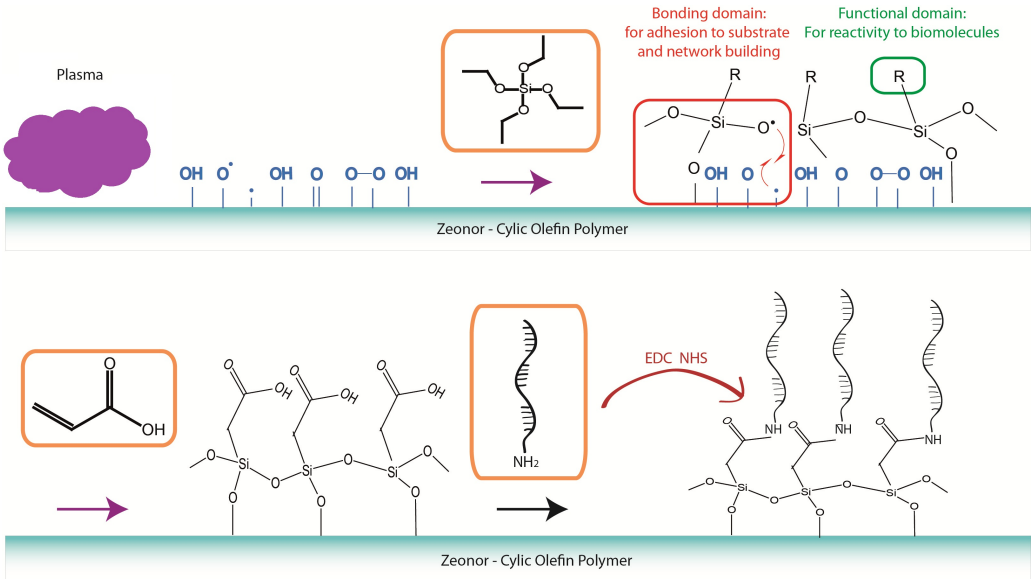

Figure 3.14: Schematic of binding scenario.

ate layer. The addition of a silicon oxide layer improves carboxy retention by creating a bonding domain for improved adhesion to the substrate and a network building layer for high binding capacity.

AFM measurements demonstrated a slight increase in surface roughness when TEOS & AA (1.1 nm) is used compared to AA (0.5 nm), an increase in surface roughness is associated with increased non-specific adsorption but not in this case as non-specific adsorption decreased for TEOS & AA.

Optical transmission measurements demonstrated that the surface is acceptable for fluorescently labelled biodevices, as the UV/Vis transmission remains close to transparent and as favourable to that of untreated COP. Ageing measurements of the UV/Vis transmission displayed no degredation over the time range studied.

3.5 Conclusion

In the work presented in this chapter, surfaces of COP substrates were successfully modified using plasma enhanced chemical vapour deposition to produce carboxylic groups for applications in biosensors. A technique for the modification of substrates using tetraethyl orthosilicate (TEOS) and acrylic acid (AA) as monomer sources to produce a polymer coating was presented. A silicon oxide layer has been successfully introduced as a bonding layer to the AA deposition and a comparison of the TEOS and AA film with AA deposition was given. Using a silicon oxide bonding layer and carboxylic functional layer, a novel surface has been developed that exhibits useful properties for improved biosensor device behaviour.

Chapter 4

Plasma Characterisation and Diagnostics

4.1 Background

In this chapter an exploration of the relationship between the plasma-phase chemistry and the deposition of acrylic acid is presented in order to control fundamental plasma processes like ion energies, to understand the fragmentation process and characterise the plasma. The plasma-phase chemistry has been investigated by means of mass spectrometry, a Langmuir probe and optical emission spectroscopy. The first measurements of an acrylic acid plasma using a retarding field energy anlayser are presented. Attention has been given to the influence of discharge power on the neutral and ionic species of the plasma. Combining the different diagnostic techniques the major plasma-phase reactions are elucidated and a knowledge of these help to explain how the molecular structure of plasma deposits are affected by processing parameters such as rf power and choice of background gases between argon and oxygen.

The deposited film has been studied by attenuated total reflection Fourier transform

infrared spectroscopy. The influence of the process parameters on the plasma have been investigated. The results are discussed within the context of increasing carboxylic acid functionality in the film.

Additionally, it is demonstrated that the choice of background gas for the deposition has a role in the final properties of the film; using argon as a background gas reduced the amount of CO groups in the plasma and deposited film, while oxygen as a background gas resulted in an increase the concentration of CO and OH species and offered better retention of the carboxylic acid functionalisation in the film, under the parameters discussed.

4.2 Introduction

Employing low pressure radio frequency plasma-enhanced chemical vapour deposition it is possible to obtain thin films with properties which depend strongly on the plasma-phase chemistry [63]. The plasma chemistry and thus the deposited surface depend on 'external' user-controlled processes such as gaseous pressures, discharge power, background gases and reactor configuration. Choice of these parameters demand fundamental understanding of the 'internal' plasma processes, such as monomer breakup and ion and electron energies. Diagnostic tools such as mass spectrometry, optical emission spectroscopy and retarding field energy analysers have been developed in order to investigate plasma properties. The goal of this study was to combine 'internal' and 'external' plasma parameters such as species concentrations, and ion energies, over a range of pressures, powers and background gases in an acrylic acid containing plasma so as to understand the deposition process of acrylic acid films.

Studies to date have concentrated on the use of plasmas to deposit films that feature a high degree of retention of the chemical functionality of the monomeric precursor. Retention of monomer functionality offers the possibility of exercising control over processes that depend on surface chemistry. However, understanding of the relationship between

the plasma and film deposition remain inadequate. Fragmentation and recombination events take place within the plasma, but the importance of the various processes, and the identity of those species that lead to polymer formation remain uncertain.

While the existing literature on the plasma deposition of acrylic acid is sparse, studies which are available have concentrated on the structure and application of plasma deposited thin films as opposed to the mechanisms of plasma deposition. To investigate the mechanism of plasma polymerisation, a number of techniques were applied at a range of rf power.

Firstly, mass spectrometry and optical emission spectroscopy were performed in order to track the breakup of the acrylic acid monomer and species produced in the plasma.

Secondly, Langmuir probe measurements were taken. The electron energy distribution function (EEDF) in a low pressure processing discharge is an indicator of the state of the plasma [110, 138]. Knowledge of the EEDF is important for determining plasma parameters like electron density, n_e, and electron temperature, T_e, and for optimising the plasma process [139, 140]. Chemical processes are sensitive to the EEDF which play a central role in coupling power into the desired surface reactions.

Thirdly, ion energy distributions and ion flux densities over pressure and power ranges of 60 - 120 mTorr and 0 - 500 W and background gases of argon and oxygen are presented. Ions are important in the formation of polymerised films as they transport energy to the surface, thus contributing to the deposition processes and surface functionalisation [61]. Appropriate control of ion bombardment energy is important in the context of deposition and functionalisation of substrates.

Fourthly, ATR-FTIR measurements are used to characterise the surface of the deposited film. The film depositions were carried out on cylic olefin polymer (COP).

4.3 Experimental

The plasma was investigated using the PECVD system described in section 2.1.1. The chamber had a base pressure of approximately 15 mTorr (2.0 Pa). In this investigation, oxygen and argon pretreatment had flow rate values of 100 sccm. During deposition either the oxygen or argon flow was stopped and the remaining gas flow rate value was reduced to 50 sccm.

Acrylic Acid ($C_3H_4O_2$) of 99% purity was purchased from Sigma-Aldrich. Addition of acrylic acid raised base pressure of chamber to 40 mTorr (5.3 Pa). Further addition of oxygen or argon (50 sccms) raised the final pressure of chamber to 98 mTorr (13.1 Pa). The flow of acrylic acid monomer vapour into the chamber was regulated through a manually operated needle valve. Any variations of these parameters will be identified where required.

The mass spectrometer is a quadrupole 500 model by Hiden Analytical. The spectrometer was connected to the chamber by a side port at the centre of a side wall. Species arriving at the spectrometer were ionised by electron impact with an electron kinetic energy of 20 eV. This was done to limit additional fragmentations in the mass spectrometer.

The optical emission of the plasma was detected through a sapphire quartz window by a UV/VIS spectrometer (MicroHr, Horiba Jobin Yvon, Cedex, France) with a wavelength scan range of 200 to 1100 nm. The spectrometer is a 140 mm f/3.9 Czerny-Turner with imaging optics of resolution 0.3 nm. The spectrometer was placed at a side port of the chamber which had a line of sight to the plasma.

The Langmuir probe system (Model ALP System, Impedans, Dublin) [141] consists of a probe tip which is a tungsten wire of radius 0.2 mm and 5.0 mm in length, rf compensated electronics and a high speed data acquisition unit was used to record the probe current-voltage (IV) characteristics. The IV trace was averaged over 200 sweeps and the resulting traces are analysed in the usual way [142] to calculate the electron electron temperature and the EEDF.

The use of Langmuir probes in depositing plasma, particular with insulating deposits, is generally problematic, as a solution the probe was heated prior to measurement to evapourate any insulating deposits on the surface. An automated probe tip cleaning feature is provided as standard on the Langmuir probe system to facilitate the cleaning by heating of the probe tip after prolonged use. The probe was cleaned between measurements by heating. This is achieved by pulse biasing the probe to a large positive voltage and drawing an electron current of up to 100 mA during the on period of the pulse. The power on the probe surface is calculated and maintained by varying the duty cycle so that the probe is not damaged.

Ion energy measurements were carried out using a retarding field energy analyser (Semion, Impedans, Dublin, Ireland). The analyser is 60.0 mm in diameter and 3.0 mm thick, it consists of an array of 800 μm holes over an area of 1.0 cm^2. A series of three grids is used; the first grid is maintained at the electrode floating potential, the second grid is swept to provide the ion retarding potential, only ions with energies greater than the voltage on grid two will be detected. The thrid grid is biased negatively with respect to grid one to repel electrons that may enter the analyser and to inhibit secondary electron emission from the collector. Finally a collector plate is used to attract any ions passing through the second grid. The ion energy distribution is obtained by taking the derivative of the collector current versus retarding potential, a complete description of the analyser is available elsewhere [115].

Fourier transform infrared (FTIR) spectra were recorded using a Perking Elmer FTIR system (Model Spectrum GX) used in the attenuated total reflection mode. The detector and sample chamber were purged with nitrogen to eliminate background signal of CO_2. For all data presented, unmodified COP slides were used as background. Scans were collected between 4000 and 400 cm^{-1} (25 - 2.5 μm) range with 32 scan average per image.

4.4 Results and Discussion

4.4.1 Mass Spectrometry

Fig. 4.1 and 4.2 show the electron impact (EI) mass spectra of acrylic acid for various rf powers and background gases. 0 W meaning no plasma ignition. The EI spectra are interpreted using the rules of conventional mass spectrometry analysis as detailed by McLafferty [111]. The molecular ion of acrylic acid appears at m/z 72 (CH_2=CHCOOH), while fragments are detected at m/z 17 (OH) m/z 28 (CO^+), 44 (COO^+), 45 ($COOH^+$) and 55 (CH_2CHCO^+). Also detected is water at m/z 18; at least some of the intensity of this peak is due to residual water in the vacuum system, which is observed in control spectra recorded in absence of the plasma and monomer. Precautions were taken to reduce the contribution from residual water in the system by keeping the system under vacuum for 48 hrs before measurements were carried out. No peaks were found above m/z 72.

With carboxylic acid functionalisation in mind, particular attention should be assigned to m/z 17 (OH) and m/z 28 (CO) as they have a strong contribution from the breakup of the carboxylic functional group (-COOH) within the discharge. Fragmentation increases with increasing applied power as can be seen in the Fig. 4.1 (i) and 4.2 (i). The plasma has produced considerable fragmentation of the acrylic acid but the background gas has an effect on the the quantities of new species. In particular, mass spectrometry results from Fig. 4.1 (i) show interesting behaviour with the acid fragmentation (CO and OH products). With an argon background CO shows no change with rf power input, OH shows a decrease. With oxygen as the background gas different behaviour is observed. With the rf power applied to the plasma Fig. 4.2 (ii) shows that the acid fragmentation (CO and OH products) increases with the rf power applied to the plasma. Both the OH and the CO fragments have an initial fast increase and plateau at 15 W of rf power. This is investigated further in section 4.4.4.

One would expect that when the COO species becomes fragmented the quantity of

CO species would increase. This is the case when argon is used as the background gas but when oxygen is used an increase in power results in an increased concentration of COO and CO. Thus oxygen as a background gas improves the survival of COOH (as compared to argon as background gases under identical conditions). Observations lead to the conclusion that the background oxygen gas is active in the fragmentation process, this can be seen by the loss of molecular oxygen with increased power, yet little signal is observed at m/z 16 (monatomic oxygen). The oxygen radicals are highly reactive and are thus used to maintain carboxylic acid functionality within the plasma.

The EI mass spectrum of the plasma neutrals with increasing power contain all the signals seen in the 0 W setting. The peaks can be grouped in two types, type A peaks are defined as those that arise exclusively from ionisation of the 'intact' acrylic acid in the mass spectrometer. Type B peaks are the most intense and arise from fragmentation of acrylic acid in the plasma, fragments are subsequently ionised by EI in the mass spectrometer, as laid out in Table 4.1.

Table 4.1: Grouping of acrylic acid fragments.

Type A		Type B	
72	CH_2=CHCOOH	45	COOH
55	CH_2=CHCO	44	COO
		28	CO
		26	CH=CH
		18	H_2O
		17	OH
		2	H

Reaction pathways of this fragmentation leading to different chemical structures are presented in Fig. 4.3 which was developed from Toole [143]. Here, collisions between acrylic acid species and plasma electrons results in the creation of excited state species, which then decompose homolytically to give neutral species. Most of the remaining peaks which are of low intensity are are therefore, associated with the intact acrylic acid. The

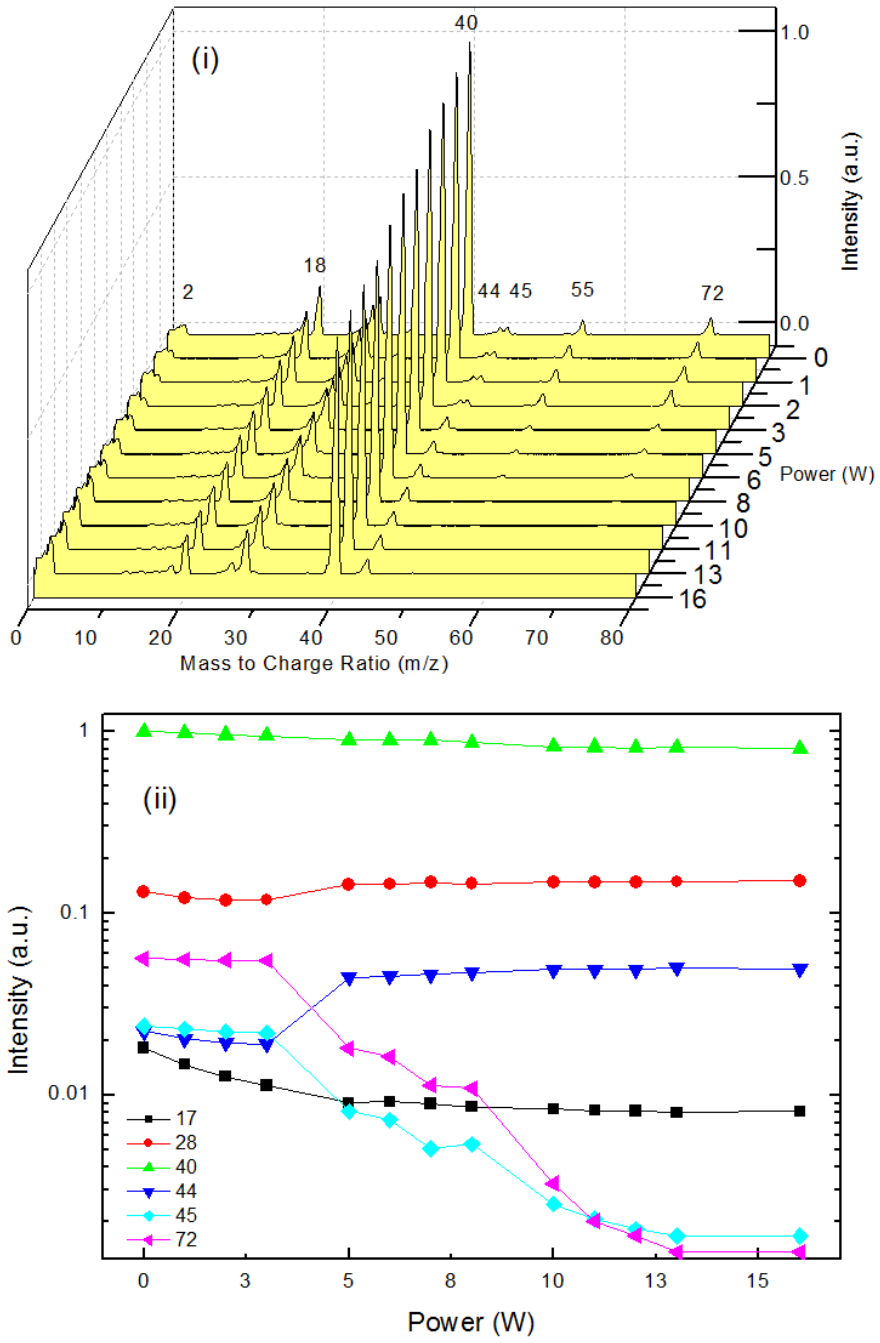

Figure 4.1: Fragmentation of acrylic acid with argon as background gas. (i) Overview of process fragmentation on a linear scale (ii) Tracking of individual fragmented species on a log scale. These figures show the mass spectra of acrylic acid for various rf powers and background gases.The molecular ion of acrylic acid appears at m/z 72 (CH2=CHCOOH), while various fragments are detected.

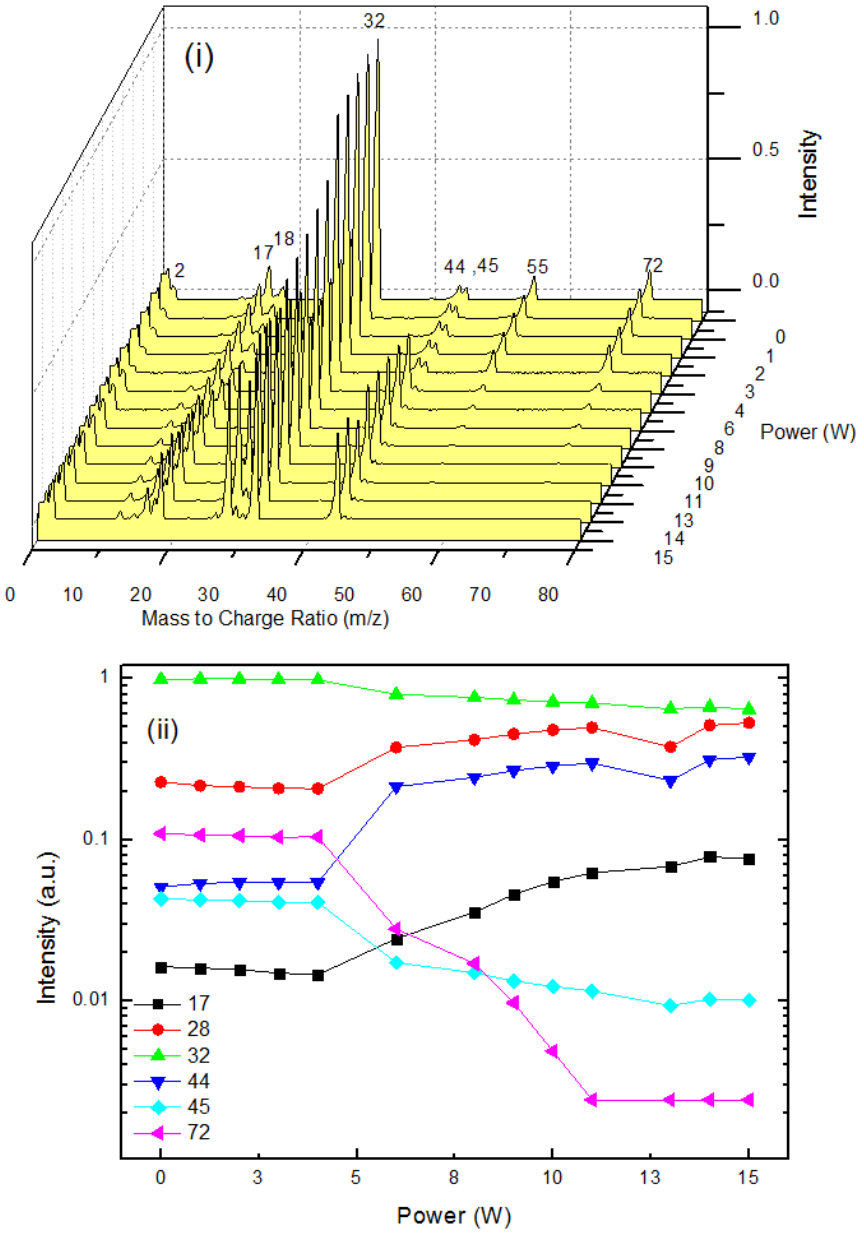

Figure 4.2: Fragmentation of acrylic acid with oxygen as background gas. (i) Overview of process fragmentation on a linear scale (ii) Tracking of individual fragmented species on a log scale.

only peak still unaccounted for is m/z 2, which corresponds to H_2^+. The same reaction pathways apply equally to argon and oxygen background gases but the quantities of the resultant fragmentation processes vary greatly as certain species creation is preferred.

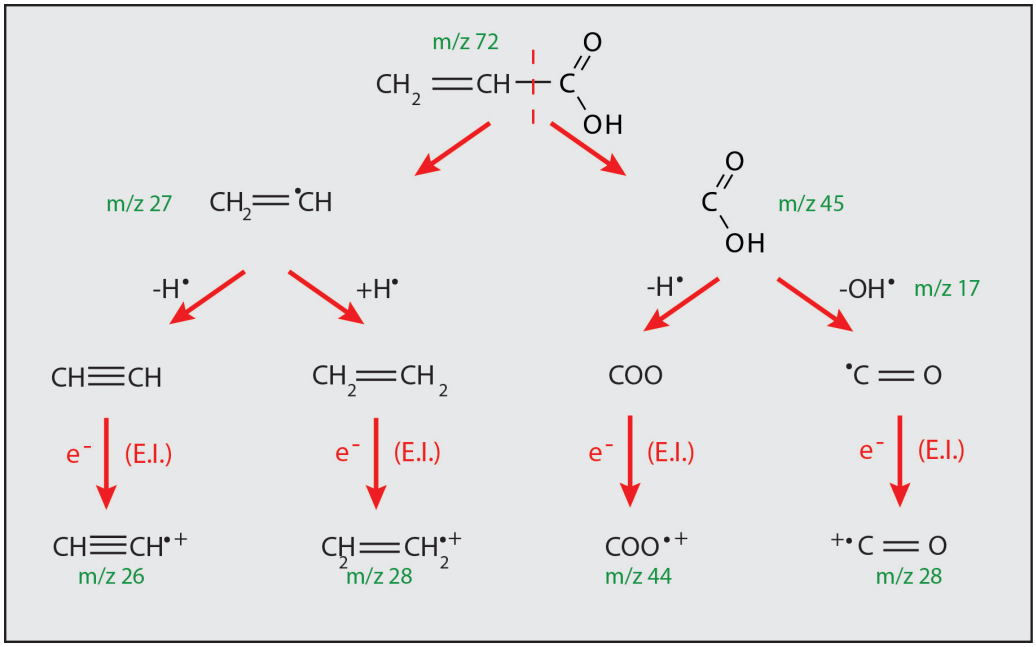

Figure 4.3: Proposed plasma fragmentation path of acrylic acid.

The plasma deposition of acrylic acid is regularly carried out with an argon background gas [144–147]. The surface density of COOH groups in the coating depends on the degree of fragmentation of the acrylic acid monomer in the discharge and from the mass spectrometry results it can be seen that an oxygen rich environment permits oxidation reactions to take place that allow greater carboxylic acid functionality retention to reach the substrate surface.

4.4.2 Langmuir Probe

Fig. 4.4 shows the EEDF distributions for argon at various rf powers. Argon was investigated at fixed gas pressure (Base chamber pressure 15 mTorr, with argon 98 mTorr) with variable rf power. The range of discharge power was limited at the low end by the stability of the discharge while the high end was limited by the desire to avoid excessive probe overheating and etching of the probe tip. Using an rf compensated probe, the plasma parameters n_e and T_e have been determined for a range of discharge powers and background gases and are tabulated in Table 4.2.

In Fig. 4.4 the electron density is observed to increase with the increase in rf power. This is because the increase in rf power generates more argon ions and hence electrons in the discharge. However, the mean electron temperature remains unchanged at ≈ 2.1 eV. As electrons are responsible for ionisation events in the plasma, lower powers will reduce the number of these events taking place, which is consistent with the mass spectra results in section (4.4.1).

Table 4.2: Plasma parameters for argon plasma at various rf powers, pressure 98 mTorr.

Power (W)	n_e (m^{-3})
20	9.7×10^{13}
40	1.6×10^{14}
60	1.9×10^{14}
80	2.5×10^{14}

A comparison of acrylic acid with the different background gases under similar plasma conditions was investigated (Fig. 4.5). The electron density in the acrylic acid discharge is higher for oxygen than for argon. One possible reason for this may be due to the lower ionisation potential of oxygen (13.6 eV) compared to argon (15.8 eV). At equal rf power, oxygen and argon exhibits different ionising abilities.

Comparing the 20 W argon EEDF (Fig. 4.4) with the 15 W acrylic acid EEDFs (Fig. 4.5) there is a lower distribution curve for AA, more than if an extrapolation to lower

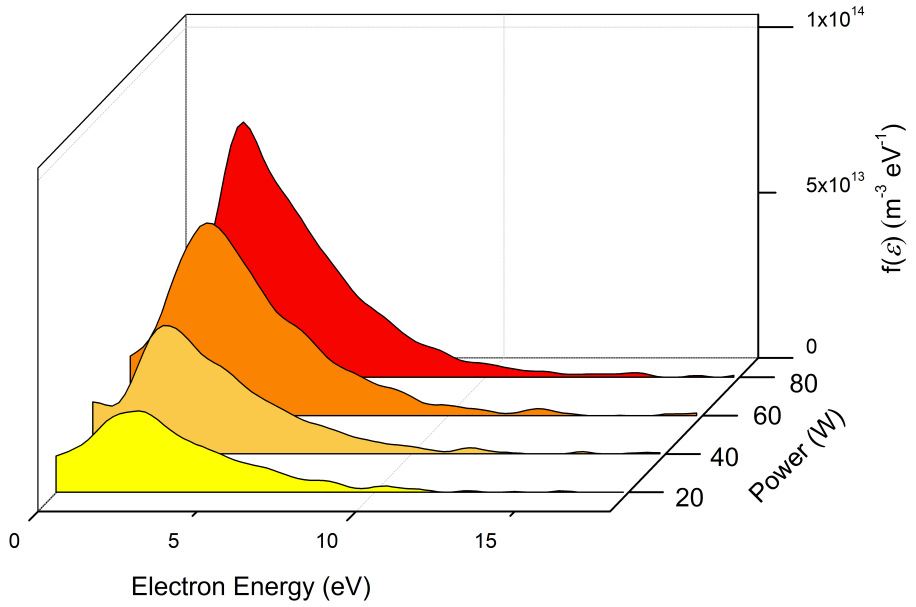

Figure 4.4: Argon EEDF for various discharge powers. The electron energy distribution function (EEDF) in a low pressure processing discharge is a good indicator of the state of the plasma. Chemical kinetics are especially sensitive to the EEDF and the electron population plays a central role in coupling power into the surface reactions. Process development and transfer will be aided by a knowledge of the EEDF and its sensitivity to various process parameters. The electron density is observed to increase with the increase in rf power. This is because the increase in rf power generates more argon ions and hence electrons in the discharge. However, the mean electron temperature remains unchanged at 2.1 eV.

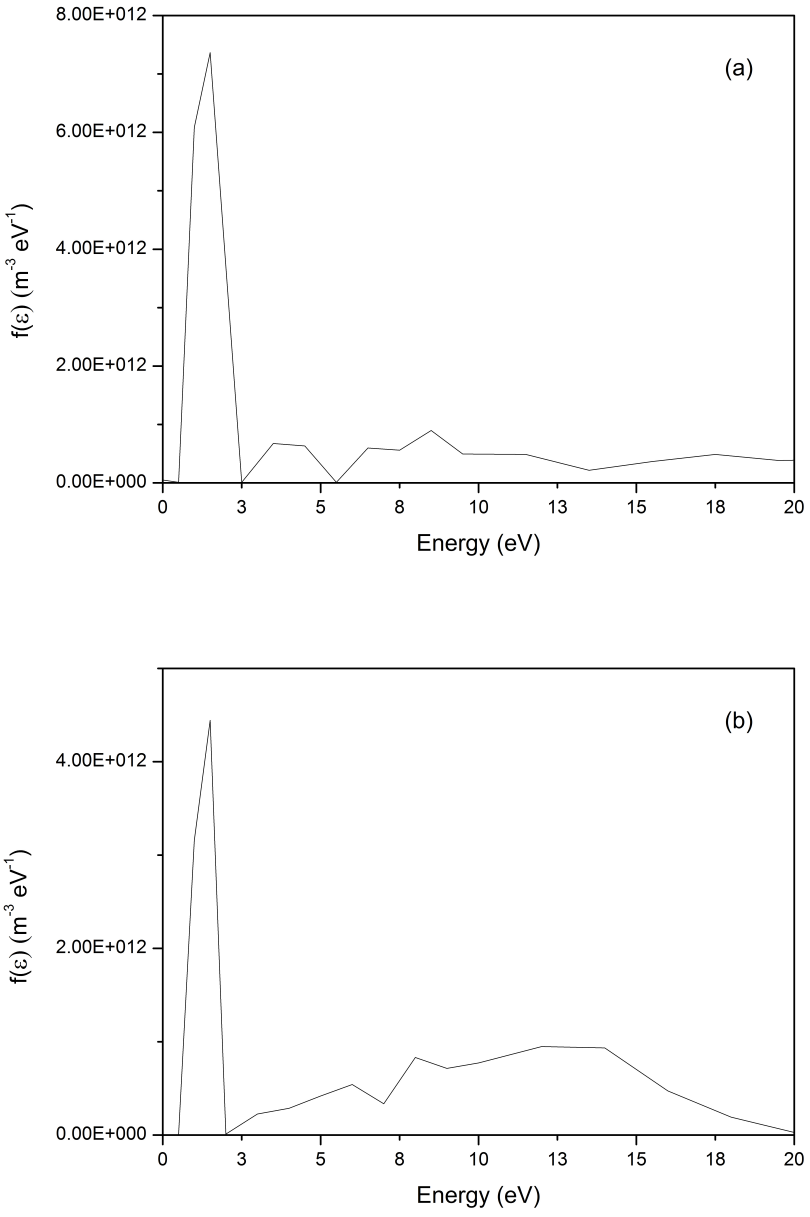

Figure 4.5: Electron energy distribution function: (a) Oxygen & AA at 15 W power, 98 mTorr chamber pressure. (b) Argon & AA at 15 W power, 98 mTorr chamber pressure. A comparison of acrylic acid with the different background gases under similar plasma conditions was investigated The electron density in the acrylic acid discharge is higher for oxygen than for argon. One possible reason for this may be due to the lower ionisation potential of oxygen (13.6 eV) compared to argon (15.8 eV).

powers were performed. The composition of the gases is different, so it can be seen that direct comparisons of argon with acrylic acid and argon cannot be achieved. However, it can be used as an indicator of the behaviour of AA and argon.

Ionisation and excitation is almost entirely dependent on electron impact. In molecular gases such as acrylic acid, the situation is more complex because of the wide variety of species (and energy states within each one) but the distribution of electron energies is still an important indicator of what chemical processes take place. Hopkins *et al.* [148] showed that in molecular nitrogen discharges, the EEDF displays significant depletion around 3 eV where there is a large cross-section for vibrational excitations of the gas molecule. The acrylic acid plasma displays a similar effect with a depletion around 3 eV although cross sectional data remains unknown.

4.4.3 Retarding Field Energy Analyser

The retarding field energy analyser (RFEA) was used to determine ion energy distribution functions (IEDF) at varying pressures and powers in acrylic acid plasma using two source gases, oxygen and argon. IEDF's are shown in Fig. 4.6 for both oxygen, argon and acrylic acid plasmas. The ratio of acrylic acid to background gases are kept constant. Ion flux densities are calculated from the IEDF and are displayed in Fig. 4.7, control over the IEDF has been achieved. Increasing the power supplied to plasma increases the ion flux density, while increasing the pressure reduces the ion flux density. Under these conditions, the observed ion energy distributions range between a broad single peak structure which is typical of those found in rf plasmas to a narrowing of the peak structure at increased power. It is seen in Fig. 4.6 that the IEDF is shifted to higher ion energies by reducing the pressure as a reduced pressure increases mean free path of the ion species. The choice of pressure and background gas affects the IEDF as shown in Table 4.3. These measurements were carried out with an rf power of 15 W as it was found in chapter 3 that at this power retention of carboxylic functionality was possible. Oxygen and AA IEDFs show a larger spread compared to argon and AA IEDFs.

Table 4.3: Ion energy distributions, the spread of the peaks are shown and peak energy is given. Measurements were taken at discharge power of 15 W.

Background Gas	Pressure (mTorr)	Spread FWHM (eV)	Energy at peak (eV)
Argon	116	7.7	7.3
	93	6.8	6.7
	78	6.5	5.8
	56	5.8	5.1
Oxygen	116	11.1	8.9
	92	8.2	8.1
	71	7.6	6.3
	56	6.0	4.2

In Fig. 4.7 it can be seen that acrylic acid with oxygen has a higher ion energy flux

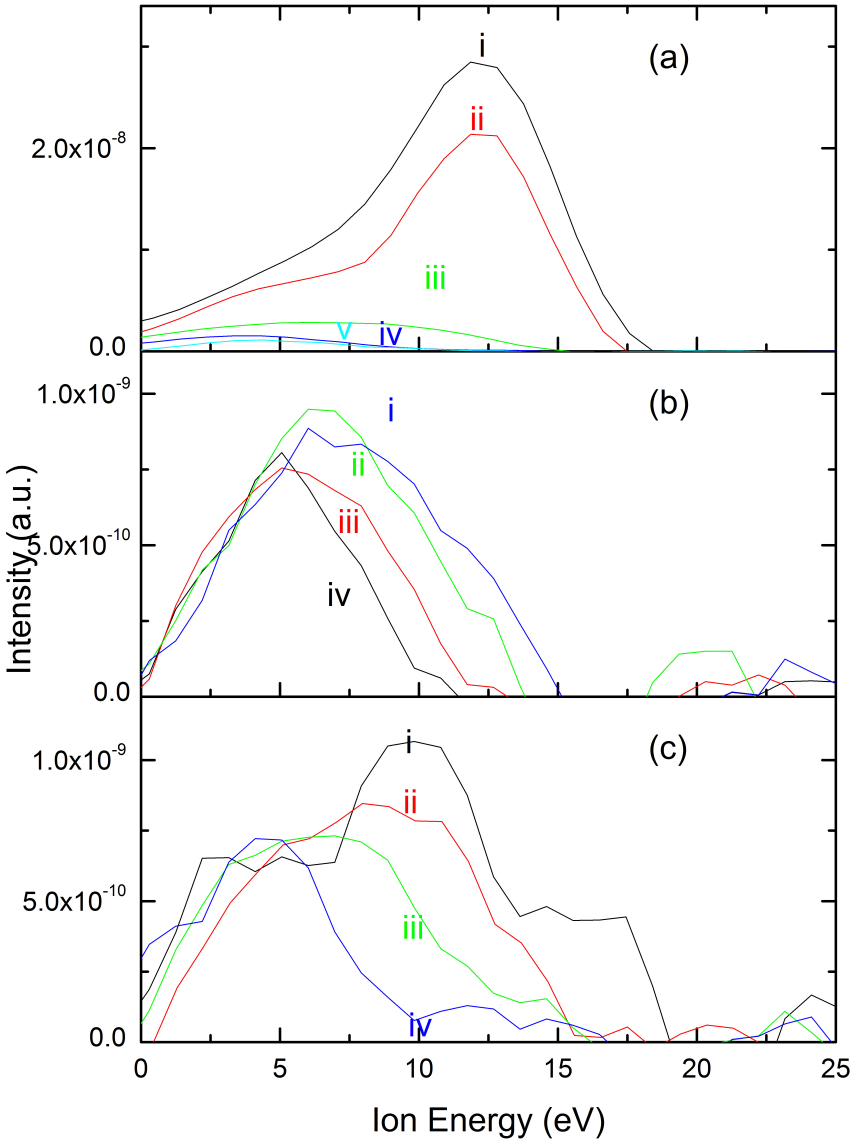

Figure 4.6: RFEA(a) Acrylic acid with argon, pressure is kept constant at 100 mTorr, applied rf power is changed (i) 440 W (ii) 312 W (iii) 125 W (iv) 59 W (v) 25 W. (b) Acrylic acid and argon, applied rf power is kept constant at 15 W, pressure is changed (iv) 116 mTorr (iii) 93 mTorr (ii) 78 mTorr (i) 56 mTorr. (c) Acrylic acid and oxygen, applied rf power is kept constant at 15 W, pressure is changed (iv) 116 mTorr (iii) 92 mTorr (ii) 71 mTorr (i) 56 mTorr. IEDF is shifted to higher ion energies by reducing the pressure as a reduced pressure increases mean free path of the ion species. The choice of pressure and background gas affects the IEDF as shown above. Oxygen and AA IEDFs show a larger spread compared to argon and AA IEDF

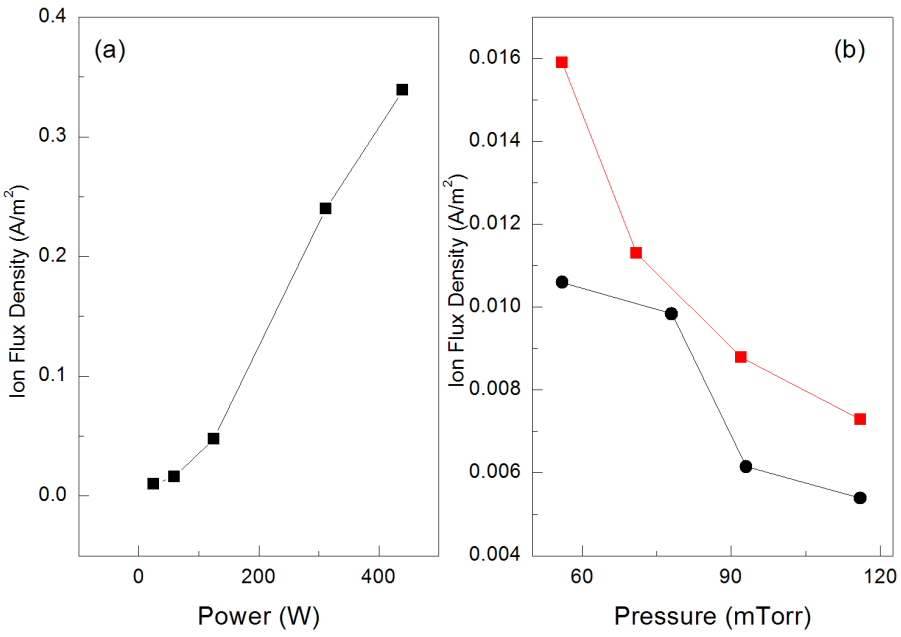

Figure 4.7: RFEA(a) Ion flux density (IFD) of acrylic acid plasma with argon with respect to increasing rf power. (b) (i) IFD of acrylic acid with oxygen as background gas. (ii) IFD of acrylic acid with oxygen as background gas.

at the same pressure and power of acrylic acid and argon.

4.4.4 Optical Emission Spectroscopy

Optical emission spectroscopy was performed under similar conditions as used for the mass spectrometry analysis. Emission from excited species such as CH, CHO and CO were identified in the acrylic acid plasma, as presented in the OES scan (200 - 1100 nm) in Fig. 4.8. In particular, emission spectra were investigated for $A^2\Sigma^+$ - $X^2\Pi$, (OH line at 306.4 nm) and $B^1\Sigma$ - $A^1\Pi$ (CO line at 519.8 nm) as they are indicative of carboxylic acid fragmentation and behaviour within the plasma. Rossini *et al.* [145] proposed that these spectral lines can be used to track the breakup of the COOH functional group. In addition, OES measurements will permit comparisons to mass spectrometry data (see section 4.4.1).

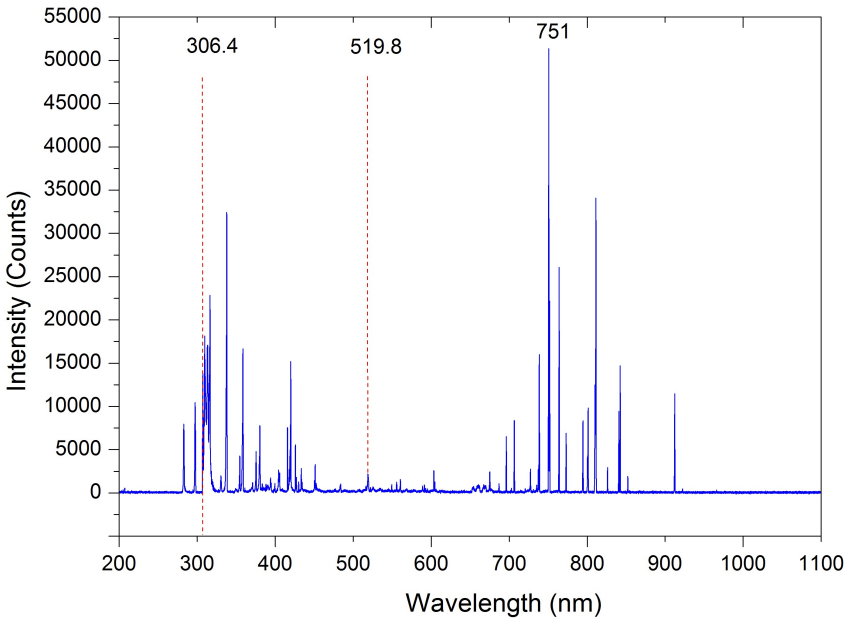

Figure 4.8: Optical emission spectrum of acrylic acid and argon, plasma at 25 W

In Fig. 4.9, OES measurements show that the acid fragmentation (CO and OH prod-

ucts) increase with the rf power to the plasma. OH species have an initial increase and reach a plateau at around 45 W. CO species exhibited a similar initial increase however CO species required higher rf power to stabalise.

Mass spectrometry and OES measurements confirm the presence of CO species. However, CO species displayed a delayed increase in mass spectrometry data and a rapid increase in OES readings. While increased power resulted in increased CO species in both instances, the rate of CO species creation is conflicting.

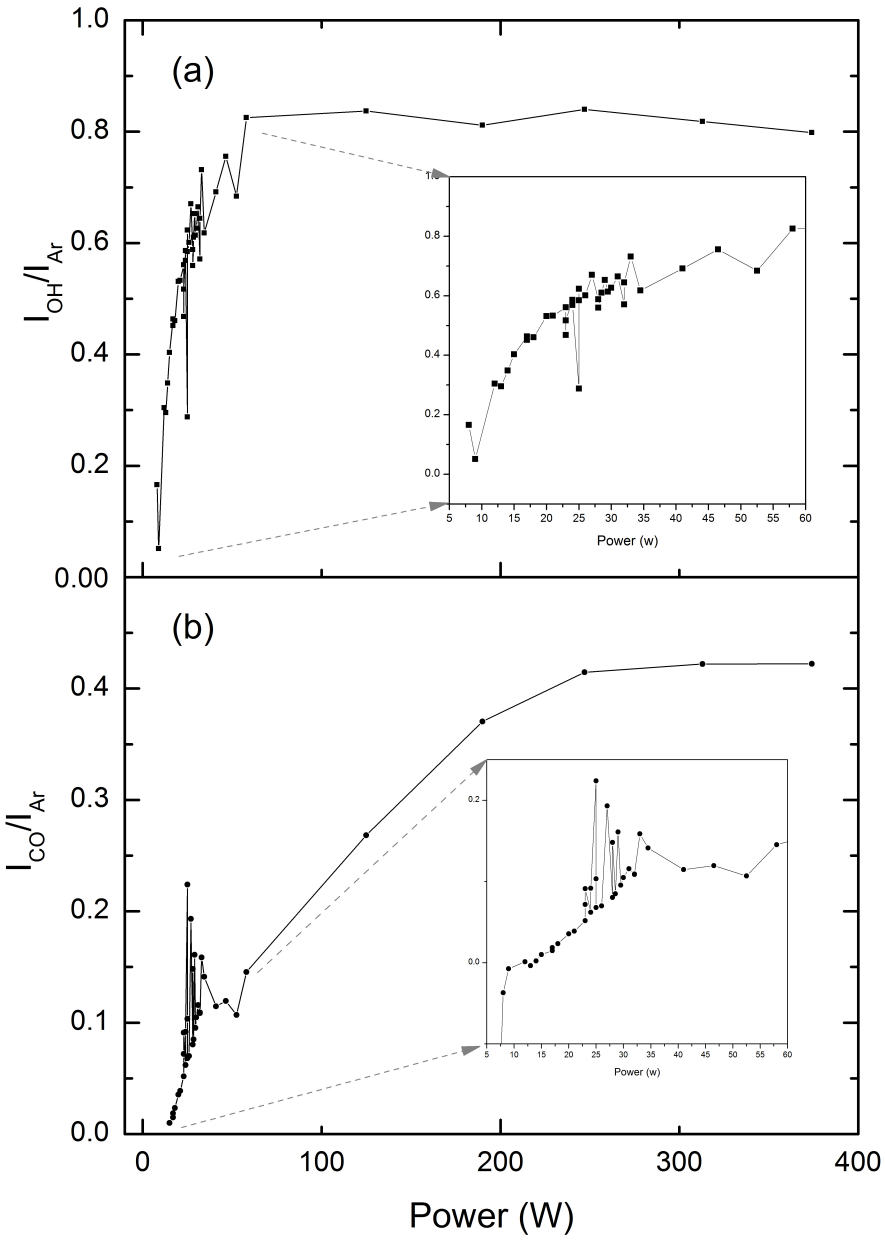

Figure 4.9: (a) OH line at 307 nm to argon line 751 nm (b) CO line 519 nm to argon line 751 nm emission liners were analysed in order to link these results to those of the MS and to the monomer functionality retention.

4.4.5 Surface Behaviour

The effect of plasma power on the film properties was investigated using ATR-FTIR. In order to study the influence of processing parameters on the deposited film structures. Films were deposited at powers of 6.0, 10.0, 16.0, 25.0 W and 50 W on COP substrates. From Fig. 4.10 it can be seen that carboxylic acid functionality increases when depositions take place with an oxygen background gas. Increasing the power beyond 16 W results in a decrease in the carboxylic acid peak and an increase in CO and OH species. A typical FTIR spectrum, which has been labelled with the important functional groups is shown in Fig. 4.10. The scan region of 400 to 4000 cm^{-1} shows the bands CO 1280-1200 cm^{-1}, wagging mode from polymer backbone 1453 cm^{-1}, carbonyl (stretch) at 1700 cm^{-1} which is characteristic of carboxylic groups, polymer CH (stretch) 2950-2850 cm^{-1} and OH (stretch) 3000-3500 cm^{-1}. From Fig. 4.12 and 4.13 it is clear that increasing the applied power to the system has a strong influence on the final deposited surface functional groups. The presence of the COOH functionality has been confirmed by ATR-FTIR acrylic acid as shown in Fig. 4.10. A full description of the surface characteristics of the film is described in Chapter 3.

Fig. 4.11 summarises the behaviour of the functional groups of greatest interest i.e. COOH, CO and OH retained on the surface of the COP. With the increased destruction of the carboxylic acid group, CO and OH species are seen to increase in the deposits. This agrees with previous mass spectrometry and OES plasma phase measurements.

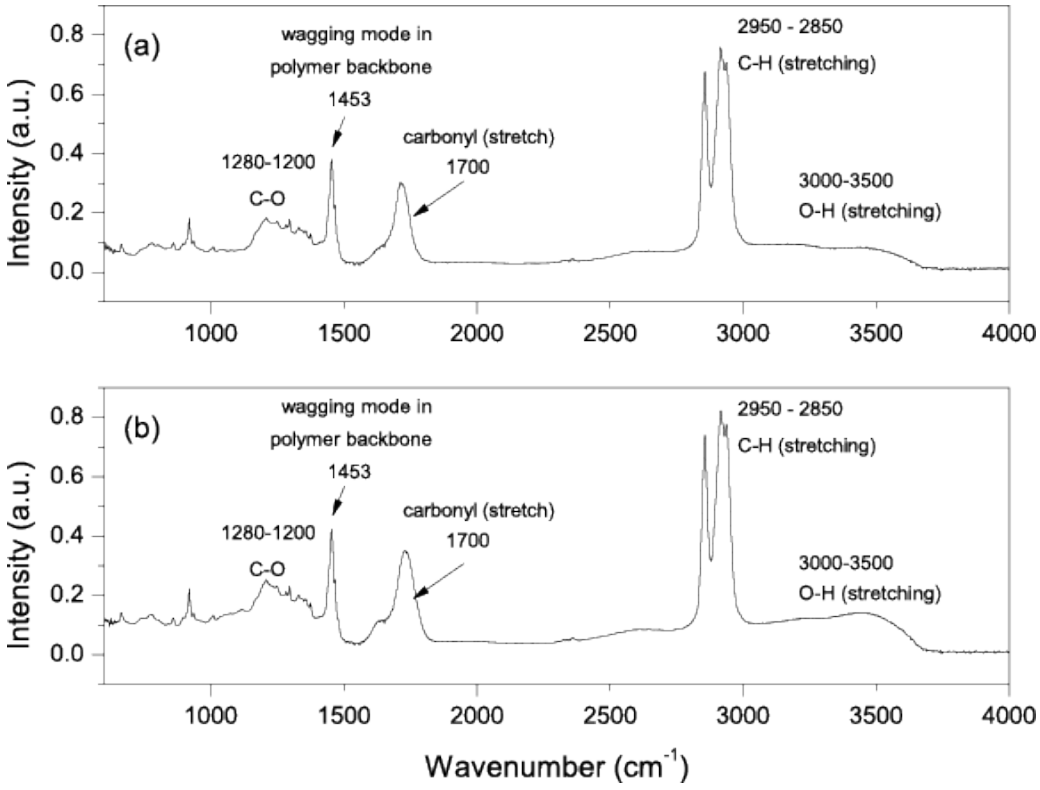

Figure 4.10: ATR-FTIR spectra on COP substrates carried out at rf power of 15W (a) Acrylic acid plasma deposition with argon as background gas. (b) Acrylic acid plasma deposition with oxygen as background gas.

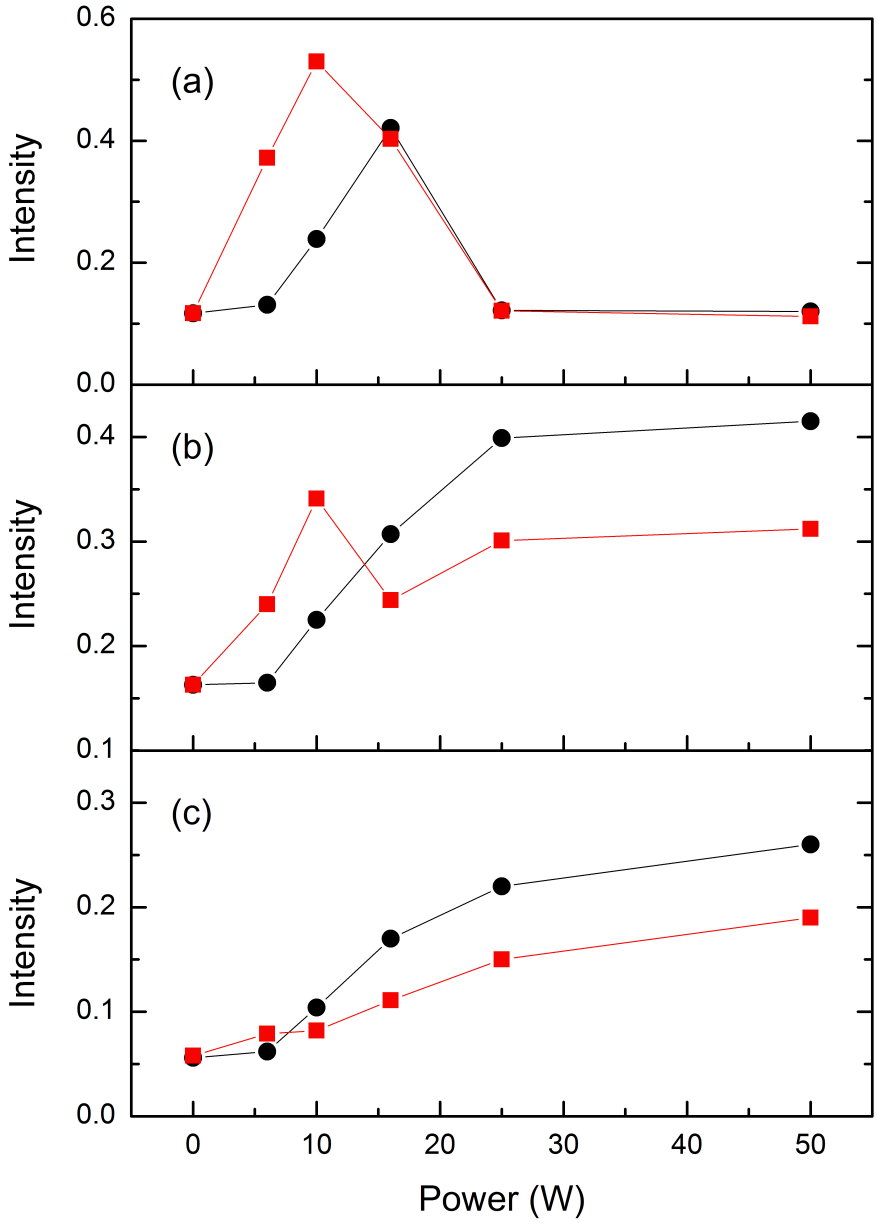

Figure 4.11: (a) COOH (b) CO (c) OH Black circle Oxygen, Red square Argon. In order to study the influence of this acid fragmentation on the deposited film structures, different films have been deposited at different power, 6, 10, 16, 25 and 50 W, respectively

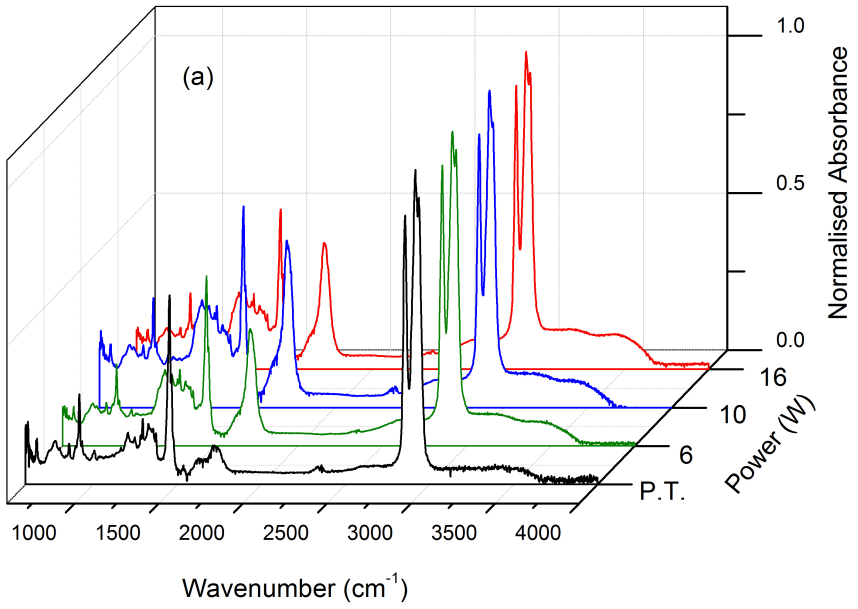

Figure 4.12: Acrylic acid deposition with respect to RF power. Background gas is argon at 50 sccm. (P.T. means plasma treated substrate with no deposition)

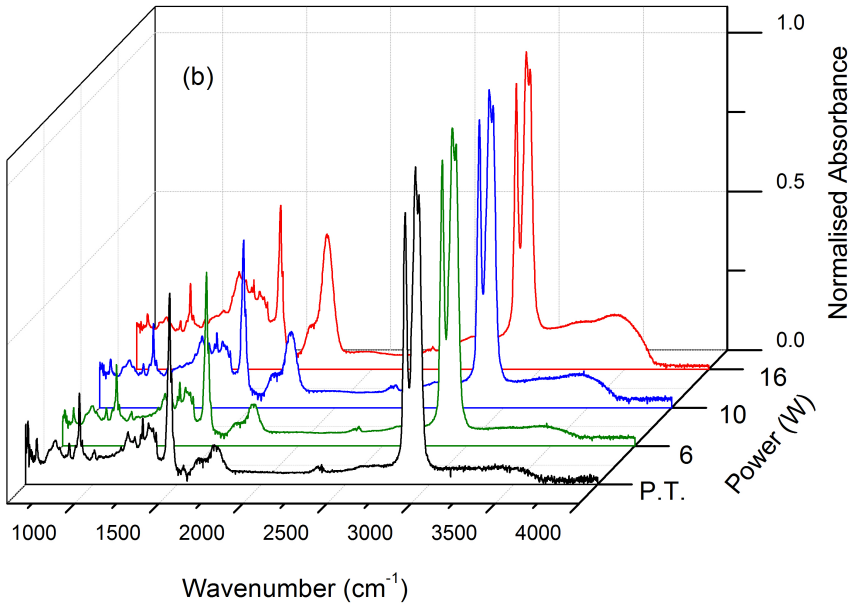

Figure 4.13: Acrylic acid deposition with respect to RF power. Background gas is oxygen at 50 sccm. (P.T. means plasma treated substrate with no deposition)

4.5 Further Discussion

The peaks detected in the plasma mass spectrometry of the neutrals arise from one of two processes. In the first process, the acrylic acid drifts into the EI source and is ionised. The ionised monomer fragments leading to a number of lower mass molecules. These are seen in the EI of acrylic acid at 0 W. In the second process, within the plasma the acrylic acid monomer is excited by energy transfer from an electron. The neutral mass spectrum of argon contains no evidence of significant amounts of radical-neutral or radical-radical combination, except for reactions involving H. The neutral mass spectrum of oxygen contains similar neutral species but with higher concentrations of COO, CO and OH.

At low power, COOH functional group retention is high, with an increase in power there is a loss of functionality. As power increased the concentration of CO and OH functional groups in the deposits increased. This result reflects the fact that as power increases there is more extensive fragmentation taking place in the plasma, greater ion fluxes arriving at surfaces in contact with the plasma and more energy being deposited per ion at the surface.

The combination of mass spectrometry, Langmuir probe and OES analysis with FTIR enables a number of important conclusions to be drawn concerning the plasma polymerisation of acrylic acid. It is possible to make a distinction between conditions of low and high power. This is illustrated most clearly in the mass spectrometry and Langmuir probe results. It was observed that the plasma electron density attains values up to 7×10^{12} m^{-3} for oxygen background and to 4×10^{12} m^{-3} for an argon background under identical pressure and power regime. The plasma density was found to increase strongly with increased power, however T_e was only weakly dependent on the applied power. Overall the results give a picture of relatively cool and low density plasma but with sufficient energy to cause ionisation and maintain the plasma. The data obtained from the probe provides valuable information with regard to process reproducibility.

A number of critical plasma process parameters in PECVD for carboxylic acid us-

ing acrylic acid has been investigated. It has been shown the importance of rf power and pressure in the monomer fragmentation and functional group retention of carboxylic acid groups. Background gases significantly influence the plasma phase i.e. ion energy distributions and monomer breakup. The choice of background gas also affects the final state of the deposited film, although oxygen has a higher ion flux density it is a more suitable substitute for argon as oxidisation processes offers increased level of carboxylic acid functionality.

Appropriate control and knowledge of ion bombardment energy is important in the context of deposition and functionalisation on substrates and offers a method of controlling surface properties. It has been shown that the IEDF can be controlled by choice of process pressure and RF power to the system. Optical emission from species such as CO and OH were observed in acrylic acid and argon discharges. The spectral lines $A^2\Sigma$-X^2, (OH line at 306.4 nm) and $B^1\Sigma$-A^1 (CO line at 519.8 nm) offer a method of tracking fragmentation of the monomer but disagree with the rate of creation of these species. It can be considered that the radical species recombine or are further fragmented before reaching the mass spectrometer. Oxygen in aliphatic molecular structure which is readily liberated in the plasma enviornment, the liberated oxygen acts as a radical scavenger and combines to form stable species.

4.6 Conclusion

In the work presented in this chapter, the acrylic acid plasma was successfully characterised. The experimental techniques employed serve to elucidate the mechanism of plasma polymerisation to the extent that detailed plasma-phase reaction schemes can be proposed. Knowledge of those reactions, plus an understanding of the influence of the plasma process parameters, point the way to the fabrication of 'designer' materials, featuring finely-tuned surface chemistries, for use in specialised applications such as biodevices.

Chapter 5

Deposition of Hexamethyldisiloxane for Bioapplications

5.1 Background

This chapter presents work on the study of hexamethyldisiloxane (HMDSO). HMDSO is an inexpensive and safe organosilicon monomer. It is the most commonly described monomer in the literature with regard to PECVD, particularly in silicon oxide thin film deposition [19, 149–151]. HMDSO has been employed in a wide range of applications using plasma processes [152–156]. Recently HMDSO plasma deposited films have been recognised as useful in bio-applications [157].

This chapter aims to modify a substrate using HMDSO deposited films to control the interaction between a biomaterial (316L stainless steel) and a biological component (fibrinogen). In the case of in-vivo medical implants the importance of the surface prop-

ertires is crucial [120, 158]. Thus, surface properties of deposited films were investigated using FTIR, SIMS, fibrinogen binding measurements and water contact angle measurements. An understanding of the factors that influence fibrinogen adsorption in plasma depositions are elucidated .

5.2 Introduction

It has been found previously that the deposition of HMDSO with and without oxygen background gas results in different film structures [159–161]. A change in oxygen content during plasma deposition significantly alters the species in the plasma and results in higher and lower carbon content in the film. In this work then two different types of coatings were deposited on 316L stainless steel by PECVD. The first deposition used pure HMDSO, the second deposition used oxygen and HMDSO gas mixture. Plasma-phase and surface characterisation was carried out by mass spectroscopy, FTIR, water contact angle measurements and fibrinogen bioresponse was measured using enzyme linked immunosorbent assay (ELISA).

In order to understand the surface behaviour it is necessary to understand the mechanisms that lead to the surface structures, mass spectrometry was employed in this work. Mass spectrometry permitted the investigation of the fragmentation process in the plasma which helped elucidate the reactions at the substrate surface. Electron-impact ionisation is the dominant process for formation of charge carriers in the plasma and it is also responsible for creation of reactive species via dissociative ionisation [162, 163]. Basner *et al.* [164] showed that dissociative ionisation is the principal process for complex molecules like HMDSO, where the dominant channel is the removal of the methyl group CH_3 from HMDSO to produce the ion $Si_2O(CH_3)_5{}^+$.

5.3 Experimental

The films were deposited in the plasma chamber described in section 2.1.1. Two types of films have been deposited, one using pure HMDSO plasma at 100 sccm of HMDSO flow and the other oxygen and HMDSO plasma at 375 sccm oxygen and 12 sccm HMDSO. The system base pressure was 15 mTorr (2 Pa) and the operating pressures for HMDSO and oxygen & HMDSO plasma were 85 mTorr (11 Pa) and 260 mTorr (35 Pa), respectively. The substrates were subjected to 3.0 min plasma pretreatment at an rf power of 250 W with an argon flow rate of 100 sccm and oxygen flow rate of 100 sccm.

Polished 316L stainless steel substrates were obtained from GoodFellow, Huntingdon, England. Polished Si (100) wafers were used as the substrate for FTIR and SIMS measurements.

Mass spectroscopic data were acquired using a Prisma 80 quadrupole mass spectrometer (Pfeiffer vacuum, Berlin, Germany). Mass spectra were recorded in the m/z range of 0 - 200 with a resolution 1.0 amu.

The nature of chemical bonding present in the film was investigated by FTIR spectroscopic system (Perkin ElmerSpectrum GX FTIR) used in transmission mode. The detector and the sample chamber were purged with nitrogen gas during measurements. For all FTIR data presented, silicon wafers were used as substrates and unmodified silicon wafer used as the background. Scans were collected over the 4000 to 400 cm^{-1} wavenumber range with a 32 scan average per image.

A quadrupole Mini Secondary Ion Mass Spectrometry (MiniSIMS Millbrook Instruments Ltd., Manchester, England) was used for surface analysis of samples. A gallium ion beam (6.0 keV) used in positive mode was focused perpendicularly on the samples, resolution of 0.3 amu and a scan area of 100×100 mm^2 was used. The operating pressure in the SIMS chamber was 3.1×10^{-5} Pa

2.0 mL of human fibrinogen (SigmaAldrich) was used at a concentration of 100 mg/mL was added to the stainless steel surface. The uncoated stainless steel was used to make

a calibration series (100, 75, 50, 25, 12.5 ng/mL). The stainless steel controls and the samples were incubated for 60.0 min at room temperature with gentle agitation. The test sample dose was 100 ng/mL. Following incubation, a blocking solution consisting of 1.0% gelatin in phosphate buffered saline (PBS) was added to the fibrinogen coating solution. The blocking solution was incubated for a further 60.0 min at room temperature with gentle agitation. The controls and samples were subjected to three 5.0 min washes in phosphate buffered saline tween (PBST). Washing reduced nonspecific bound material by a combination of the detergent action and dilution. Goat anti-fibrinogen antiserum was diluted with 1% gelatin in PBST. This dilutent reduces non-specific binding. The antiserum incubation was performed for 60.0 min at room temperature with gentle agitation and the samples were washed three times (5.0 min per wash) with PBST. Rabbit antigoat IgG horseradish peroxidase (HRP, SigmaAldrich) conjugate was prepared in 1% gelatin PBST. This was added to the samples and incubated for 30.0 min at room temperature. The samples were then washed three times (5.0 min per wash) with PBST. A final 5.0 min wash with PBST was performed. The purpose of peroxidase conjugation in the secondary antibody was to give a coloured reaction after its reaction with tetramethylbenzidine (3,3′, 5,5′ Tetramethylbenzidine, Sigma T0440), which is proportional to the primary antibody bound to fibrinogen. The reaction could be stopped by adding 1 N sulphuric acid, the colour reaction was measured using Genesys 2 spectrophotometer at 450 nm.

Water contact angles (CA) were measure with a contact angle goniometer (First Ten Angstroms FTA200) using a high purity HPLC grade water (Sigma Aldrich) as the probe liquid. The CA was measured in air at room temperature. Uniform droplets with a volume of 17.24 mL were dropped on the surface and after the drops had reached a stable configuration, approximately 15 s, digital images of the drops were recorded. Using FTA32 Video 2.0 software CAs were calculated from the images. Three data points were taken for each sample and the water CA were measured in different locations on the sample.

5.4 Results and Discussion

5.4.1 Mass Spectrometry

The mass spectrometry spectra are shown in Figs. 5.1, 5.2, 5.3, showing the fragmentation of HMDSO for rf powers, 0 W (no plasma ignition), 100 W and 300 W, respectively; the electron energy of mass spectrometer ioniser was 40 eV for all measurements. In the pure HMDSO spectrum (Figs. 5.1 a(i), 5.2 b(i), 5.3 c(i)) various fragments appear, the strongest peak at m/z 147 is attributed to $Si_2O(CH_3)_5{}^+$ which is produced by dissociative ionisation of HMDSO under dissociation of a methyl group in agreement with Basner *et al.* and Jiao *et al.* [164**?**]. Table 5.1 shows the different species that appear in the mass spectrometry results. These results are in agreement with those found in previous studies of HMDSO plasmas [165, 166].

The addition of oxygen to HMDSO in the plasma results in the spectra shown in Fig. 5.1 a(ii), 5.2 b(ii), 5.3 c(ii). A contrast is evident between the pure HMDSO plasma and the oxygen and HMDSO plasma in which the latter exhibited no species above m/z 44 and a change in ratios of the lower mass species. The new species that appeared with the addition of oxygen include m/z 44 (SiO^+), m/z 32 ($O_2{}^+$), and m/z 16 (O^+), peaks corresponding to hydrocarbon species bonded to Si disappeared. This change in the lower mass range can be concluded to be that the produced species are the result of oxidation reactions. The intensity of of hydrocarbon species is very low compared to oxygenated species which indicate that oxidation reactions are dominant in oxygen & HMDSO plasmas.

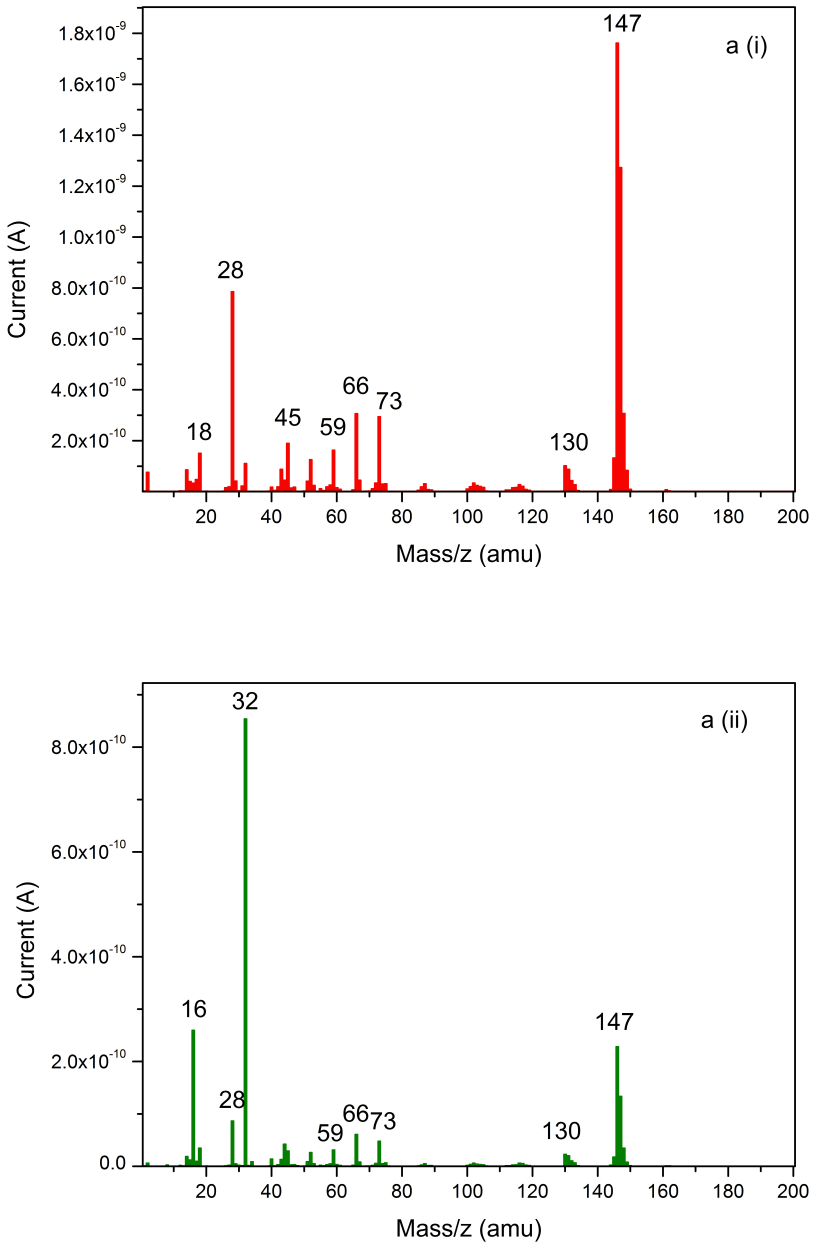

Figure 5.1: A (i) Pure HMDSO without plasma ignition, (ii) Oxygen and HMDSO (365:12) without plasma ignition

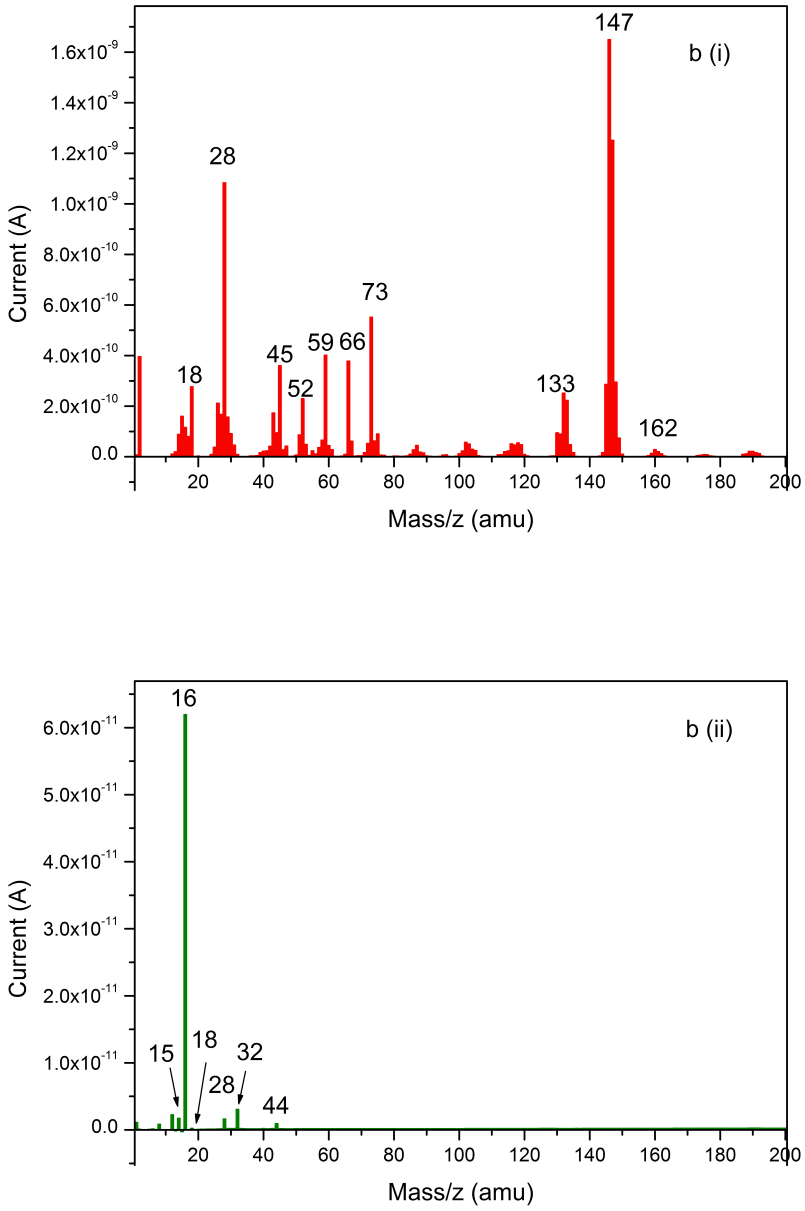

Figure 5.2: B (i) Pure HMDSO at 100 W rf power, (ii) Oxygen and HMDSO (365:12) 100 W rf power

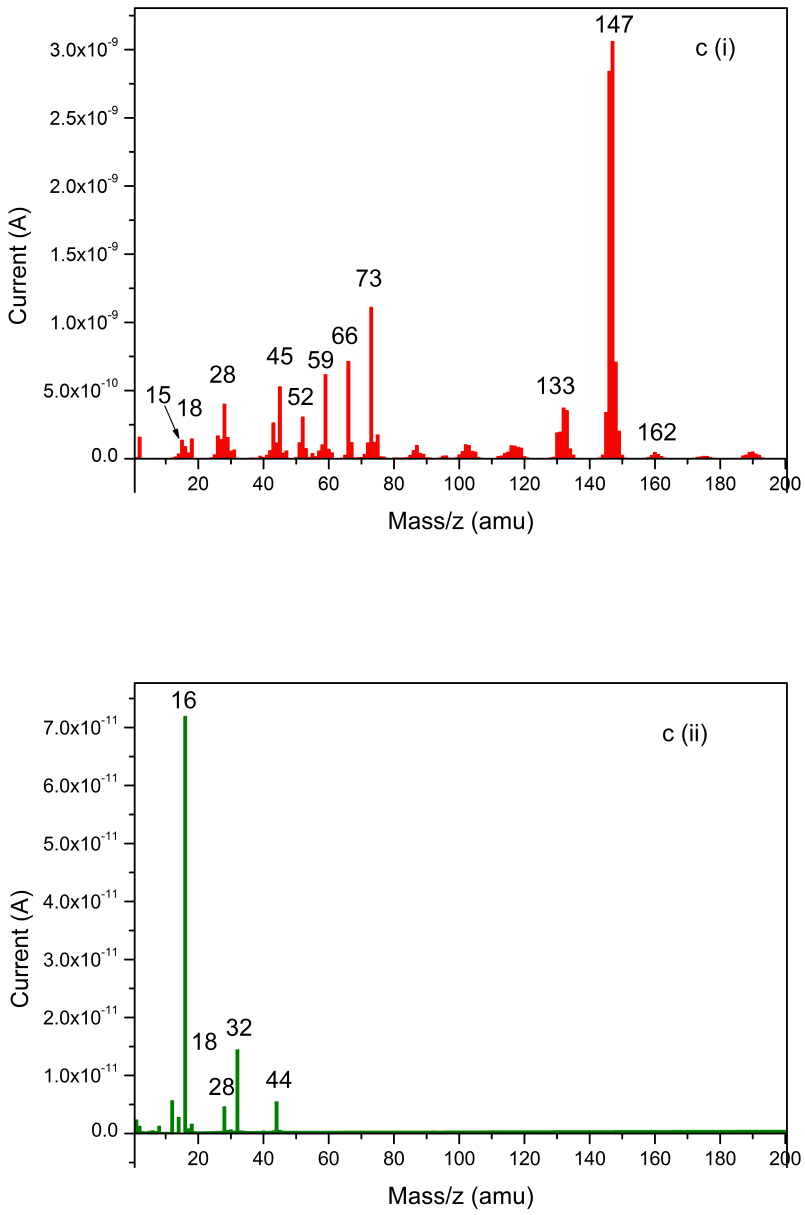

Figure 5.3: C (i) Pure HMDSO at 300 W rf power, (ii) Oxygen and HMDSO (365:12) 300 W rf power

Table 5.1: Chemical assignment of HMDSO fragmentation.

Mass (amu)	Assignment	Mass (amu)	Assignment
15	$SiCH_3^+$	59	$SiC_2H_7^+$
16	$SiCH_4^+$ and/or O^+	66	$Si_2OC_4H_{12}^+$
18	H_2O^+	73	Si_2OH^+
28	$C_2H_4^+$ and/or Si^+	73	$(CH_3)_3Si^+$
32	O_2^+	131	$Si_2OC_4H_{11}^+$
43	$SiCH_3^+$	133	$Si_2OC_4H_{13}^+$
44	COO^+ and/or SiO^+	147	$Si_2OC_5H_{15}^+$
45	$SiOH^+$	162	$Si_2OC_6H_{18}^+$
52	$Si_2OC_2H_8^+$		

5.4.2 Surface Analysis

The composition of the coatings determined through FTIR is shown in Fig. **??**. The characteristic peaks of Si-O-Si appear at 450 cm^{-1}, 800 cm^{-1} and 1070 cm^{-1}. The peak at 450 cm^{-1} corresponds to the symmetric stretching vibration of Si-O-Si, 800 cm^{-1} corresponds to bending vibration of Si-O-Si and 1070 cm^{-1} peak corresponds to asymmetric stretching vibration of Si-O-Si. The peak at 1278 cm^{-1} corresponds to the symmetric deformation vibration of methyl silyl, the asymmetric stretching vibration of CH in Si-CH_3 occurs at 2960 cm^{-1}, symmetric stretching vibration of CH in Si-CH_3 occurs at 2905 cm^{-1} and the Si-CH_3 rocking vibration occurs at 840 cm^{-1}. Peaks at 930 cm^{-1}, 3380 cm^{-1} and 3650 cm^{-1} corresponds to hydroxyl groups bonded to Si . SiC stretching vibration occurs at 668 cm^{-1} and 800 cm^{-1}. The peak at 801 corresponds to Si-C and Si-(CH_3) vibrations.

For the films deposited with pure HMDSO plasma, the methyl silyl peaks at 845 cm^{-1}, 1278 cm^{-1} and 2965 cm^{-1} are large and negligible for the films deposited under the oxygen & HMDSO plasma. As the oxygen flow is increased, the methyl group present in HMDSO is oxidised to carbon dioxide and water. Additionally, as the oxygen is increased the fragmented molecules from $(CH_3)_3$-Si-O-Si-$(CH_3)_3$ are oxidised to carbon dioxide and water, stripping off the hydrocarbons from Si, which accounts for decreased methyl silyl peak with increase in oxygen flow. This result is in agreement with the observed mass spectroscopic studies. As the samples coated in a pure HMDSO plasma is rich in hydrocarbon, the resultant film is called, polymer-like and for deposited films coated using oxygen & HMDSO plasmas which are rich in Si-O-Si network are called, silica-like.

It is observed from the FTIR spectra Fig. **??** that the polymer-like film is rich in methylsilyl (1278 and 840 cm^{-1}) components as well as SiO bonds. In Fig. 5.4a the surface SIMS analysis shows that the polymer-like film has a significantly high amount of methlsily group at m/z = 43 and $SiOCH_2$ at m/z = 56 scanned in the positive SIMS mode. However, for silica-like films Fig. 5.4b shows these peaks are reduced and the SiO peak at m/z = 44 is predominant. Thus, the SIMS analysis is in agreement with the FTIR results.

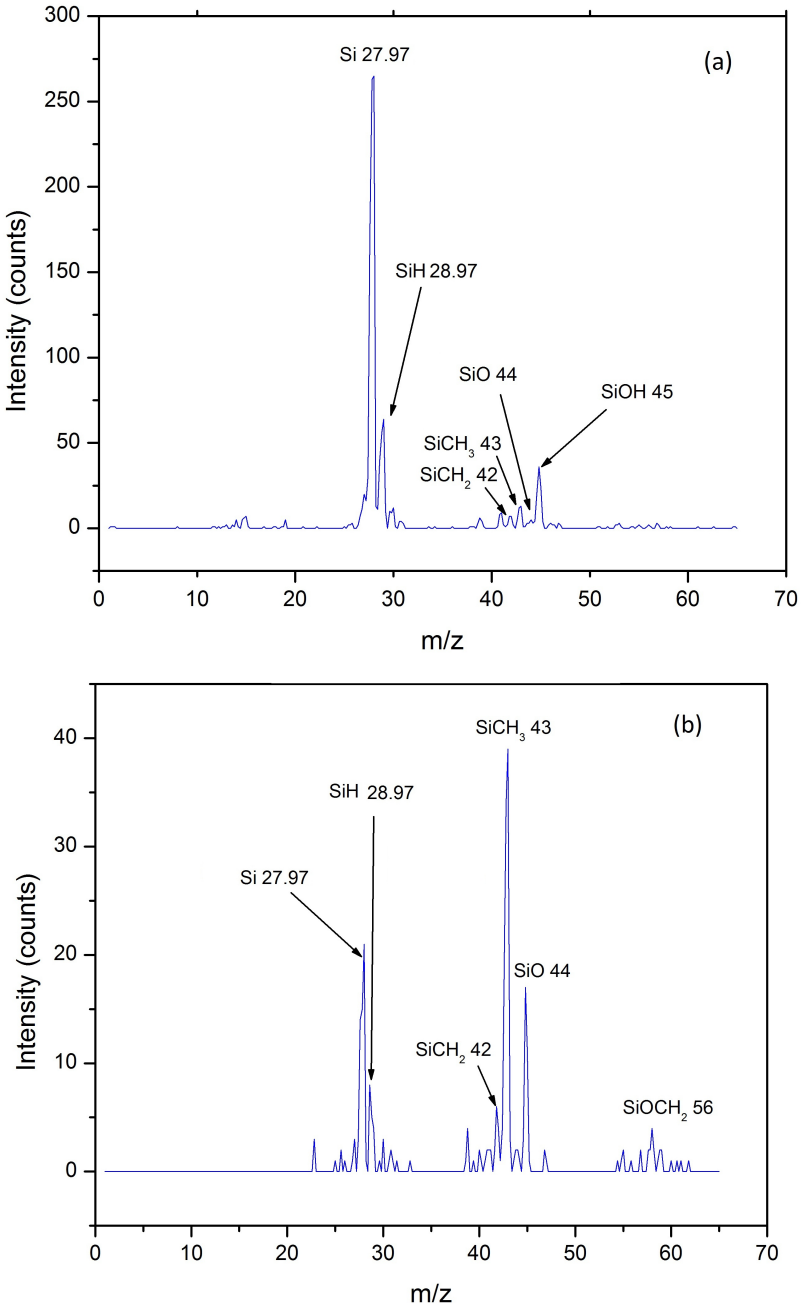

Figure 5.4: SIMS analysis of (a) silica-like coatings (b) polymer-like coatings, taken in positive SIMS mode. Investigations using SIMS demonstrates the polymer like film contains high amounts of SiCH3

5.4.3 Fibrinogen Adsorption

Fibrinogen adsorption was evaluated using an enzyme immunosorbent assay (ELISA) [167]. The ELISA method determines the identity and quantity of biological species such as antibodies in bodily fluids or tissues. As shown in Fig. 5.5, fibrinogen adsorption was higher on the polymer-like film with a binding percentage relative to 316L stainless steel of 42%. Silica-like films demonstrated a binding of 23%. With regards to wettability, according to literature [58, 60], it is expected that fibrinogen adsorption be minimum at hydrophilic surfaces and to increase with increasing hydrophobicity. However, untreated 316L stainless steel with a CA of 72° has adsorbed a higher amountof fibrinogen than the hydrophobic polymer-like coating. Additionally, it has been demonstrated elsewhere that metallic nature of the steel surface leads to fibrinogen binding through charge transfer mechanisms [168, 169] which explains the fibrinogen binding of the 316L steel.

Several groups have reported the effects of surface hydrophobicity on protein denaturation. For example, Wertz et al. [170] studied the spreading of bovine serum albumin (BSA) and human fibrinogen on hydrophobic and hydrophilic selfassembled monolayers (SAMs) using total internal reflection fluorescence. For both proteins, fast and extensive spreading was observed on the hydrophobic surface (greater increase of protein footprint as a function of time), whereas very little spreading was observed on the hydrophilic surface.

At low protein concentrations, however, the quantity of adsorbed proteins was greater on a hydrophobic surface. Although faster spreading of protein occurred on the hydrophobic surface, the proteins spread to a far lesser extent at low protein concentration. These studies contradict several general findings that greater protein surface coverage was obtained on hydrophobic surfaces, where protein spreading is usually not accounted for [171]. This work demonstrates fibrinogen adsorption is

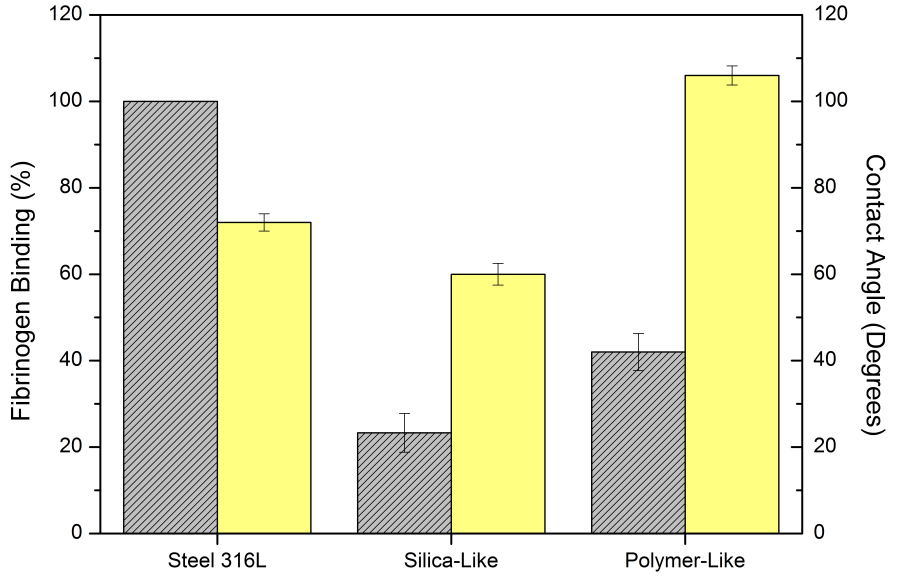

Figure 5.5: Fibrinogen adsorption (grey lined), Contact angle data (solid yellow).Fibrinogen adsorption of the coatings deposited on 316L stainless steel measured using enzyme immunosorbent assay showed adsorption on polymer-like coating was 42% relative to untreated stainless steel, silica-like coatings showed adsorption of 23%. Measurements of the water drop contact angle were also made on these investigations. Typical contact angles for the deposited films were 60 for silica-like and 106 for polymer-like coatings.

5.4.4 Contact Angle

Water contact angles (CA) were investigated and are displayed in Fig. 5.5. The polymer-like film surface has a water contact angle of 106°. The hydrophobic nature of the polymer-like $SiO_xC_yH_z$ films, deposited from pure HMDSO, is due to the presence of methyl groups and hydrocarbons in the film. It has been shown previously [172] that film hydrophobicity depends on the oxygen concentration in the plasma. So, by reducing the hydrocarbons through an increase in the oxygen content it was possible to create polarity at the surface, hence increased hydrophilicity. The SiO_x film has a water contact angle of 60°, as a consequence of the formation of a polar Si-O-Si network. This network allows the formation of hydrogen bonds with water molecules, resulting in lower water contact angles. According to literature [58, 60], fibrinogen adsorption is expected to be at a minimum on hydrophilic surfaces and to increase with increasing hydrophobicity. However, untreated 316L stainless steel with a CA of 72° has adsorbed a higher amount of fibrinogen than the hydrophobic polymer-like coating. Apart from the wettability, another factor must have been contributed for the observed higher adsorption in stainless steel. It has been demonstrated by Huang et al. [169] that the metallic nature of the steel surface leads to fibrinogen binding through charge transfer mechanisms - hence the adsorption of fibrinogen on the stainless steel 316L

5.5 Further Discussion

Mass spectrometry results effectively demonstrate how reactive species produced can be tailored depending on background gas and their quantities altered by rf power input to the plasma, allowing tailored selection of surface properties.

The mass spectrometry analysis of the plasma showed that in the formation of polymer-like coatings the plasma predominantly contains silicon bonded to methoxy, ethoxy groups and silanols. SiO^+ and O_2^+ species were dominant during the silica-like film formation

due to oxidation of the precursor molecule with the oxygen acting as a radical scavenger. As the discharge power was increased, the fragmentation of the monomer increased. As demonstrated in section 4.4.2 higher rf power enhances electron densities and the concentration of reactive fragments grows with the discharge power due to increased particle collisions.

At high rf power of oxygen and HMDSO, the dissociation process is increased, which results in higher oxygen content and thus more oxidation reactions can take place. A relative increase in some reactive species is observed e.g. m/z 44 and 28. Additionally, the addition of oxygen to the plasma may serve to increase the number of active sites on the surface for radical adsorption.

Two different types of silicon-based coatings with varying surface characteristics have been deposited from HMDSO by PECVD. FTIR analysis indicate that the polymer-like film spectrum included several new bands which were absent in the silica-like spectrum. Both surfaces exhibited a strong SiO peak at 1070 cm^{-1} but the polymer-like coating included SiCH and CH bands. Characterisation of the different surfaces is also achieved using SIMS, which demonstrated strong emission of SiO and SiOH in the silica-like coating and $SiCH_3$, $SiCH_2$, SiO and $SiOCH_2$ in the polymer-like coating. SIMS analysis confirmed results attained from the FTIR analysis i.e Pure HMDSO deposition results in a polymer like deposition and oxygen & HMDSO results in a silica-like deposition.

Medical applications should have an excellent barrier property that prevents direct contact of the blood with thrombogenic stainless steel surface and also offer imperturbable surface characteristics in a harsh biological environment. Fibrinogen adsorption of the coatings deposited on 316L stainless steel measured using ELISA showed adsorption on polymer-like coating was 42% relative to untreated stainless steel, silica-like coatings showed adsorption of 23%. Thus silica-like coatings are promising as coatings for in-vivo medical applications.

Measurements of the water drop contact angle were also made on these investigations.

Typical contact angles for the the deposited films were 60° for silica-like and 106° for polymer-like coatings. The increasing concentrations of oxygen in the plasma gas results in a decrease of this contact angle. The surface wettability, being a property that relies on the surface chemical composition of the film, becomes increasingly enhanced by the oxygen plasma process that produces a strong modification of the film composition but concentrated in the surface region.Labarre [173] showed that adsorbed fibrinogen proteins undergo conformational changes after getting adsorbed on the implant surface. Studies have demonstrated that fibrinogen conformational change takes place on hydrophobic surfaces, where the adsorbed fibrinogen takes up an extended conformation to facilitate exposure of its hydrophobic components, thus enabling more protein adsorption on hydrophobic surfaces [174]. Malmsten et al. [175] showed that the adsorption of proteins on hydrophilic and hydrophobic surfaces depends on the nature of proteins.

5.6 Conclusion

In the work presented in this chapter, surfaces of 316L stainless steel substrates were successfully modified using plasma enhanced chemical vapour deposition. An antifouling fibrinogen coating was produced for applications in in-vivo bioimplants using plasma polymerised HMDSO. The film deposition was attempted with different gas mixtures of a) pure HMDSO monomer vapour and b) HMDSO monomer vapour with oxygen. Plasma and surface characteristics were investigated using a combination of techniques; mass spectrometry, FTIR, SIMS, fibrinogen adsorption techniques and water contact angles. The wetting potential of the substrates was found to be dependent on the presence of oxygen in the deposition. The fibrinogen adsoroption was expected to be at a minimum on hydrophilic surfaces and to increase with increasing hydrophobicity. However, it was found that untreated 316L stainless steel which is more hydrophilic adsorbed a higher amount of fibrinogen than the hydrophobic polymer-like coating.

Chapter 6

Conclusion

6.1 Summary of Thesis

This work gave a contribution to the complex argument of plasma polymerisation presenting; a novel surface that exhibits high signal to noise ratio, long term stability, that is reproducible, simple to manufacture and doesn't alter the bulk properties of the substrate. The work presented in this thesis can be broadly labelled as an investigation of plasma enhanced chemical vapour depostition for applications in biodevices, including bioassays and bioimplants. The results can be further classified into two catergories; the first concerned the development of a carboxylated surface that exhibited favourable properties for biosensors, included in this first catergory is the characterisation of acrylic acid plasma, which led to better understandings of the processes that lead to carboxy functional group retention of the surface of COP substrates and the influence power and background gases oxygen and argon.

The second class of experiment saw the investigation of non-fouling coatings, with particlular interest in reducing fibrinogen adsorption on medical grade stainless steel. A thourough characterisation of both the surface and the plasma elucidated important pa-

rameters that help in the reduction of thrombosis effects of in-vivo implants. This includes the development of polymer-like and silica-like coatings from hexamethyldisiloxane.

PECVD provides an effective means for precisely tailoring surface properties such as hydrophobicity, type and density of functional groups, and for the incorporation of a diverse array of biomolecules by independently coupling different molecules selectively based on compatible surface chemistries, as demonstrated by the covalent attachement of amino terminated ssDNA on carboxy surfaces and the development of non-fouling coatings.

The thesis has described the creation of a plasma deposited surface that exhibited low NSA through a combination of a tetraehtyloxysilane bonding layer and acrylic acid functional layer. An extensive investigation was undertaken to characterise the surface properties of the deposited film. The covalent attachment of biomarkers has been demonstrated, with a 16.4% coverage of COOH. The stability and resistance to washing was examined and the influence of surface morphology discussed. The plasma characterisation and investigation of acrylic acid plasma under various plasma conditions that leads to carboxy retention, growth mechanisms were discussed.

The development of an anti-fouling surface for in-vivo implantations using hexamethyldisiloxane. The surface was characterised and an investigation into the plasma phase was undertaken. It has been demonstrated that a reduction in the adsorption of fibrinogen can be achieved by tailoring surface properties with 23% binding on a silica-like coating compared to 42% on a polymer-like coating. Fibrinogen adsorption was expected to be at a minimum on hydrophilic surfaces and to increase with hydrophobicity. However, it was found that untreated 316L stainless steel which is more hydrophilic adsorbed a higher amount of fibrinogen that the hydrophobic polymer-like coating.

6.2 Future Work

The TEOS and acrylic acid deposited film developed in this thesis is now being employed by the Biomedical Dignositics Institute, Dublin City University, Ireland. Both the deposited film and the plasma phase have been finely tuned and characterised, this has permitted the deposition process to be moved relatively easily to a new plasma process chamber. Experiments have begun in a new plasma chamber (Oxford Instruments Plasma Etch and Deposition, Plasma Pro), this chamber allows for finer control over monomer flow rates, faster pump down times and greater throughput of substrates. It is hoped that with the extra sensitivity offered by this chamber that the process can be improved further.

The TEOS and acrylic acid deposited film discussed in this thesis has been discussed for use in 'labelled' biosensors. But the deposited film can be used on gold surfaces with appropriate linker chemistry this would allow the coatings to be used for both label free surface plasmon resonance based detection as well as on fluorescence based detection.

The hydration of the surface layer, orientation of the surface bound biomolecules (proteins and DNA) and their activity are crucial factors determining the bioassay performance and further investigation is required into these areas. Neutron reflection will allow the determination of the swelling of the coatings in-situ, the distribution of water through the layer and changes consequent upon biomolecular interaction and to deduce conformation of surface-bound biomolecules through the thickness increment upon their binding. Neutron reflectivity studies will help understand the surface-biomolecule interaction.

Superior control and manipuatlion of plasma chemistry is important, one method is the implementation of a dual frequency plasma source which can offer better control and improved surface properties. Dual frequency sources permit independent control of ion energy and ion flux, they have not as of yet been employed in the study of acrylic acid deposition for biodevices but have been applied in other work [176].

Future investigations of process control could include a more comprehensive process model as the current model may be an over simplification of the actual chemistry in the discharge. In order to analyse these, a reliable mass detection system would be required. Techniques such as laser induced fluorescence could be employed to get an absolute density of species and this in turn could be used to calibrate other sensors such as the mass spectrometer.

It is expected that the use of plasma processes will continue to expand, because they have unique capabilities, are economically attractive and are 'friendly' towards the environment.

Bibliography

[1] H. Yasuda. *Luminous chemical vapor deposition and interface engineering.* CRC, 2005.

[2] H.F. Sterling and R.C.G. Swann. Chemical vapour deposition promoted by rf discharge. *Solid-State Electronics*, 8(8):653–654, 1965.

[3] H. Yasuda. Plasma for modification of polymers. *Journal of Macromolecular ScienceChemistry*, 10(3):383–420, 1976.

[4] H. Yasuda, M.O. Bumgarner, H.C. Marsh, and N. Morosoff. Plasma polymerization of some organic compounds and properties of the polymers. *Journal of Polymer Science: Polymer Chemistry Edition*, 14(1):195–224, 1976.

[5] A.R. Reinberg. Plasma deposition of inorganic thin films. *Annual Review of Materials Science*, 9(1):341–372, 1979.

[6] E.M. Liston, L. Martinu, and M.R. Wertheimer. Plasma surface modification of polymers for improved adhesion: a critical review. *Journal of adhesion science and technology*, 7(10):1091–1127, 1993.

[7] J. Behnisch, H. Zimmermann, and J. Friedrich. Topokinetics of the polyene formation in poly (vinyl chloride) films during treatment with nonoxidative plasma. *International Journal of Polymeric Materials*, 16(1-4):139–142, 1992.

[8] E.E. Johnston and B.D. Ratner. Surface characterization of plasma deposited organic thin films. *Journal of electron spectroscopy and related phenomena*, 81(3):303–317, 1996.

[9] B.D. Ratner. Plasma deposition for biomedical applications: a brief review. *Journal of Biomaterials Science, Polymer Edition*, 4(1):3–11, 1993.

[10] R. Förch, Z. Zhang, and W. Knoll. Soft plasma treated surfaces: tailoring of structure and properties for biomaterial applications. *Plasma processes and polymers*, 2(5):351–372, 2005.

[11] K.S. Siow, L. Britcher, S. Kumar, and H.J. Griesser. Plasma methods for the generation of chemically reactive surfaces for biomolecule immobilization and cell colonization-a review. *Plasma processes and polymers*, 3(6-7):392–418, 2006.

[12] I. Bisson P. Frey B. Gupta, C. Plummer and J. Hilborn. Plasma-induced graft polymerization of acrylic acid onto poly(ethylene terephthalate) films: characterization and human smooth muscle cell growth on grafted films. *Biomaterials*, 23(3):863 – 871, 2002.

[13] F. Rossi and P. Colpo. Plasma processes and applications in nanobiotechnology. *Journal of Physics: Conference Series*, 252(1):012001, 2010.

[14] B. Gupta, C. Plummer, I. Bisson, P. Frey, and J. Hilborn. Plasma-induced graft polymerization of acrylic acid onto poly (ethylene terephthalate) films: characterization and human smooth muscle cell growth on grafted films. *Biomaterials*, 23(3):863–871, 2002.

[15] J.D. Whittle, N.A. Bullett, R.D. Short, C.W.I. Douglas, A.P. Hollander, and J. Davies. Adsorption of vitronectin, collagen and immunoglobulin-g to plasma polymer surfaces by enzyme linked immunosorbent assay (ELISA). *J. Mater. Chem.*, 12(9):2726–2732, 2002.

[16] L. De Bartolo, S. Morelli, L.C. Lopez, L. Giorno, C. Campana, S. Salerno, M. Rende, P. Favia, L. Detomaso, R. Gristina, et al. Biotransformation and liver-specific functions of human hepatocytes in culture on RGD-immobilized plasma-processed membranes. *Biomaterials*, 26(21):4432–4441, 2005.

[17] Z.F. Li, E.T. Kang, K.G. Neoh, and K.L. Tan. Covalent immobilization of glucose oxidase on the surface of polyaniline films graft copolymerized with acrylic acid. *Biomaterials*, 19(1-3):45 – 53, 1998.

[18] D. B. Haddow, D. A. Steele, R. D. Short, R. A. Dawson, and S. Macneil. Plasma-polymerized surfaces for culture of human keratinocytes and transfer of cells to an in vitro wound-bed model. *Journal of Biomedical Materials Research Part A*, 64A(1):80–87, 2003.

[19] M.R. Alexander, R.D. Short, F.R. Jones, W. Michaeli, and C.J. Blomfield. A study of HMDSO/O2 plasma deposits using a high-sensitivity and-energy resolution XPS instrument: curve fitting of the Si 2p core level. *Applied surface science*, 137(1-4):179–183, 1999.

[20] D.B. Haddow, R.M. France, R.D. Short, S. MacNeil, R.A. Dawson, G.J. Leggett, and E. Cooper. Comparison of proliferation and growth of human keratinocytes on plasma copolymers of acrylic acid/1, 7-octadiene and self-assembled monolayers. *Journal of biomedical materials research*, 47(3):379–387, 1999.

[21] R. Daw, S. Candan, A.J. Beck, A.J. Devlin, I.M. Brook, S. MacNeil, R.A. Dawson, and R.D. Short. Plasma copolymer surfaces of acrylic acid/1, 7 octadiene: Surface characterisation and the attachment of ROS 17/2.8 osteoblast-like cells. *Biomaterials*, 19(19):1717–1725, 1998.

[22] A.J. Beck, F.R. Jones, and R.D. Short. Plasma copolymerization as a route to the fabrication of new surfaces with controlled amounts of specific chemical functionality. *Polymer*, 37(24):5537–5539, 1996.

[23] L. Detomaso, R. Gristina, G.S. Senesi, R. d'Agostino, and P. Favia. Stable plasma-deposited acrylic acid surfaces for cell culture applications. *Biomaterials*, 26(18):3831–3841, 2005.

[24] V. Sciarratta, U. Vohrer, D. Hegemann, M. Müller, and C. Oehr. Plasma functionalization of polypropylene with acrylic acid. *Surface and Coatings Technology*, 174:805–810, 2003.

[25] R. Jafari, M. Tatoulian, W. Morscheidt, and F. Arefi-Khonsari. Stable plasma polymerized acrylic acid coating deposited on polyethylene (PE) films in a low frequency discharge (70 khz). *Reactive and Functional Polymers*, 66(12):1757–1765, 2006.

[26] B.R. Pistillo, A. Perrotta, R. Gristina, G. Ceccone, M. Nardulli, R. d'Agostino, and P. Favia. Water resistant ethylene/acrylic acid plasma-deposited coatings. *Surface and Coatings Technology*, 2011.

[27] T.M. Ko, J.C. Lin, and S.L. Cooper. Surface characterization and platelet adhesion studies of plasma-carboxylated polyethylene. *Journal of colloid and interface science*, 156(1):207–217, 1993.

[28] R. Cueff, G. Baud, M. Benmalek, JP Besse, JR Butruille, and M. Jacquet. X-ray photoelectron spectroscopy studies of plasma-modified PET surface and alumina/PET interface. *Applied surface science*, 115(3):292–298, 1997.

[29] I. Gancarz, G. Pozniak, and M. Bryjak. Modification of polysulfone membranes CO_2 plasma treatment. *European polymer journal*, 35(8):1419–1428, 1999.

[30] N. Inagaki, S. Tasaka, and K. Hibi. Surface modification of Kapton film by plasma treatments. *Journal of Polymer Science Part A: Polymer Chemistry*, 30(7):1425–1431, 1992.

[31] M.S. Sheu, A.S. Hoffman, B.D. Ratner, J. Feijen, and J.M. Harris. Immobilization of polyethylene oxide surfactants for non-fouling biomaterial surfaces using an argon glow discharge treatment. *Journal of adhesion science and technology*, 7(10):1065–1076, 1993.

[32] P. Kingshott and H.J. Griesser. Surfaces that resist bioadhesion. *Current Opinion in Solid State and Materials Science*, 4(4):403–412, 1999.

[33] B. Lassen, K. Holmberg, C. Brink, A. Carlen, and J. Olsson. Binding of salivary proteins and oral bacteria to hydrophobic and hydrophilic surfaces in vivo and in vitro. *Colloid & Polymer Science*, 272(9):1143–1150, 1994.

[34] H. Chen, Z. Zhang, Y. Chen, M.A. Brook, and H. Sheardown. Protein repellant silicone surfaces by covalent immobilization of poly (ethylene oxide). *Biomaterials*, 26(15):2391–2399, 2005.

[35] K. Uchida, H. Otsuka, M. Kaneko, K. Kataoka, and Y. Nagasaki. A reactive poly (ethylene glycol) layer to achieve specific surface plasmon resonance sensing with a high S/N ratio: the substantial role of a short underbrushed peg layer in minimizing nonspecific adsorption. *Analytical chemistry*, 77(4):1075–1080, 2005.

[36] H. Ogi, Y. Fukunishi, H. Nagai, K. Okamoto, M. Hirao, and M. Nishiyama. Nonspecific-adsorption behavior of polyethylenglycol and bovine serum albumin studied by 55-MHz wireless-electrodeless quartz crystal microbalance. *Biosensors and Bioelectronics*, 24(10):3148–3152, 2009.

[37] M.M. Dudek, R.P. Gandhiraman, C. Volcke, S. Daniels, and A.J. Killard. Evaluation of a Range of Surface Modifications for the Enhancement of Lateral Flow Assays on Cyclic Polyolefin Micropillar Devices. *Plasma Processes and Polymers*, 6(10):620–630, 2009.

[38] I. Beaulieu, M. Geissler, and J. Mauzeroll. Oxygen plasma treatment of polystyrene

and Zeonor: substrates for adhesion of patterned cells. *Langmuir*, 25(12):7169–7176, 2009.

[39] M. Morra, E. Occhiello, and F. Garbassi. Hydrophobic recovery and misting behavior of plasma treated PS and PC surfaces. *Die Angewandte Makromolekulare Chemie*, 189(1):125–136, 1991.

[40] M. Poksinski and H. Arwin. Total internal reflection ellipsometry: ultrahigh sensitivity for protein adsorption on metal surfaces. *Optics letters*, 32(10):1308–1310, 2007.

[41] M. Advincula, X. Fan, J. Lemons, and R. Advincula. Surface modification of surface sol-gel derived titanium oxide films by self-assembled monolayers (SAMs) and nonspecific protein adsorption studies. *Colloids and Surfaces B: Biointerfaces*, 42(1):29–43, 2005.

[42] K. Rechendorff, MB Hovgaard, M. Foss, VP Zhdanov, and F. Besenbacher. Enhancement of protein adsorption induced by surface roughness. *Langmuir*, 22(26):10885–10888, 2006.

[43] B. Walivaara, B.O. Aronsson, M. Rodahl, J. Lausmaa, and P. Tengvall. Titanium with different oxides: in vitro studies of protein adsorption and contact activation. *Biomaterials*, 15(10):827–834, 1994.

[44] D. Hegemann, E. Körner, and S. Guimond. Plasma polymerization of acrylic acid revisited. *Plasma Processes and Polymers*, 6(4):246–254, 2009.

[45] R.D. Short and D.A. Steele. Testing the hypothesis: Comments on plasma polymerisation of acrylic acid revisited. *Plasma Processes and Polymers*, 7(5):366–370, 2010.

[46] D. Hegemann, E. Körner, and S. Guimond. Reply to:testing the hypothesis: Com-

ments on plasma polymerization of acrylic acid revisited. *Plasma Processes and Polymers*, 7(5):371–375, 2010.

[47] J.D. Whittle, R.D. Short, and D.A. Steele. Reply to Testing the Hypothesis: Comments on Plasma Polymerization of Acrylic Acid Revisited. *Plasma Processes and Polymers*, 2011.

[48] J. Andrade and V. Hlady. Protein adsorption and materials biocompatibility: a tutorial review and suggested hypotheses. *Biopolymers/Non-Exclusion HPLC*, pages 1–63, 1986.

[49] L. Vroman and E.F. Leonard. *The behavior of blood and its components at interfaces.* New York Academy of Sciences, 1977.

[50] B.D. Ratner. *Biomaterials science: an introduction to materials in medicine.* Academic press, 2004.

[51] T.H. Groth, E.J. Campbell, K. Herrmann, and B. Seifert. Application of enzyme immunoassays for testing haemocompatibility of biomedical polymers. *Biomaterials*, 16(13):1009–1015, 1995.

[52] L. Tang, Y. Wu, and R.B. Timmons. Fibrinogen adsorption and host tissue responses to plasma functionalized surfaces. *Journal of biomedical materials research*, 42(1):156–163, 1998.

[53] J.L. Ortega-Vinuesa, P. Tengvall, and I. Lundstrom. Aggregation of HSA, IgG, and fibrinogen on methylated silicon surfaces. *Journal of colloid and interface science*, 207(2):228–239, 1998.

[54] R.J. Green, M.C. Davies, C.J. Roberts, and S.J.B. Tendler. Competitive protein adsorption as observed by surface plasmon resonance. *Biomaterials*, 20(4):385–391, 1999.

[55] P. Yang, N. Huang, Y.X. Leng, J.Y. Chen, H. Sun, J. Wang, and G.J. Wan. Inhibition of adherent platelet activation produced by Ti–O thin film fabricated by PIII. *Surface and Coatings Technology*, 186(1):265–269, 2004.

[56] A.G. Hemmersam, M. Foss, J. Chevallier, and F. Besenbacher. Adsorption of fibrinogen on tantalum oxide, titanium oxide and gold studied by the QCM-D technique. *Colloids and Surfaces B: Biointerfaces*, 43(3-4):208–215, 2005.

[57] M. Malmsten. Ellipsometry studies of the effects of surface hydrophobicity on protein adsorption. *Colloids and Surfaces B: Biointerfaces*, 3(5):297–308, 1995.

[58] H. Elwing. Protein absorption and ellipsometry in biomaterial research. *Biomaterials*, 19(4-5):397–406, 1998.

[59] T. Yoshioka, K. Tsuru, S. Hayakawa, and A. Osaka. Preparation of organotitanium molecular layers for biomedical applications. *Materials Science and Engineering: C*, 24(6):901–905, 2004.

[60] O. Joshi, H.J. Lee, J. McGuire, P. Finneran, and K.E. Bird. Protein concentration and adsorption time effects on fibrinogen adsorption at heparinized silica interfaces. *Colloids and Surfaces B: Biointerfaces*, 50(1):26–35, 2006.

[61] M.A. Lieberman and A.J. Lichtenberg. *Principles of Plasma Discharges and Materials Processing, 2nd edition.* Wiley, 2005.

[62] H. Yasuda. *Luminous chemical vapor deposition and interface engineering.* CRC, 2005.

[63] R. d'Agostino. *Plasma Deposition, Treatment, and Etching of Polymers.* Academic Press Inc, Bari, Italy, 1990.

[64] M.D. Dange, J.Y. Lee, and K. Sooriakumar. New applications of low temperature PECVD silicon nitride films for microelectronic device fabrication. *Microelectronics Journal*, 22(7-8):19 – 26, 1991.

[65] F. Jansen. Plasma-Enhanced Chemical Vapor Deposition (AVS monograph series). *New York, American Vacuum Society*, 1998.

[66] P.N. Prasad. *Introduction to biophotonics*. John Wiley and Sons, 2003.

[67] J. Castillo, S. Gaspar, S. Leth, M. Niculescu, A. Mortari, I. Bontidean, V. Soukharev, S.A. Dorneanu, A.D. Ryabov, and E. Csoregi. Biosensors for life quality:: Design, development and applications. *Sensors and Actuators B: Chemical*, 102(2):179–194, 2004.

[68] M.N. Velasco-Garcia. Optical biosensors for probing at the cellular level: A review of recent progress and future prospects. In *Seminars in cell & developmental biology*, volume 20, pages 27–33. Elsevier, 2009.

[69] L. Pavesi and P.M. Fauchet. *Biophotonics*. Springer Verlag, 2008.

[70] J.A. Hansen, R. Mukhopadhyay, J.Ø. Hansen, and K.V. Gothelf. Femtomolar electrochemical detection of DNA targets using metal sulfide nanoparticles. *Journal of the American Chemical Society*, 128(12):3860–3861, 2006.

[71] A. Janshoff, H.J. Galla, and C. Steinem. Piezoelectric mass-sensing devices as biosensors: An alternative to optical biosensors? *Angew. Chem. Int. Ed*, 39:4004–4032, 2000.

[72] C.M. Ferreira and M. Moisan. *Microwave discharges : fundamentals and applications*. New York : Plenum Press, 1993.

[73] W.L. Kruer. *The physics of laser plasma interactions*. Reading, MA (US): Addison-Wesley Publishing Co., 1988.

[74] O.A. Popov. *High density plasma sources: design, physics, and performance*. William Andrew, 1995.

[75] B. Chapman. *Glow discharge processes: sputtering and plasma etching*. Wiley New York, 1980.

[76] I.U.P. Raizer, M.N. Shneider, and N.A. Yatsenko. *Radio-frequency capacitive discharges*. CRC, 1995.

[77] P. Favia, LC Lopez, E. Sardella, R. Gristina, M. Nardulli, and R. d'Agostino. Low temperature plasma processes for biomedical applications and membrane processing. *Desalination*, 199(1-3):268–270, 2006.

[78] F. Palumbo, P. Favia, A. Rinaldi, M. Vulpio, and R. d'Agostino. PE-CVD of Organic Thin Films with Controlled Surface Concentration of Carboxylic Groups. *Plasmas and Polymers*, 4(2):133–145, 1999.

[79] J.R. Hollahan and A.T. Bell. *Techniques and applications of plasma chemistry*. John Wiley & Sons, 1974.

[80] J. Mort and F. Jansen. *Plasma-deposited thin films*. CRC Press Inc., Boca Raton, FL, 1986.

[81] D.L. Smith. *Thin-film deposition: principles and practice*. McGraw-Hill Professional, 1995.

[82] J.R. Roth. *Industrial plasma engineering: Applications to nonthermal plasma processing*, volume 2. Taylor & Francis, 2001.

[83] A.A. Fridman and L.A. Kennedy. *Plasma physics and engineering*. CRC, 2004.

[84] F.C. Chen. *Introduction to Plasma Physics and Controlled Fusion*. Springer, 1974.

[85] H. Biederman and Y. Osada. *Plasma polymerization processes*. Elsevier, 1992.

[86] J.M. Slocik, E.R. Beckel, H. Jiang, J.O. Enlow, J.S. Zabinski Jr, T.J. Bunning, and R.R. Naik. Site-specific patterning of biomolecules and quantum dots on function-

alized surfaces generated by plasma-enhanced chemical vapor deposition. *Advanced Materials*, 18(16):2095–2100, 2006.

[87] H. Yasuda and Y. Matsuzawa. Economical advantages of low-pressure plasma polymerization coating. *Plasma Processes and Polymers*, 2(6):507–512, 2005.

[88] C. Haag and H. Suhr. Improved adhesion of Cu on pre-etched polytetrafluoroethylene by PECVD deposited thin metallic layers. *Applied Physics A: Materials Science & Processing*, 47(2):199–203, 1988.

[89] D. Kim, M.A. Scibioh, S. Kwak, I.H. Oh, and H.Y. Ha. Nano-silica layered composite membranes prepared by PECVD for direct methanol fuel cells. *Electrochemistry communications*, 6(10):1069–1074, 2004.

[90] V. Bursikova, V. Navratil, L. Zajickova, and J. Janca. Temperature dependence of mechanical properties of DLC/Si protective coatings prepared by PECVD. *Materials Science and Engineering: A*, 324(1):251–254, 2002.

[91] A. Grill. *Cold plasma in materials fabrication.* IEEE press, 1994.

[92] A.J. Beck, F.R. Jones, and R.D. Short. Mass spectrometric study of the radiofrequency-induced plasma polymerisation of styrene and propenoic acid. *J. Chem. Soc., Faraday Trans.*, 94(4):559–565, 1998.

[93] Menno T. van Os. *Surface Modification by Plasma Polymerization: Film Deposition, Tailoring of Surface Properties and Biocompatibility.* PhD thesis, 2000.

[94] P.N. Prasad. *Introduction to biophotonics.* LibreDigital, 2003.

[95] J.R. Lakowicz. *Principles of fluorescence spectroscopy.* New York, Plenum Press, 1983.

[96] K.S. Ma, F. Reza, I. Saaem, and J. Tian. Versatile surface functionalization of

cyclic olefin copolymer (COC) with sputtered SiO2 thin film for potential BioMEMS applications. *Journal of Materials Chemistry*, 19(42):7914–7920, 2009.

[97] J. Raj, G. Herzog, M. Manning, C. Volcke, B.D. MacCraith, S. Ballantyne, M. Thompson, and D.W.M. Arrigan. Surface immobilisation of antibody on cyclic olefin copolymer for sandwich immunoassay. *Biosensors and Bioelectronics*, 24(8):2654–2658, 2009.

[98] H. Becker and C. Gartner. Polymer microfabrication technologies for microfluidic systems. *Analytical and Bioanalytical Chemistry*, 390(1):89–111, 2008.

[99] G.A. Diaz-Quijada, R. Peytavi, A. Nantel, E. Roy, M.G. Bergeron, M.M. Dumoulin, and T. Veres. Surface modification of thermoplasticstowards the plastic biochip for high throughput screening devices. *Lab on a Chip*, 7(7):856–862, 2007.

[100] M.A. Lieberman and A.J. Lichtenberg. *Principles of plasma discharges and materials processing*. Wiley-Blackwell, 2005.

[101] A. Kurella and N.B. Dahotre. Review paper: surface modification for bioimplants: the role of laser surface engineering. *Journal of biomaterials applications*, 20(1):5–50, 2005.

[102] P.K. Chu, J.Y. Chen, L.P. Wang, and N. Huang. Plasma-surface modification of biomaterials. *Materials Science and Engineering: R: Reports*, 36(5-6):143–206, 2002.

[103] L. Feng and J.D. Andrade. *Structure and adsorption properties of fibrinogen*, volume 602. ACS Publications, 1995.

[104] R.F. Doolittle. Fibrinogen and fibrin. *Encyclopedia of Life Sciences*, 1984.

[105] R.J. Good. Contact angle, wetting, and adhesion: a critical review. *Journal of adhesion science and technology*, 6(12):1269–1302, 1992.

[106] J.F. Watts, J. Wolstenholme, and J. Wiley. *An introduction to surface analysis by XPS and AES*. Wiley Online Library, 2003.

[107] P.J. Hendra. How does FTIR work? *Internet journal of vibrational spectroscopy*, 5(5):2, 2001.

[108] V.T. Cherepin. *Secondary ion mass spectroscopy of solid surfaces*. Utrecht, Netherlands: VSP Books, 1987.

[109] S.N. Magonov and M.H. Whangbo. Surface analysis with STM and AFM. 3(527), 1996.

[110] M.A. Lieberman and A.J. Lichtenberg. *Principles of plasma discharges and materials processing*. Wiley-Blackwell, 2005.

[111] F.W. McLafferty and F. Turecek. *Interpretation of mass spectra*. Univ Science Books, 1993.

[112] T. Fujimoto. *Plasma spectroscopy*, volume 123. Oxford University Press, USA, 2004.

[113] H. Schneckenburger. Total internal reflection fluorescence microscopy: technical innovations and novel applications. *Current Opinion in Biotechnology*, 16(1):13 – 18, 2005. Analytical biotechnology.

[114] Glasnevin Dublin 9 Ireland Imedans Ltd. Invent Centre, DCU. URL: http://www.impedans.com., 2011.

[115] D. Gahan, B. Dolinaj, and M.B. Hopkins. Retarding field analyzer for ion energy distribution measurements at a radio-frequency biased electrode. *Review of Scientific Instruments*, 79:033502, 2008.

[116] C.C. Shih, C.M. Shih, Y.Y. Su, L.H.J. Su, M.S. Chang, and S.J. Lin. Effect of

surface oxide properties on corrosion resistance of 316L stainless steel for biomedical applications. *Corrosion science*, 46(2):427–441, 2004.

[117] L. Detomaso, R. Gristina, G.S. Senesi, R. d'Agostino, and P. Favia. Stable plasma-deposited acrylic acid surfaces for cell culture applications. *Biomaterials*, 26(18):3831–3841, 2005.

[118] M.R. Alexander and T.M. Duc. The chemistry of deposits formed from acrylic acid plasmas. *Journal of Materials Chemistry*, 8(4):937–943, 1998.

[119] R.P. Gandhiraman, V. Gubala, L.C.H. Nam, C. Volcke, C. Doyle, B. James, S. Daniels, and D.E. Williams. Deposition of chemically reactive and repellent sites on biosensor chips for reduced non-specific binding. *Colloids and Surfaces B: Biointerfaces*, 79(1):270–275, 2010.

[120] B. Kasemo. Biological surface science. *Surface Science*, 500(1-3):656–677, 2002.

[121] WA Pliskin and HS Lehman. Structural evaluation of silicon oxide films. *Journal of The Electrochemical Society*, 112:1013, 1965.

[122] K.S. Ma, F. Reza, I. Saaem, and J. Tian. Versatile surface functionalization of cyclic olefin copolymer (COC) with sputtered SiO2 thin film for potential BioMEMS applications. *J. Mater. Chem.*, 19(42):7914–7920, 2009.

[123] V. Gubala, N.C.H. Le, R.P. Gandhiraman, C. Coyle, S. Daniels, and D.E. Williams. Functionalization of cyclo olefin polymer substrates by plasma oxidation: Stable film containing carboxylic acid groups for capturing biorecognition elements. *Colloids and Surfaces B: Biointerfaces*, 2010.

[124] L. Detomaso, R. Gristina, R. d'Agostino, GS Senesi, and P. Favia. Plasma deposited acrylic acid coatings: Surface characterization and attachment of 3T3 murine fibroblast cell lines. *Surface and Coatings Technology*, 200(1-4):1022–1025, 2005.

[125] S. Mourtas, M. Kastellorizios, P. Klepetsanis, E. Farsari, E. Amanatides, D. Mataras, BR Pistillo, P. Favia, E. Sardella, R. d'Agostino, et al. Covalent immobilization of liposomes on plasma functionalized metallic surfaces. *Colloids and Surfaces B: Biointerfaces*, 2011.

[126] A. Cros, R. Saoudi, G. Hollinger, CA Hewett, and SS Lau. An X-ray photoemission spectroscopy investigation of oxides grown on AuxSi1-x layers. *Journal of Applied Physics*, 67(4):1826–1830, 1990.

[127] E. Paparazzo. X-ray photo-emission and Auger spectra of damage induced by Ar+-ion etching at SiO2 surfaces. *Journal of Physics D: Applied Physics*, 20:1091, 1987.

[128] Nist X-ray photoelectron spectroscopy database 20.

[129] V.G. Pol, S.V. Pol, Y. Gofer, J. Calderon-Moreno, and A. Gedanken. Thermal decomposition of tetraethylorthosilicate (TEOS) produces silicon coated carbon spheres. *Journal of Materials Chemistry*, 14(6):966–969, 2004.

[130] W.J. Ma, A.J. Ruys, R.S. Mason, P.J. Martin, A. Bendavid, Z. Liu, M. Ionescu, and H. Zreiqat. DLC coatings: Effects of physical and chemical properties on biological response. *Biomaterials*, 28(9):1620–1628, 2007.

[131] D. Liu, A. Bruckbauer, C. Abell, S. Balasubramanian, D.J. Kang, D. Klenerman, and D. Zhou. A reversible pH-driven DNA nanoswitch array. *J. Am. Chem. Soc*, 128(6):2067–2071, 2006.

[132] S. Roy, X. Chen, M.H. Li, Y. Peng, F. Anariba, and Z. Gao. Mass-Produced Nanogap Sensor Arrays for Ultrasensitive Detection of DNA. *J. Am. Chem. Soc*, 131(34):12211–12217, 2009.

[133] J. Hu, M. Wang, H.U.G. Weier, P. Frantz, W. Kolbe, DF Ogletree, and M. Salmeron. Imaging of Single Extended DNA Molecules on Flat (Aminopropyl) triethoxysilane-Mica by Atomic Force Microscopy. *Langmuir*, 12(7):1697–1700, 1996.

[134] R.M. Pasternack, S.R. Amy, and Y.J. Chabal. Attachment of 3-(Aminopropyl) triethoxysilane on Silicon Oxide Surfaces: Dependence on Solution Temperature. *Langmuir*, 24(22):12963–12971, 2008.

[135] A. Kasry, P. Borri, P.R. Davies, A. Harwood, N. Thomas, S. Lofas, and T. Dale. Comparison of Methods for Generating Planar DNA-Modified Surfaces for Hybridization Studies. *ACS Applied Materials & Interfaces*, 1(8):1793–1798, 2009.

[136] C. Charlton, V. Gubala, R.P. Gandhiraman, J. Wiechecki, N.C.H. Le, C. Coyle, S. Daniels, B.D. MacCraith, and D.E. Williams. TIRF microscopy as a screening method for non-specific binding on surfaces. *Journal of Colloid and Interface Science*, 354(1):405–409, 2011.

[137] E.S. Kim, Q. Yu, and B. Deng. Plasma surface modification of nanofiltration (nf) thin-film composite (tfc) membranes to improve anti organic fouling. *Applied Surface Science*, 2011.

[138] N.S.J. Braithwaite. Electron energy distribution functions in processing plasmas. *Pure and applied chemistry*, 62(9):1721–1728, 1990.

[139] VA Godyak, RB Piejak, and BM Alexandrovich. Electron energy distribution function measurements and plasma parameters in inductively coupled argon plasma. *Plasma Sources Science and Technology*, 11:525, 2002.

[140] T. Tsankov, Z. Kissovski, N. Djermanova, and S. Kolev. Electron energy distribution function measurements in an inductively driven tandem plasma source. *Plasma Processes and Polymers*, 3(2):151–155, 2006.

[141] D. Gahan, B. Dolinaj, and MB Hopkins. Comparison of plasma parameters determined with a Langmuir probe and with a retarding field energy analyzer. *Plasma Sources Science and Technology*, 17:035026, 2008.

[142] F. Chen. *Langmuir Probe Diagnostics Notes.* IEEE-ICOPS meeting, Jeju, Korea., 2003.

[143] L. O'Toole, A.J. Beck, A.P. Ameen, F.R. Jones, and R.D. Short. Radiofrequency-induced plasma polymerisation of propenoic acid and propanoic acid. *J. Chem. Soc., Faraday Trans.*, 91(21):3907–3912, 1995.

[144] E. Sardella, P. Favia, E. Dilonardo, L. Petrone, and R. d'Agostino. PE-CVD of acid/base coatings from acrylic acid and allylamine vapours. *Plasma Processes and Polymers*, 4(S1):S781–S783, 2007.

[145] P. Rossini, P. Colpo, G. Ceccone, K. D. Jandt, and F. Rossi. Surfaces engineering of polymeric films for biomedical applications. *Materials Science and Engineering: C*, 23(3):353 – 358, 2003.

[146] C. Bayram, A.K. Mizrak, S. Akturk, H. Kursaklioglu, A. Iyisoy, A. Ifran, and E.B. Denkbas. In vitro biocompatibility of plasma-aided surface-modified 316L stainless steel for intracoronary stents. *Biomedical Materials*, 5:055007, 2010.

[147] F. Palumbo, P. Favia, A. Rinaldi, M. Vulpio, and R. d'Agostino. PE-CVD of Organic Thin Films with Controlled Surface Concentration of Carboxylic Groups. *Plasmas and Polymers*, 4(2):133–145, 1999.

[148] M.B. Hopkins, C.A. Anderson, and W.G. Graham. Time-resolved electron energy distribution function measurements in a low-frequency rf glow discharge. *EPL (Europhysics Letters)*, 8:141, 1989.

[149] M.S. Hedenqvist and K.S. Johansson. Barrier properties of SiOx-coated polymers: multi-layer modelling and effects of mechanical folding. *Surface and Coatings Technology*, 172(1):7–12, 2003.

[150] S. Sahli, Y. Segui, S. Ramdani, and Z. Takkouk. Rf plasma deposition from hexamethyldisiloxane-oxygen mixtures. *Thin solid films*, 250(1-2):206–212, 1994.

[151] D. Hegemann, U. Vohrer, C. Oehr, and R. Riedel. Deposition of SiOx films from O2/HMDSO plasmas. *Surface and Coatings Technology*, 116:1033–1036, 1999.

[152] F. Benıtez, E. Martı´nez, and J. Esteve. Improvement of hardness in plasma polymerized hexamethyldisiloxane coatings by silica-like surface modification. *Thin Solid Films*, 377:109–114, 2000.

[153] C. Vautrin-Ul, F. Roux, C. Boisse-Laporte, J.L. Pastol, and A. Chausse. Hexamethyldisiloxane (hmdso)-plasma-polymerised coatings as primer for iron corrosion protection: influence of rf bias. *J. Mater. Chem.*, 12(8):2318–2324, 2002.

[154] F. Fracassi, R. d'Agostino, F. Palumbo, E. Angelini, S. Grassini, and F. Rosalbino. Application of plasma deposited organosilicon thin films for the corrosion protection of metals. *Surface and Coatings Technology*, 174:107–111, 2003.

[155] E. Vassallo, L. Laguardia, D. Ricci, and G. Bonizzoni. Innovative plasma processes for consolidation of biodeteriorated ancient papers. 238(1):46–51, 2006.

[156] F. Rombaldoni, R. Mossotti, A. Montarsolo, M.B. Songia, R. Innocenti, and G. Mazzuchetti. Thin film deposition by PECVD using HMDSO-O 2-Ar gas mixture on knitted wool fabrics in order to improve pilling resistance. *Fibers and Polymers*, 9(5):566–573, 2008.

[157] L. Akesso, P. Navabpour, D. Teer, M.E. Pettitt, M.E. Callow, C. Liu, X. Su, S. Wang, Q. Zhao, C. Donik, et al. Deposition parameters to improve the fouling-release properties of thin siloxane coatings prepared by PACVD. *Applied Surface Science*, 255(13-14):6508–6514, 2009.

[158] B. Kasemo. Biological surface science. *Current Opinion in Solid State and Materials Science*, 3(5):451–459, 1998.

[159] C. Vautrin-Ul, C. Boisse-Laporte, N. Benissad, A. Chausse, P. Leprince, and

R. Messina. Plasma-polymerized coatings using HMDSO precursor for iron protection. *Progress in organic coatings*, 38(1):9–15, 2000.

[160] G.R. Prasad, S. Daniels, D.C. Cameron, B.P. McNamara, E. Tully, and R. O'Kennedy. Pecvd of biocompatible coatings on 316L stainless steel. *Surface and Coatings Technology*, 200(1):1031–1035, 2005.

[161] R. Morent, N. De Geyter, S. Van Vlierberghe, P. Dubruel, C. Leys, and E. Schacht. Organic-inorganic behaviour of HMDSO films plasma-polymerized at atmospheric pressure. *Surface and Coatings Technology*, 203(10-11):1366–1372, 2009.

[162] W.M. Huo, V. Tarnovsky, and K.H. Becker. Total electron-impact ionization cross-sections of CFx and NFx (x = 1-3). *Chemical physics letters*, 358(3-4):328–336, 2002.

[163] K.H. Becker and V. Tarnovsky. Electron-impact ionization of atoms, molecules, ions and transient species. *Plasma Sources Science and Technology*, 4:307, 1995.

[164] R. Basner, R. Foest, M. Schmidt, K. Becker, and H. Deutsch. Absolute total and partial electron impact ionization cross sections of hexamethyldisiloxane. *International journal of mass spectrometry*, 176(3):245–252, 1998.

[165] D.S. Wavhal, J. Zhang, M.L. Steen, and E.R. Fisher. Investigation of gas phase species and deposition of SiO2 films from HMDSO/O2 plasmas. *Plasma Processes and Polymers*, 3(3):276–287, 2006.

[166] M.R. Alexander, F.R. Jones, and R.D. Short. Mass spectral investigation of the radio-frequency plasma deposition of hexamethyldisiloxane. *The Journal of Physical Chemistry B*, 101(18):3614–3619, 1997.

[167] T. Groth, EJ Campbell, K. Herrmann, and B. Seifert. Application of enzyme immunoassays for testing haemocompatibility of biomedical polymers. *Biomaterials*, 16(13):1009–1015, 1995.

[168] S. Windecker, I. Mayer, G. De Pasquale, W. Maier, O. Dirsch, P. De Groot, Y.P. Wu, G. Noll, B. Leskosek, B. Meier, et al. Stent coating with titanium-nitride-oxide for reduction of neointimal hyperplasia. *Circulation*, 104(8):928–933, 2001.

[169] N. Huang, P. Yang, YX Leng, JY Chen, H. Sun, J. Wang, GJ Wang, PD Ding, TF Xi, and Y. Leng. Hemocompatibility of titanium oxide films. *Biomaterials*, 24(13):2177–2187, 2003.

[170] C.F. Wertz and M.M. Santore. Effect of surface hydrophobicity on adsorption and relaxation kinetics of albumin and fibrinogen: single-species and competitive behavior. *Langmuir*, 17(10):3006–3016, 2001.

[171] G. Raffaini and F. Ganazzoli. Protein adsorption on a hydrophobic surface: a molecular dynamics study of lysozyme on graphite. *Langmuir*, 26(8):5679–5689, 2010.

[172] I. Beaulieu, M. Geissler, and J. Mauzeroll. Oxygen plasma treatment of polystyrene and Zeonor: substrates for adhesion of patterned cells. *Langmuir*, 25(12):7169–7176, 2009.

[173] D. Labarre. Improving blood-compatibility of polymeric surfaces. *Trends Biomater Artif Organs*, 15:1–3, 2001.

[174] C. Yongli, Z. Xiufang, G. Yandao, Z. Nanming, Z. Tingying, and S. Xinqi. Conformational changes of fibrinogen adsorption onto hydroxyapatite and titanium oxide nanoparticles. *Journal of colloid and interface science*, 214(1):38–45, 1999.

[175] M. Malmsten. Ellipsometry studies of the effects of surface hydrophobicity on protein adsorption. *Colloids and Surfaces B: Biointerfaces*, 3(5):297–308, 1995.

[176] E.P. Van de Ven, I.W. Connick, and A.S. Harrus. Advantages of dual frequency PECVD for deposition of ILD and passivation films. In *VLSI Multilevel Interconnec-*

tion Conference, 1990. Proceedings., Seventh International IEEE, pages 194–201. IEEE, 1990.